PARAMETRIC AND POSTERIOR CRAMÉR-RAO LOWER BOUNDS FOR EXTENDED TARGET TRACKING IN A RANDOM MATRIX FRAMEWORK

A THESIS SUBMITTED TO
THE GRADUATE SCHOOL OF NATURAL AND APPLIED SCIENCES
OF
MIDDLE EAST TECHNICAL UNIVERSITY

BY

ELİF SARITAŞ

IN PARTIAL FULFILLMENT OF THE REQUIREMENTS
FOR
THE DEGREE OF MASTER OF SCIENCE
IN
ELECTRICAL AND ELECTRONICS ENGINEERING

SEPTEMBER 2015

Approval of the thesis:

PARAMETRIC AND POSTERIOR CRAMÉR-RAO LOWER BOUNDS FOR EXTENDED TARGET TRACKING IN A RANDOM MATRIX FRAMEWORK

submitted by **ELİF SARITAŞ** in partial fulfillment of the requirements for the degree of **Master of Science in Electrical and Electronics Engineering Department, Middle East Technical University** by,

Prof. Dr. Gülbin Dural Ünver
Dean, Graduate School of **Natural and Applied Sciences** _____

Prof. Dr. Gönül Turhan Sayan
Head of Department, **Electrical and Electronics Engineering** _____

Assoc. Prof. Dr. Umut Orguner
Supervisor, **Electrical and Electronics Engg. Dept., METU** _____

Examining Committee Members:

Prof. Dr. Mübeccel Demirekler
Electrical and Electronics Engineering Department, METU _____

Assoc. Prof. Dr. Umut Orguner
Electrical and Electronics Engineering Department, METU _____

Prof. Dr. Çağatay Candan
Electrical and Electronics Engineering Department, METU _____

Assoc. Prof. Dr. Afşar Saranlı
Electrical and Electronics Engineering Department, METU _____

Assoc. Prof. Dr. M. Burak Güldoğan
Electrical and Electronics Engg. Dept., Turgut Özal Uni. _____

Date: **08.09.2015**

I hereby declare that all information in this document has been obtained and presented in accordance with academic rules and ethical conduct. I also declare that, as required by these rules and conduct, I have fully cited and referenced all material and results that are not original to this work.

Name, Last Name: ELİF SARITAŞ

Signature :

ABSTRACT

PARAMETRIC AND POSTERIOR CRAMÉR-RAO LOWER BOUNDS FOR EXTENDED TARGET TRACKING IN A RANDOM MATRIX FRAMEWORK

Sarıtaş, Elif
M.S., Department of Electrical and Electronics Engineering
Supervisor : Assoc. Prof. Dr. Umut Orguner

September 2015, 91 pages

This thesis presents the parametric and posterior Cramér-Rao lower bounds (CRLB) for extended target tracking (ETT) in a random matrix framework. ETT is an area of target tracking in which the common assumption of point targets does not hold due to the recent improvements in sensor technology. With the increased sensor capability, targets can generate more than one measurement in a single scan depending on their size. Therefore, not only the target's kinematical state but also its extension can be estimated. Although there are different methods in literature that deals with ETT, random matrix based ETT algorithms are the subject of this thesis. In this Bayesian approach, the extents of the targets are assumed to be ellipsoidal and they are represented with positive definite matrices which are called as the extent states. The kinematic and extent states are estimated recursively in a Bayesian framework. When these estimators are applied, their performances come into question. Cramér-Rao Lower

Bound (CRLB) which gives a lower bound on the achievable mean-square-error (MSE) of an unbiased estimator is a commonly used method to evaluate estimator performance in estimation theory. CRLB is the inverse of the Fisher Information which is a measure of information that a measured random variable carries about the parameter to be estimated; and in this study, it is applied for ETT algorithms. First, parametric and posterior CRLBs for ETT in a random matrix framework are obtained. Formulae for CRLBs for both kinematic and extent states are computed by using both analytical and numerical tools, and then compared with the performance of a state-of-the-art random matrix based ETT algorithm.

Keywords: Extended target tracking, Bayesian approach, random matrix, posterior CRLB, parametric CRLB

ÖZ

RASTGELE MATRİS ÇERÇEVESİNDE GENİŞLETİLMİŞ HEDEF İZLEME İÇİN PARAMETRİK VE SONSAL CRAMÉR-RAO ALT SINIRI

Sarıtaş, Elif
Yüksek Lisans, Elektrik ve Elektronik Mühendisliği Bölümü
Tez Yöneticisi : Doç. Dr. Umut Orguner

Eylül 2015 , 91 sayfa

Bu tezde rastgele matris çerçevesinde genişletilmiş hedef izleme (GHİ) için parametrik ve sonsal Cramér-Rao alt sınırları (CRAS) sunulmaktadır. GHİ, yakın zamanda gerçekleşen sensör teknolojisindeki ilerlemeler dolayısıyla yaygın olarak yapılan noktasal hedef varsayımının geçerli olmadığı hedef izleme alanıdır. Artan sensör yetenekleri ile hedefler tek bir sensör raporunda birden fazla ölçüm üretir hale gelmiştir. Böylelikle, hedefin kinematik durumunun yanı sıra genişliği de tahmin edilebilir olmuştur. Kaynaklarda çeşitli GHİ algoritmaları olsa da, bu çalışmada rastgele matris tabanlı GHİ algoritmaları üzerinde durulmuştur. Bu yaklaşımda hedeflerin şekillerinin elips şeklinde olduğu varsayılır ve şekil durum değişkeni kesin pozitif matrisler ile temsil edilir. Bayes teorisi çerçevesinde, kinematik ve şekil durumları yinelemeli olarak kestirilir. Bu tezde bu kestiriciler kullanıldıkları zaman elde edilen kestirim başarımları sorgulanmaktadır. CRAS yansız kesitiricilerin başarabileceği ortalama karesel hata için bir alt sınırdır ve

başarım ölçümü için kestirim teorisinde sıklıkla kullanılır. Ölçümü alınan rastgele bir değişkenin tahmin edilmek istenen parametre ile ilgili taşıdığı bilginin ölçüsü olan Fisher bilgi matrisinin tersi olan bu sınır, bu çalışmada GHİ algoritmaları için uygulanmıştır. Öncelikle rastgele matris çerçevesinde GHİ için parametrik ve sonsal CRAS'lar elde edilmiştir. Çözümlemeli ve sayısal araçlar kullanılarak kinematik ve şekil durumları için CRAS formülleri türetilip rastgele matris tabanlı güncel bir GHİ algoritmasının başarımları ile karşılaştırılmıştır.

Anahtar Kelimeler: Genişletilmiş hedef izleme, Bayes yaklaşımı, rastgele matris, sonsal CRAS, parametrik CRAS

Teyzoşum Ayşe Kurt'a

ACKNOWLEDGMENTS

Foremost, I am truly indebted and thankful to my supervisor Assoc. Prof. Dr. Umut Orguner for his patient guidance and support he provided in every step of this thesis work. With his assistance, he made it much easier for me to get through this challenging period.

I should thank to Turkish Scientific and Technological Research Council (TÜBİTAK) for their financial support during my M.Sc. studies.

I owe my deepest gratitude to my grandmother Hafize Zambak for all the effort she put for raising me.

Moreover, I owe much to Murat Kumru for his invaluable support and inspiration. His friendship has always made me feel at ease.

It is a great pleasure to express my gratitude to my dearest sister Selen Naz. Besides her help with proof-reading, she has always put up with me with patience, when I am struggling with this dissertation study.

Last but not least, I am sincerely grateful to my parents for all the support they provided in my entire life. Without their faith in me, I would not have been able make it this far.

TABLE OF CONTENTS

ABSTRACT v

ÖZ vii

ACKNOWLEDGMENTS x

TABLE OF CONTENTS xi

LIST OF TABLES xv

LIST OF FIGURES xvi

LIST OF ABBREVIATIONS xviii

CHAPTERS

1 INTRODUCTION 1

1.1 Motivation of the Thesis 1

1.2 Organization of the Thesis 3

2 BACKGROUND 5

2.1 Extended Target Tracking 5

2.1.1 ETT with Random Matrices 7

2.1.1.1 Formulation 9

2.2 Cramér-Rao Lower Bound 12

2.2.1 Parametric Cramér-Rao Lower Bound 12

2.2.2 Posterior Cramér-Rao Lower Bound 14

2.3 Literature Research on Performance Measures on Extended Target Tracking 15

3 PARAMETRIC CRAMÉR-RAO LOWER BOUND FOR EXTENDED TARGET TRACKING 19

3.1 Parametric Cramér-Rao Lower Bound for Dynamic Systems 19

3.2 Fisher Information Matrix for ETT 20

3.2.1 Score Function 21

3.2.2 Fisher Information Matrix 25

3.3 Initialization of the Parametric CRLB 31

3.4 Parametric CRLB for Semi-Major and Semi-Minor Axes 32

4 POSTERIOR CRAMÉR-RAO LOWER BOUND FOR EXTENDED TARGET TRACKING 35

4.1 Definition of Posterior Cramér-Rao Lower Bound for Dynamic Systems 35

4.2 Derivations of Posterior CRLB for the Case of ETT . . 37

4.2.1 Derivations for the Kinematical State 39

4.2.2 Derivations for the Extent State 41

4.3 Initialization of Posterior Cramér-Rao Lower Bound . . 51

4.3.1 Initialization for the Posterior CRLB of the Kinematic State 51

4.3.2 Initialization for the Posterior CRLB of the Extent State 52

4.4 Computation of Posterior Cramér-Rao Lower Bound for Semi-Major and Semi-Minor Axes 54

5 SIMULATIONS 55

5.1 Parametric Cramér-Rao Lower Bound 55

5.1.1 Implementation 55

5.1.1.1 True Target & Measurement Parameters 55

5.1.1.2 ETT Algorithm Parameters 59

5.1.2 Results 60

5.2 Posterior Cramér-Rao Lower Bound 65

5.2.1 Implementation 65

5.2.1.1 Trajectory and Measurement Generation 65

5.2.1.2 Computation of Posterior Cramér-Rao Lower Bound 66

5.2.1.3 ETT Algorithm Parameters 68

5.2.2 Results 69

5.3 Dependence of the Estimator Performance on Some Parameters 73

5.3.1 Dependence on Process Noise Covariance Matrix Q 74

5.3.2 Dependence on Measurement Noise Covariance Matrix R 76

5.3.3 Dependence on Forgetting Factor τ 77

6 CONCLUSIONS 85

REFERENCES 89

LIST OF TABLES

TABLES

Table 5.1 Average RMS errors and average parametric CRLBs for kinematical states. 64

Table 5.2 Average RMS errors and average parametric CRLBs for extension. 64

Table 5.3 Average RMS errors and average parametric CRLBs for semi-major and semi-minor axes. 64

Table 5.4 Average standard deviations of RMS errors for kinematical states. 64

Table 5.5 Average standard deviations of RMS errors for extension states. 65

Table 5.6 Average RMS errors and average posterior CRLB values for kinematical states. 72

Table 5.7 Average RMS errors and average posterior CRLB values for extension. 72

Table 5.8 Average RMS errors and average posterior CRLB values for semi-major and semi-minor axes. 73

Table 5.9 Average standard deviations of RMS errors for kinematical states. 73

Table 5.10 Average standard deviations of RMS errors for extension states. 73

LIST OF FIGURES

FIGURES

Figure 5.1 True trajectory and a single realization of measurements. . . 58

Figure 5.2 RMS errors and parametric CRLB values for kinematical states with $m = 5$, $m = 20$ and $m = 80$. 60

Figure 5.3 RMS errors and parametric CRLB values for extension with $m = 5$, $m = 20$ and $m = 80$. 62

Figure 5.4 RMS errors and parametric CRLB values for major and minor semi-axes with $m = 5$, $m = 20$ and $m = 80$. 63

Figure 5.5 Random trajectories and a single realization of measurements. 67

Figure 5.6 RMS errors and posterior CRLB values for kinematical states with $m = 5$, $m = 20$ and $m = 80$. 71

Figure 5.8 RMS errors and posterior CRLB values for major and minor semi-axes with $m = 5$, $m = 20$ and $m = 80$. 71

Figure 5.7 RMS errors and posterior CRLB values for extension states with $m = 5$, $m = 20$ and $m = 80$. 72

Figure 5.9 RMS errors and parametric CRLB values for kinematical states with different process noise covariance matrices. 75

Figure 5.10 RMS errors and posterior CRLB values for kinematical states with different process noise covariance matrices. 76

Figure 5.11 RMS errors and parametric CRLB values for extension with different measurement noise covariance matrices. 79

Figure 5.12 RMS errors and posterior CRLB values for extension estimates with different measurement noise covariance matrices. 80

Figure 5.13 RMS errors and parametric CRLB values for semi-major and semi-minor axes estimates with different measurement noise covariance matrices. 80

Figure 5.14 RMS errors and posterior CRLB values for semi-major and semi-minor axes estimates with different measurement noise covariance matrices. 81

Figure 5.15 RMS errors and parametric CRLB values for extension with $\tau = 5$, $\tau = 10$, $\tau = 20$ and $\tau = 100$. 82

Figure 5.16 RMS errors and posterior CRLB values for extension with $\tau = 5$, $\tau = 10$, $\tau = 20$ and $\tau = 100$. 83

Figure 5.17 RMS errors and parametric CRLB for major and minor semi-axes with $\tau = 5$, $\tau = 10$, $\tau = 20$ and $\tau = 100$. 83

Figure 5.18 RMS errors and posterior CRLB values for major and minor semi-axes with $\tau = 5$, $\tau = 10$, $\tau = 20$ and $\tau = 100$. 84

LIST OF ABBREVIATIONS

CRLB	Cramér-Rao lower bound
CV	Constant velocity
EKF	Extended Kalman filter
ETT	Extended target tracking
FIM	Fisher information matrix
HCRLB	Hybrid Cramér-Rao lower bound
IMM	Interacting multiple model
KF	Kalman filter
LOS	Line of sight
MHT	Multiple hypothesis tracking
MSE	Mean-square-error
MVU	Minimum variance unbiased
pdf	Probability density function
PF	Particle filter
RMS	Root-mean-square
RBUKF	Rao-Blackwellised unscented Kalman filter
UKF	Unscented Kalman filter
TT	Target tracking

CHAPTER 1

INTRODUCTION

1.1 Motivation of the Thesis

In broad sense, target tracking (TT) can be refers to the field of research that deals with the problem of estimating the kinematical features of some targets using the measurements gathered from one or more sensors. Most of the time, the number of targets is unknown, and it is conventionally assumed that these objects are points as a consequence of low sensor resolution compared to the target extent or the object being in the far-field of the sensor. Therefore, it is common to assume that each target generates at most a single measurement in a sensor report. On the other hand, with the recent improvements in sensor technology, this assumption is not valid any longer. For instance, the increase in radar resolution capabilities results in the fact that targets can generate more than one measurement in a single scan depending on their size.

This area of target tracking where the point target assumption does not hold is known as extended target tracking (ETT). With the increased sensor capability, the estimation of not only the kinematical features but also the extension of the object are made possible. Moreover, the extent estimation contributes to resolving the attributes of the object, such as target type. Some examples of the problems which make use of ETT methods are given in [1] as vehicles that use radar sensors to track other road-users, ground radar stations tracking airplanes which are sufficiently close to the sensor, or mobile robotics when pedestrians are tracked using laser range sensors. Furthermore, clusters of targets that

are closely spaced can be examined via ETT algorithms as well. There are different approaches to extent estimation. The extent can be modelled as a rigid body with a predefined shape, or described with a spatial distribution of a set of measurements. Several methods in the literature that deal with ETT can be exemplified as spatial distributions, random matrix based methods and Monte Carlo methods. In this study, the random matrix based ETT algorithms are investigated. In this approach, the extents of the targets are assumed to be ellipsoidal and they are represented with positive definite matrices which are called as the extent states. The kinematic and extent states are estimated recursively in a Bayesian framework with a filter that resembles a Kalman Filter.

When an estimator is applied, its performance should be investigated. The use of lower bounds on the achievable estimation error is a common methodology to evaluate estimator performance in estimation theory. The most well-known and important family of lower bounds is Cramér-Rao Lower Bound (CRLB) which provides a lower bound on the achievable error of an unbiased estimator in terms of mean-square-error (MSE). CRLB is defined as the inverse of the Fisher Information Matrix (FIM) which is a measure of information that a measured random variable carries about the parameter to be estimated. CRLB can be calculated for both deterministic and random parameter estimation. The bound obtained for random parameter estimation is called as Bayesian CRLB. CRLB expressions are also available for the state estimation of discrete-time systems in the literature. The deterministic and Bayesian CRLBs used for state estimation are called as parametric and posterior CRLBs respectively.

In the literature, there are few studies that examine the performance of ETT techniques, none of which focus on the random matrix approach. The existing methods are all restricted to the comparison of some earliest methods in ETT. Therefore, the aim of this study is to calculate the parametric and posterior CRLBs for ETT in a random matrix framework. In this thesis, first, the analytical formulae for CRLBs for both kinematic and extent states are obtained by using analytical and numerical tools and then compared with the performance of the state-of-the-art random matrix based ETT algorithms. The results provide valuable insight for the performances of the recently proposed ETT algorithms

and give an indication of how much size estimation capability can be expected from such methods.

1.2 Organization of the Thesis

The thesis has been organized as follows. It begins with an introductory chapter that expresses the motives behind this study. Chapter 2 provides a general background on the topic. Some ETT algorithms are summarized and random matrix approach is discussed in detail. Moreover, the concept of a lower bound is introduced and CRLB is defined. Finally, some studies on the performance measures are surveyed in this chapter. In Chapter 3, parametric CRLB is explained and its derivation for ETT with random matrices is presented. Posterior CRLB is described and its derivation is given for ETT in Chapter 4. These bounds are implemented and the corresponding results are discussed in Chapter 5. The thesis concludes with a summary in Chapter 6 where final remarks on the study and future work are also discussed.

CHAPTER 2

BACKGROUND

In this chapter, some background information on the concepts utilized throughout this study is provided. The main topics addressed in this section are ETT, CRLB and performance measures on ETT. First, the notion of ETT is introduced and an overview of literature on this problem is given. Then, Bayesian approach using random matrices is explained in detail including the problem formulation. The second concept examined in this part is CRLB. After the theorem of CRLB is stated, the brief history of performance measures on ETT is summarized.

2.1 Extended Target Tracking

In conventional target tracking, targets are assumed to be points. Therefore, only one measurement is expected for a target in radar plot, when the target is detected. After receiving the measurements, the first task is to decide which measurement belongs to which target, i.e., to make data association. Then by exploiting the associated measurement, the kinematical features, such as position and velocity, are estimated and attributes of a target are deduced with the help of these estimates. There are many well-established algorithms in the literature, for TT is a mature field; and [2] and [3] provide detailed discussions on every aspect of this area.

The progress in the radar technology in recent years led to new research areas in which conventional methods of TT are not applicable. For example, the

point target assumption does not hold any more when one works with a high resolution radar. More than one measurements at a single scan is possible for a target, especially for short-range applications, due to improved radar resolutions. Increased number of measurements which is proportional to the target's size make it possible to estimate not only the kinematical state but also the extension size and orientation of the target. The estimated extension may also cover a group of closely spaced objects. This field of target tracking where multiple measurements are possible for a single target is named as extended target tracking (ETT).

ETT is a newly arising field of research; yet, there exists various methods that deal with it in literature such as multiple hypothesis tracking(MHT), spatial distributions, Bayesian methods with random matrices, so and so forth. One of the earliest papers in this topic belongs to Salmond et al. [4], where the problem of tracking of an elliptic target with a radar that gives range, bearing and along-range target extent measurements is considered. Target length is embedded into the state vector and its contribution to the track maintenance is examined by implementing the extended Kalman filter (EKF), unscented Kalman filter (UKF) and particle filter (PF). In another study conducted by Salmond et al. [5], the extent is modeled as a set of point sources. Moreover, it is assumed that number of measurements arising from the target at a scan is Poisson distributed and these measurements are independent having a spatial probability density function (pdf) which is convolved with the sensor model later. Eventually, a Bayesian filter is derived and implemented with both multiple hypothesis KF and PF.

Track before detect methods are also applied to ETT problems. One may find the application of this approach to a one dimensional extended target in the paper [6] proposed by Boers et al. Nonlinear Kalman filters are also utilized for ETT. One example is Rao-Blackwellised unscented Kalman filter (RBUKF) used by Xu et al. in [7]. In this paper, down-range extent and cross-range extent are included in the state. These static parameters are coupled to kinematical features in a highly nonlinear manner that RBUKF is preferred. The reasons for this choice of the filter were the divergent behavior of EKF and the compu-

tational complexity of UKF. It was seen that RBUKF is immune to divergence problems with a relatively low computational cost.

The study [8] carried out by Angelova et al. utilizes Monte Carlo techniques for an ETT problem with range, bearing and down-range measurements. The kinematical states and extension parameters are estimated separately. Kinematic state estimates are obtained by interacting multiple model (IMM)-KF, whereas Monte Carlo techniques, IMM with data augmentation, mixture KF and IMM-PF are implemented for extension parameter estimation. Angelova et al. concluded that IMM with data augmentation is the most accurate algorithm; however, its computation cost is greater than the others and performance of IMM-PF depends on the parameter selection. Moreover, they claim that "mixture KF provides a reasonable compromise between accuracy and computational time".

Probability hypothesis density filters have also been made use of for ETT. A detailed example is given in [9] by Granström et al. In this work, probability hypothesis density refers to the first-order moment of a random set of target states. Probability hypothesis density filter is implemented by Gaussian mixture approximation. Clustering methods are applied in order to reduce the computational cost. They indicate that tracking performance is quite satisfactory even in a cluttered environment. Moreover, it is claimed by the authors that the algorithm handles closely spaced targets effectively.

2.1.1 ETT with Random Matrices

In this study, a Bayesian approach, which assumes that targets or groups of target have ellipsoidal form represented by positive semi-definite symmetric random matrices, is considered. With this method, the target extent is also a state variable to be estimated using multiple measurements enabling the estimation of size, orientation and aspect ratio of the target.

This approach is first suggested by Koch in [10]. In this paper, a Bayesian estimator is established deriving its recursive equations for all phases of tracking:

prediction, filtering and smoothing. The second paper on this subject [11] belongs to Feldmann et al. In [11], the authors propose an improvement on the measurement model of the previous paper [10], while using the same formulation. The last work considered here is presented by Granström et al. [1]. In this work, a new prediction method is suggested claiming that it is superior to the previous ones. In this section, details of the ETT with random matrices is presented. First of all, notations used throughout this thesis are introduced.

Notations:

- $x_k \in \mathbb{R}^n$ denotes kinematical state at time t_k. It includes of position and velocity components. In this study, only x and y axes are considered. Therefore, the state x_k is a vector with 4 elements, i.e., $n = 4$.
- $X_k \in \mathbb{S}^d$ represents the extension of the target at t_k. X_k is a 2×2 positive definite symmetric matrix, i.e., $d = 2$.
- $\xi_k = (x_k, X_k)$ is the augmented state at time t_k which is the union of x_k and X_k.
- $Y_k = \left\{y_k^i\right\}_{i=1}^{m_k}$ stands for the set of m_k measurements, each named as y_k^i, received at time instant k.
- $Y^k = \{Y_\ell\}_{\ell=0}^{k}$ refers to the set of whole measurements from the initial time instant t_0 to time t_k.
- Multivariate Gaussian pdf for a random variable x with mean μ and Σ is denoted as
$$\mathcal{N}(x; \mu, \Sigma) \triangleq \frac{e^{-\frac{1}{2}(x-\mu)^T \Sigma^{-1}(x-\mu)}}{\sqrt{(2\pi)^n |\Sigma|}}$$
where the random vector $x \in \mathbb{R}^n$.
- Pdf of Wishart distribution for a positive semi-definite random matrix X with degrees of freedom v and scale matrix V is given as
$$\mathcal{W}_d(X; v, V) \triangleq \frac{|X|^{\frac{v-d-1}{2}}}{2^{\frac{vd}{2}} \Gamma_d\left(\frac{v}{2}\right) |V|^{\frac{v}{2}}} e^{\mathrm{tr}\left(-\frac{1}{2}XV^{-1}\right)}$$
where the subscript d ($v \geq d$) indicates that X is a $d \times d$ random matrix, i.e., $X \in \mathbb{S}^d$.

- The inverse Wishart pdf for a positive semi-definite random matrix X with degrees of freedom v and scale matrix Ψ is given as

$$\mathcal{IW}_d(X; v, V) \triangleq \frac{|\Psi|^{\frac{v}{2}}}{2^{\frac{vd}{2}}\Gamma_d\left(\frac{v}{2}\right)|X|^{\frac{v+d+1}{2}}} e^{\mathrm{tr}\left(-\frac{1}{2}\Psi X^{-1}\right)}$$

where the subscript d ($v \geq d$) indicates that X is a $d \times d$ random matrix, i.e., $X \in \mathbb{S}^d$.

2.1.1.1 Formulation

In ETT, multiple measurements are generated by the sensor at each scan. These measurements are independent from each other. According to the measurement model used in [10], measurements are produced from an ellipse whose center is the entries of kinematical state corresponding to position and they are spread to the space in proportion to its extension size and orientation. The likelihood function for a measurement set at a given time is defined by Koch as

$$p(Y_k|x_k, X_k) = \prod_{i=1}^{m_k} \mathcal{N}(y_k^i; Hx_k, X_k) \tag{2.1}$$

where H is the measurement matrix and m_k represents the number of measurements at time k which is possibly random and dependent on the kinematical and extent states at time k, i.e., $m_k = m_k(x_k, X_k)$.

This model neglects the contribution of sensor errors to the spread of the measurements. The absence of measurement error in the model can result in overestimated extension in the presence of large sensor errors. Thus in [11], Feldmann et al. modifies (2.1) so that the effects of the sensor noise on the measurement distribution can be taken into account. The new model is given as

$$p(Y_k|x_k, X_k) = \prod_{i=1}^{m_k} \mathcal{N}(y_k^i; Hx_k, sX_k + R) \tag{2.2}$$

where s is a scaling factor and R is the measurement error covariance matrix.

The posterior pdf of the augmented state is then expressed in [10] and [11] as

$$\begin{aligned} p(\xi_k|Y^k) &= p(x_k|X_k, Y^k)p(X_k|Y^k), \\ &\approx p(x_k|Y^k)p(X_k|Y^k), \\ &= \mathcal{N}(x_k; \mu_{k|k}, \Sigma_{k|k})\mathcal{IW}(X_k; v_{k|k}, V_{k|k}). \end{aligned} \tag{2.3}$$

It is worth to remind that the state ξ_k is the concatenation of kinematical state and extension.

The predicted pdf for the augmented state is derived as below in [10].

$$p(\xi_k|Y^{k-1}) = \int p(\xi_k|\xi_{k-1}, Y^{k-1})p(\xi_{k-1}|Y^{k-1})dx_{k-1}dX_{k-1}, \tag{2.4}$$

$$= \int p(x_k|X_k, \xi_{k-1}, Y^{k-1})p(X_k|x_{k-1}, X_{k-1}, Y^{k-1})p(\xi_{k-1}|Y^{k-1})dx_{k-1}dX_{k-1}, \tag{2.5}$$

$$= \int p(x_k|X_k, x_{k-1})p(X_k|X_{k-1})p(\xi_{k-1}|Y^{k-1})dx_{k-1}dX_{k-1}. \tag{2.6}$$

The last term in the integral (2.6) is the posterior pdf for the previous time instant. Note that while obtaining (2.6) from (2.5), there are some assumptions made. First of all, the process is assumed to be Markovian. Additionally, the kinematical state should not depend on the previous extension so that the following equality can be written.

$$p(x_k|X_k, \xi_{k-1}, Y^{k-1}) = p(x_k|X_k, x_{k-1}). \tag{2.7}$$

The final assumption regarding this derivation is that the extension evolves independently from the previous kinematical state so that the following equality holds.

$$p(X_k|x_{k-1}, X_{k-1}, Y^{k-1}) = p(X_k|X_{k-1}). \tag{2.8}$$

As indicated by Granström et al. in [1], this assumption is valid for some models such as constant velocity or constant acceleration. Yet, it turns out to be untrue for some other models; for instance, the coordinated-turn model. This is the main motivation for Granström et al.'s paper [1], that suggests a prediction update model valid for extension evolutions depending on the kinematic state.

The transition pdfs for the prediction are defined in [11] by Feldmann et. al. and in [10] by Koch as follows.

$$p(x_{k+1}|x_k) = \mathcal{N}(x_{k+1}; f(x_k), Q_{k+1}), \tag{2.9}$$

$$p(X_{k+1}|X_k) = \mathcal{W}\left(X_{k+1}; n_{k+1}, \frac{X_k}{n_{k+1}}\right), \tag{2.10}$$

where Q_{k+1} is the process noise covariance matrix and $f(\cdot)$ is state transition function. Whereas, the following version is proposed by Granström et al. in [1] so that extension can evolve depending on the kinematical state.

$$p(X_{k+1}|x_k, X_k) = \mathcal{N}\left(X_{k+1}; n_{k+1}, \frac{M_{x_k} X_k M_{x_k}^T}{n_{k+1}}\right) \tag{2.11}$$

where M_{x_k} is an invertible matrix function of the kinematic state x_k. The steps of the estimator proposed in [11] is given below. ETT algorithm whose performance is going to be compared to CRLB in this study is implemented according to this description.

Prediction Update:

$$x_{k+1|k} = f(x_{k|k}) \tag{2.12}$$

$$P_{k+1|k} = F P_{k|k} F + Q \tag{2.13}$$

$$X_{k+1|k} = X_{k|k} \tag{2.14}$$

$$\alpha_{k+1|k} = 2 + \exp(-T/\tau)(\alpha_{k|k} - 2) \tag{2.15}$$

where F is the Jacobian of $f(\cdot)$ and $\alpha_{k|k} = n_{k|k} - d - 1$.

Measurement Update:

$$x_{k+1|k+1} = x_{k+1|k} + K_{k+1|k}(\bar{y}_{k+1} - H x_{k+1|k}), \tag{2.16}$$

$$P_{k+1|k+1} = P_{k+1|k} - K_{k+1|k} S_{k+1|k} K_{k+1|k}^T, \tag{2.17}$$

$$X_{k+1|k+1} = \frac{1}{\alpha_{k+1|k+1}}\left(\alpha_{k+1|k} X_{k+1|k} + \hat{N}_{k+1|k} + \hat{Y}_{k+1|k}\right), \tag{2.18}$$

$$\alpha_{k+1|k+1} = \alpha_{k+1|k} + n_{k+1}, \tag{2.19}$$

where

$$\bar{y}_{k+1} = \frac{1}{n_{k+1}} \sum_{i=1}^{m_{k+1}} y_{k+1}^{i}, \tag{2.20}$$

$$S_{k+1|k} = H P_{k+1|k} H^T + \frac{Y_{k+1|k}}{n_{k+1}}, \tag{2.21}$$

$$K_{k+1|k} = P_{k+1|k} H^T S_{k+1|k}^{-1}, \tag{2.22}$$

$$Y_{k+1|k} = s X_{k+1|k} + R, \tag{2.23}$$

$$\bar{Y}_{k+1} = \sum_{i=1}^{m_{k+1}} \left(y_{k+1}^{i} - \bar{y}_{k+1}\right) \left(y_{k+1}^{i} - \bar{y}_{k+1}\right)^T, \tag{2.24}$$

$$N_{k+1|k} = \left(\bar{y}_{k+1} - H x_{k+1|k}\right) \left(\bar{y}_{k+1} - H x_{k+1|k}\right)^T, \tag{2.25}$$

$$\hat{N}_{k+1|k} = X_{k+1|k}^{1/2} S_{k+1|k}^{-1/2} N_{k+1|k} \left(S_{k+1|k}^{-1/2}\right)^T \left(X_{k+1|k}^{1/2}\right)^T, \tag{2.26}$$

$$\hat{Y}_{k+1|k} = X_{k+1|k}^{1/2} Y_{k+1|k}^{-1/2} \bar{Y}_{k+1} \left(Y_{k+1|k}^{-1/2}\right)^T \left(X_{k+1|k}^{1/2}\right)^T. \tag{2.27}$$

Note that $X_{k+1|k}^{-1/2}$ is defined as follows.

$$X_{k+1|k} = X_{k+1|k}^{1/2} \left(X_{k+1|k}^{-1/2}\right)^T. \tag{2.28}$$

2.2 Cramér-Rao Lower Bound

Estimation theory is developed with the aim of inferring some set of parameters using measurements. Its area of interest includes systems from a wide range of subjects such as control, communications, image processing, radar and so forth [12]. It is desired to estimate the parameter as accurately as possible, which brings the necessity to establish some performance measures on the estimator.

2.2.1 Parametric Cramér-Rao Lower Bound

Parametric (or deterministic) Cramér-Rao Lower Bound (CRLB) is one of the performance measures setting a limit on the achievable estimator performance. In fact, it defines a lower bound on the mean-square-error (MSE) that an unbiased estimator of a deterministic parameter can accomplish. Therefore, performances of different estimators can be compared by examining the closeness of

MSE of an estimator to this bound. The closer the result to the bound, the better the performance of the estimator is. Furthermore, if the CRLB is attained by MSE for an estimator, then the estimator is said to be efficient.

Before presenting the theorem for parametric CRLB, the definitions for an unbiased estimator and the score function are given using [12].

Definition 1. *An estimate $\hat{x}(y)$ of a deterministic parameter $x \in \mathbb{R}^{n_x}$ based on the random measurements $y \in \mathbb{R}^{n_y}$ is unbiased if and only if*

$$E\left[\hat{x}(y)|x\right] = x \qquad \forall x. \tag{2.29}$$

■

Definition 2. *The score function, $S(\cdot,\cdot)$, is the gradient, with respect to some vector of parameters x, of the logarithm of the likelihood function.*

$$S(y,x) \triangleq \nabla_x \log p(y|x) \tag{2.30}$$

where $\nabla_x \triangleq \left[\begin{array}{ccc} \dfrac{\partial}{\partial x_1} & \dfrac{\partial}{\partial x_2} & \cdots \dfrac{\partial}{\partial x_{n_x}} \end{array}\right]^T$ *denotes the gradient operator.* ■

Now that the expressions above are presented, the theorem of parametric CRLB for a deterministic parameter $x \in \mathbb{R}^{n_x}$ is given as follows.

Theorem 1 (Adopted from Theorem 3.1 from [12])**.** *It is assumed that the likelihood $p(y|x)$ satisfies the regularity condition*

$$E\left[\nabla_x \log p(y|x)\right] = 0, \quad \forall x. \tag{2.31}$$

Then, the covariance matrix of any unbiased estimator $\hat{x}(y)$ of the deterministic parameter x based on the measurement y must satisfy

$$\mathrm{cov}(\hat{x}(y)) \geq \left(E\left[-\Delta_x^x \log p(y|x)\right]\right)^{-1} \tag{2.32}$$

where the notation Δ_x^s denote the Hessian operation, i.e., $\Delta_x^s = \nabla_x \nabla_s^T$, and the derivatives inside the expectation are evaluated at the true value of x. The right hand side of (2.32) is called as the parametric CRLB of the parameter x and shown as $\mathcal{J}^x$. ■

The matrix $E\left[-\Delta_x^x \log p(y|x)\right]$ in (2.32) is named as Fisher information matrix (FIM) and it is a measure of information that the measurement y conveys about the estimated parameter x. We show the Fisher information matrix as $\mathcal{I}^x$. Note that for some problems, finding the second order derivatives in (2.32) may be a pretty cumbersome task. To overcome this problem, following property from [12] can be used.

Property 1. *The following equality is satisfied.*

$$E\left[-\Delta_x^x \log p(y|x)\right] = E\left[\nabla_x \log p(y|x) \nabla_x^T \log p(y|x)\right]. \tag{2.33}$$

■

The last property given below is related to how to find the parametric CRLB of a function of a parameter whose parametric CRLB is known.

Property 2. *If $z = g(x)$ is to be estimated, where $g(\cdot)$ is, in general, a nonlinear function, then the parametric CRLB for z can be found from the parametric CRLB for x as follows*

$$\mathcal{J}^z \geq \nabla_x^T g(x) \mathcal{J}^x \nabla_x g(x). \tag{2.34}$$

where the notation $\nabla_x g(\bar{x})$ denotes the Jacobian of the vector valued function $g(\cdot)$ evaluated at the value $\bar{x}$. ■

2.2.2 Posterior Cramér-Rao Lower Bound

Posterior (Bayesian) CRLB is the random parameter counterpart of parametric CRLB. In this case, the estimated parameter x is random; therefore, it has a prior distribution. The posterior CRLB is much more powerful than parametric CRLB, since it gives a lower bound on the mean square error (MSE) of any estimator, i.e., not only the unbiased estimators like the parametric CRLB. The posterior CRLB is defined in the following theorem.

Theorem 2 (Adopted from Equation 217 of [13])**.** *The MSE matrix of any estimator $\hat{x}(y)$ of the random parameter x satisfies*

$$\mathrm{MSE}(\hat{x}(y)) \geq \left(E\left[-\Delta_x^x \log p(y,x)\right]\right)^{-1} \tag{2.35}$$

The right hand side of (2.35) *is called as the posterior CRLB of the parameter* x *and shown as* $\tilde{\mathcal{J}}_x$. ■

The differences between the expressions for the parametric and posterior CRLBs, i.e., between (2.32) and (2.35), are listed as follows:

- In (2.32) the score function, i.e., the derivatives of the logarithm of the likelihood, is used while in (2.35) the logarithm of the joint density (of the parameter and the measurement) is used.
- The expectation in (2.32) is with respect to only the measurement y (since the parameter x is deterministic) while the expectation in (2.32) is with respect to both the measurement y and the parameter x.

A similar property to Property 1 holds also for the random parameter case as below.

Property 3. *The following equality is satisfied.*

$$E\left[-\Delta_x^x \log p(y,x)\right] = E\left[\nabla_x \log p(y,x) \nabla_x^T \log p(y,x)\right]. \tag{2.36}$$

■

The random parameter counterpart for Property (2) is given as follows.

Property 4 (Adopted from Section 1.2.8.2 of [14])**.** *If* $z = g(x)$ *is to be estimated, where* $g(\cdot)$ *is, in general, a nonlinear function, then the posterior CRLB for* z *can be found from the posterior CRLB for* x *as follows*

$$\tilde{\mathcal{J}}^z \geq E\left[\nabla_x^T g(x)\right] \tilde{\mathcal{J}}^x E\left[\nabla_x g(x)\right]. \tag{2.37}$$

where the notation $\nabla_x g(\bar{x})$ *denotes the Jacobian of the function* $g(\cdot)$ *evaluated at* $\bar{x}$. ■

2.3 Literature Research on Performance Measures on Extended Target Tracking

ETT is a relatively new area with various algorithms suggested, and more is revealing. In order to evaluate the performances of these techniques, some per-

formance measure studies exist in the literature. Papers related to some of these works are surveyed in this section.

The first study was conducted by Ristic et al. in [15]. The scenario here is an elliptical target moving in a way that the angle between the major axis of the target and the target-observer line of sight (LOS) remains constant throughout the scenario. The joint state vector includes the target length and the ratio of minor and major axes of the ellipse as well as the kinematical features. The sensor provides the measurements of range, bearing and target extent along the LOS. The system dynamics is a linear one; however, the measurement equation is highly nonlinear due to the relationship between the states and the target extent. In this study, posterior CRLB is used to evaluate the performance. The authors first investigate the change in posterior CRLB with respect to the changes in each element of the state. Later, they implement EKF and UKF and compare their performance to posterior CRLB. Finally, they conclude that these filters are not satisfactory in terms of extent estimation due to high nonlinearity.

A different version of CRLB is offered by Xu et al. in the study [16]. The so-called hybrid CRLB (HCRLB) was developed to investigate the performance of the algorithms for ground moving extended targets with high range resolution ground moving target indicator. In the scenario of [16], the targets are modelled as rectangles; and range, bearing, Doppler and down-range extent measurements are collected with a radar. The authors give a performance measure on the estimation of the state vector which consists of the kinematical state and deterministic parameters: length and width of the extent rectangle. As the state vector includes both random variables and deterministic parameters, Xu et al. suggest to use the recursive HCRLB that handles both types of variables. They examine the effects of changing the uncertainty in the state elements on the HCRLB behavior. However, they do not implement any estimator to analyze the performance using HCRLB.

The third work which belongs to Zhong et al. [17] makes a comparison between the performance bounds for point TT and ETT with the aid of posterior CRLB. In this paper, system and measurement models are the same as those in [15]. The

contribution of extension information coming in the form of down-range extent measurements to the kinematic estimation, i.e., to the estimation of the center of the ellipse, is investigated. The authors make the following assumptions claiming that they are valid premises most of the time: States in point TT are elements of the state vector in ETT, representing kinematical features. Furthermore, the dynamics of the kinematic states in ETT is the same as those in point TT. Finally, it is accepted that the measurements related to the extension are correlated to the kinematical measurements; however, vice versa is not true. Under these assumptions, recursive posterior CRLB equations are derived for both ETT and point TT. As a result, posterior CRLB for ETT turns out to be smaller than that of point TT.

In another study [17], Zhang et al. extend their work by examining posterior CRLB for two different ETT models in [18]. The first model is the one that is used in [17]. The authors derive posterior CRLB for both ETT and point TT with this model, and concluded that the information carried by extent measurements reduces the velocity error bound drastically. Moreover, they find out that posterior CRLB for ETT is better than that for point TT in terms of kinematical states. The other model covered in the paper is the spatial probability distribution model where multiple independent measurements are expected at a scan due to the high resolution of the sensor. The measurement number is random and they are distributed in space independently. Radar supplies range and azimuth angle measurements. Here in posterior CRLB calculation, the unknown measurement number is involved in the equations and it is averaged out via the Extended Information Reduction Factor method. Complicated expectations are handled with Monte Carlo integration. It turns out that the more measurements are obtained, the more information is gathered about the states, which leads to more accurate estimates. In addition, when the mean of the number of measurements is one, ETT results coincide with that of point TT. Thus, for these two models, it is understood that ETT is superior to point TT.

The last piece of research that is discussed here belongs to Meng et al. [19]. The system dynamics and measurements are modelled as in [17]; whereas, comparison of ETT and point TT is made under the existence of clutter and missed detec-

tions. Deriving posterior CRLB under these conditions is a more tricky problem, for the contribution of measurement uncertainty to the bound is obscure. This problem is handled with three methods: information reduction factor, measurement sequence conditioning and measurement existence sequence conditioning. When these techniques are compared, and it is seen that posterior CRLB of information reduction factor becomes the smallest, and the measurement sequence conditioning yields the greatest bound. Again, posterior bounds for ETT are smaller than point TT.

As it can be seen, there is not much work on performance measures for ETT, let alone on ETT with random matrices. Therefore, parametric and posterior CRLB's derived in this thesis that enables the performance evaluation of Bayesian ETT techniques are rather novel.

CHAPTER 3

PARAMETRIC CRAMÉR-RAO LOWER BOUND FOR EXTENDED TARGET TRACKING

Parametric Cramér-Rao lower bound is the first type of CRLB derived for ETT in this study. The chapter is organized as follows. First the parametric CRLB for dynamic systems is defined in Section 3.1. Then the Fisher information matrix required for the parametric CRLB recursion is obtained in Section 3.2. The chapter continues with a discussion of initialization of the parametric CRLB recursion in Section 3.3. In Section 3.4, the chapter is concluded with parametric CRLB expressions for semi-major and semi-minor axes of the extension.

3.1 Parametric Cramér-Rao Lower Bound for Dynamic Systems

Parametric CRLB assumes that the parameter, i.e., the state vector in this case, is deterministic and it is defined only for unbiased estimators. Therefore, parametric CRLB is defined for only dynamic systems with no process noise and initial state uncertainty. We consider the following state space representation.

$$\xi_{k+1} = f(\xi_k), \tag{3.1}$$

$$y_k|\xi_k \sim p(y_k|\xi_k) \tag{3.2}$$

where

- $\xi_k \in \mathbb{R}^{n_\xi}$ is the state vector of the dynamic system;
- $f(\cdot)$ is, in general, a nonlinear differentiable function;

- $p(y_k|\xi_k)$ is a known likelihood function for the measurements $y_k \in \mathbb{R}^{n_y}$.

Then, the parametric CRLB $\mathcal{J}_{k|k}$ for any unbiased estimate $\hat{\xi}_{k|k}$ for ξ_k is defined using the following recursion.

$$\mathcal{J}_{0|-1} = \bar{J}_0 \tag{3.3}$$

$$\mathcal{J}_{k|k} = \left(\mathcal{J}_{k|k-1}^{-1} + \mathcal{I}_k\right)^{-1} \tag{3.4}$$

$$\mathcal{J}_{k+1|k} = F_k \mathcal{J}_{k|k} F_k^T \tag{3.5}$$

where $\bar{J}_0$ is a fixed covariance matrix representing an initial estimate for the augmented state ξ_0; the matrix $F_k \triangleq \nabla_{\xi_k}^T f(\xi_k)$ is the Jacobian matrix of the state transition function $f(\cdot)$ evaluated at the true value of the state ξ_k. $\mathcal{I}_k$ is the Fisher information matrix at time k which is defined as

$$\mathcal{I}_k = E\left[\nabla_{\xi_k} \log p(y_k|\xi_k) \nabla_{\xi_k}^T \log p(y_k|\xi_k)\right]. \tag{3.6}$$

In the next section, the expressions for the FIM $\mathcal{I}_k$ are obtained considering the problem definition of ETT in the random matrix framework given in Section 2.1.1.1.

3.2 Fisher Information Matrix for ETT

In this section, we derive the expressions for the FIM $\mathcal{I}_k$ defined in (3.6). We consider the augmented state vector ξ_k which is composed of the kinematic state x_k and the extension state X_k as follows.

$$\xi_k \triangleq \begin{bmatrix} \xi_k^x \\ \xi_k^X \end{bmatrix} \tag{3.7}$$

where

$$\xi_k^x \triangleq x_k, \tag{3.8}$$

$$\xi_k^X \triangleq \begin{bmatrix} [X_k]_{11} & [X_k]_{12} & [X_k]_{22} \end{bmatrix}^T. \tag{3.9}$$

Note here that since X_k is a symmetric matrix, we have the equality $[X_k]_{12} = [X_k]_{21}$. Therefore, the extent component ξ_k^X of the augmented state vector ξ_k

contains only $[X_k]_{12}$ and is three dimensional. The likelihood function $p(Y_k|x_k, X_k)$ is written as

$$p(Y_k|x_k, X_k) = \prod_{i=1}^{m_k} \mathcal{N}(y_k^i; Hx_k, sX_k + R) \tag{3.10}$$

where it should be reminded that m_k represents the number of measurements at time k which is possibly random and dependent on the kinematical and extent states at time k, i.e., $m_k = m_k(x_k, X_k)$. The likelihood function $p(Y_k|\xi_k)$ for the augmented state can be obtained from $p(Y_k|x_k, X_k)$ by making the following substitutions into $p(Y_k|x_k, X_k)$.

$$x_k \leftarrow \xi_k^x, \tag{3.11}$$

$$X_k \leftarrow \begin{bmatrix} [\xi_k^X]_1 & [\xi_k^X]_2 \\ [\xi_k^X]_2 & [\xi_k^X]_3 \end{bmatrix}. \tag{3.12}$$

The score function $\nabla_{\xi_k} p(Y_k|\xi_k)$ will be obtained using the derivatives of the log-likelihood $\log p(Y_k|x_k, X_k)$ with respect to the state variables x_k and X_k defined below.

$$S_x \triangleq \nabla_x \log p(Y_k|x_k, X_k), \tag{3.13}$$

$$S_X \triangleq \nabla_X \log p(Y_k|x_k, X_k). \tag{3.14}$$

where it is emphasized here that S_x is a vector of the same size as x while S_X is a matrix with the same size as X.

3.2.1 Score Function

In the remaining parts of this chapter, the measurements and states only at a single time instant k are considered. Hence, the subscripts k in the variables are all omitted for the sake of brevity.

The log-likelihood function $\log p(Y|x, X)$ is given as

$$\log p(Y|x, X) = \sum_{p=1}^{m} \log \mathcal{N}(y^p; Hx, sX + R)) \tag{3.15}$$

$$= \sum_{p=1}^{m} -\frac{1}{2}(y^p - Hx)^T (sX + R)^{-1}(y^p - Hx) - \frac{m}{2} \log |sX + R| \tag{3.16}$$

up to an additive constant independent of both x and X. The right hand side of the expression (3.16) consists of two terms which will be called $I_1(\cdot,\cdot)$ and $I_2(\cdot)$ from now on in this section. These terms are defined as

$$I_1(x,X) \triangleq -\frac{1}{2}\sum_{p=1}^{m}(y^p - Hx)'(sX+R)^{-1}(y^p - Hx) \tag{3.17}$$

$$I_2(X) \triangleq -\frac{m}{2}\log|sX+R| \tag{3.18}$$

In order to calculate the derivatives of $I_1(\cdot,\cdot)$ with respect to x, following property from [20] is utilized.

Property 5.

$$\frac{\partial(bx+c)^T D(bx+c)}{\partial x} = b^T(D+D^T)(bx+c). \tag{3.19}$$

■

This property yields the result below.

$$\frac{\partial I_1}{\partial x}(x,X) = H^T(sX+R)^{-1}\sum_{p=1}^{m}(y^p - Hx). \tag{3.20}$$

In order to take the derivative of $I_1(\cdot,\cdot)$ with respect to X, we first bring $I_1(\cdot,\cdot)$ into the following form.

$$\begin{aligned} I_1(x,X) &= -\frac{1}{2}\sum_{p=1}^{m}(y^p - Hx)^T(sX+R)^{-1}(y^p - Hx) \\ &= -\frac{1}{2}\sum_{p=1}^{m}\mathrm{tr}\left[(sX+R)^{-1}(y^p - Hx)(y^p - Hx)^T\right] \\ &= -\frac{1}{2}\sum_{t=1}^{2}\sum_{u=1}^{2}\left[(sX+R)^{-1}\right]_{tu}\left[\sum_{p=1}^{m}(y^p - Hx)(y^p - Hx)^T\right]_{tu} \end{aligned} \tag{3.21}$$

The derivative of inverse of a matrix with respect to its elements is given by property taken from [20] below.

Property 6.

$$\frac{\partial\left[X^{-1}\right]_{tu}}{\partial X_{kl}} = -\left[X^{-1}\right]_{tk}\left[X^{-1}\right]_{lu} \tag{3.22}$$

where the notations Σ_{ij} and $[\Sigma]_{ij}$ both denote the element of the argument matrix Σ corresponding to the ith row and the jth column. ■

Using this property, the derivative of $I_1(\cdot,\cdot)$ with respect to $[sX+R]_{kl}$ is given as follows.

$$\frac{\partial I_1}{\partial [sX+R]_{kl}}(x,X) = \frac{1}{2}\sum_{t=1}^{2}\sum_{u=1}^{2}\left[(sX+R)^{-1}\right]_{tk}\left[(sX+R)^{-1}\right]_{lu} \times \left[\sum_{p=1}^{m}(y^p-Hx)(y^p-Hx)^T\right]_{tu} \tag{3.23}$$

Hence, we can write the derivative of $I_1(\cdot,\cdot)$ with respect to X_{kl} using the chain rule as follows

$$\frac{\partial I_1}{\partial X_{kl}}(x,X) = \sum_{i=1}^{2}\sum_{j=1}^{2}\frac{\partial I_1}{\partial [sX+R]_{ij}}\frac{\partial [sX+R]_{ij}}{\partial X_{kl}} \tag{3.24}$$

$$= s\frac{\partial I_1}{\partial [sX+R]_{kl}} \tag{3.25}$$

$$= \frac{s}{2}\sum_{t=1}^{2}\sum_{u=1}^{2}\left[(sX+R)^{-1}\right]_{tk}\left[\sum_{p=1}^{m}(y^p-Hx)(y^p-Hx)^T\right]_{tu}\left[(sX+R)^{-1}\right]_{lu}$$

$$= \frac{s}{2}\sum_{t=1}^{2}\sum_{u=1}^{2}\left[(sX+R)^{-1}\right]_{kt}\left[\sum_{p=1}^{m}(y^p-Hx)(y^p-Hx)^T\right]_{tu}\left[(sX+R)^{-1}\right]_{ul}$$

$$= \frac{s}{2}\left[(sX+R)^{-1}\left(\sum_{p=1}^{m}(y^p-Hx)(y^p-Hx)^T\right)(sX+R)^{-1}\right]_{kl} \tag{3.26}$$

where we used the facts that

$$\frac{\partial [sX+R]_{ij}}{\partial X_{kl}} = \begin{cases} s, & \text{if } i=k \text{ and } j=l \\ 0, & \text{otherwise} \end{cases}, \tag{3.27}$$

and $sX+R$ is symmetric.

We now consider the second term in the log-likelihood function, $I_2(\cdot)$, which is independent of x. We have

$$\frac{\partial I_2}{\partial x}(X) = 0. \tag{3.28}$$

To be able to take the derivative of $I_2(\cdot)$ with respect to X, the following rule from [20] is employed.

Property 7.

$$\frac{\partial \log|X|}{\partial X_{ij}} = [X^{-1}]_{ji}. \tag{3.29}$$

■

Using (3.29), the derivative is found as below.

$$\begin{aligned}\frac{\partial I_2}{\partial X_{ij}}(X) &= -\frac{\partial\left(0.5m\log|sX+R|\right)}{\partial\left[sX+R\right]_{ij}}\frac{\partial\left[sX+R\right]_{ij}}{\partial X_{ij}} \\ &= -0.5sm\left[(sX+R)^{-1}\right]_{ji} \end{aligned} \tag{3.30}$$

which gives

$$\frac{\partial I_2}{\partial X}(X) = -0.5sm\,(sX+R)^{-1} \tag{3.31}$$

since $sX+R$ is a symmetric matrix. Overall results for the derivatives S_x and S_X are given below.

$$S_x = \frac{\partial I_1}{\partial x}(x,X) + \frac{\partial I_2}{\partial x}(X), \tag{3.32}$$

$$S_X = \frac{\partial I_1}{\partial X}(x,X) + \frac{\partial I_2}{\partial X}(X). \tag{3.33}$$

Using the results presented above, we get

$$S_x = H^T(sX+R)^{-1}\sum_{p=1}^{m}(y^p - Hx), \tag{3.34}$$

$$\begin{aligned} S_X =& \frac{s}{2}(sX+R)^{-1}\left(\sum_{p=1}^{m}(y^p-Hx)(y^p-Hx)^T\right)(sX+R)^{-1} \\ &- 0.5sm(sX+R)^{-1}. \end{aligned} \tag{3.35}$$

It should be reminded here that S_x is a vector of the same size as x while S_X is a matrix with the same size as X. Note that ξ_k defined in (3.7) is composed of $\xi_k^x \triangleq x_k$ and ξ_k^X given in (3.9). Therefore, the gradient of the likelihood $p(Y|\xi)$ with respect to ξ, which we call as S_ξ is given as

$$S_\xi \triangleq \nabla_\xi p(Y|\xi) = \begin{bmatrix} \nabla_x \log p(Y|\xi) \\ \nabla_{\xi^X} \log p(Y|\xi) \end{bmatrix} = \begin{bmatrix} S_x \\ S_{\xi^X} \end{bmatrix}. \tag{3.36}$$

where

$$S_{\xi^X} \triangleq \nabla_{\xi^X} \log p(Y|\xi). \tag{3.37}$$

Since the matrix X is symmetric, we have the constraint $[X]_{12} = [X]_{21}$. Under this constraint, we have

$$S_{\xi^X} = \begin{bmatrix} [S_X]_{11} \\ [S_X]_{12} + [S_X]_{21} \\ [S_X]_{22} \end{bmatrix} \tag{3.38}$$

where the summation in the second derivative comes from the chain rule under the constraint $[X]_{12} = [X]_{21}$.

3.2.2 Fisher Information Matrix

Once the score function is obtained, the expected values have to be calculated. The FIM, $\mathcal{I}_k$, defined in (3.6) is given as

$$\mathcal{I}_k \triangleq E[\nabla_\xi \log p(Y|\xi) \nabla_\xi^T \log p(Y|\xi)] \tag{3.39}$$

$$= \begin{bmatrix} E\left[S_x S_x^T\right] & E\left[S_x S_{\xi^X}^T\right] \\ E\left[S_{\xi^X} S_x^T\right] & E\left[S_{\xi^X} S_{\xi^X}^T\right] \end{bmatrix}. \tag{3.40}$$

We are now going to calculate the partitions of $\mathcal{I}_k$ one by one below.

- **Calculation of $E\left[S_x S_x^T\right]$:**

$$S_x S_x^T = H^T (sX + R)^{-1} \sum_{p=1}^{m} (y^p - Hx) \sum_{p=1}^{m} (y^p - Hx)^T (sX + R)^{-1} H. \tag{3.41}$$

  Taking the expected values of both sides given m, we obtain

$$E[S_x S_x^T | m] = H^T (sX + R)^{-1} E\left[\sum_{p=1}^{m} (y^p - Hx) \sum_{p=1}^{m} (y^p - Hx)^T \middle| m \right] \times (sX + R)^{-1} H \tag{3.42}$$

$$= H^T (sX + R)^{-1} m (sX + R)(sX + R)^{-1} H \tag{3.43}$$

$$= m H^T (sX + R)^{-1} H \tag{3.44}$$

  where we used the fact that the measurements $\{y^p\}_{p=1}^m$ are distributed as $y^p \sim \mathcal{N}(Hx, sX + R)$ and they are independent. If we take the expected value of both sides of (3.44) with respect to m, we get

$$E[S_x S_x^T] = \bar{m} H^T (sX + R)^{-1} H \tag{3.45}$$

  where $\bar{m}$ is the expected value of the number of measurements, i.e., $\bar{m} \triangleq E[m]$, which can be a function of the true states x and X, i.e., $\bar{m} = \bar{m}(x, X)$.

- **Calculation of $E\left[S_x S_{\xi^X}^T\right]$:** Due to the definition of the gradient S_ξ^X given in (3.38), this expectation involves the expectation of the terms of the form $[S_x]_j[S_X]_{kl}$. We can write these terms as the multiplication $e_j^T S_x e_k^T S_X e_l$ where each of e_j, e_k and e_l is a column vector composed of all zeros except for its jth entry which is equal to unity. Note that with the extended target state definitions, the possible values for j and k, l are $j = 1, \ldots, 4$ and $k, l = 1, \ldots, 2$, respectively. As a result, defining $B \triangleq (sX + R)^{-1}$, we can write $[S_x]_j[S_X]_{kl}$

$$
\begin{aligned}
[S_x]_j[S_X]_{kl} &= e_j^T S_x e_k^T S_X e_l && (3.46)\\
&= [S_x e_k^T S_X]_{jl} && (3.47)\\
&= \Bigg[H^T B \sum_{p=1}^{m} (y^p - Hx) \\
&\quad \times e_k^T \left(-0.5smB + 0.5sB \sum_{r=1}^{m} (y^r - Hx)(y^r - Hx)^T B \right) \Bigg]_{jl} \\
&= -0.5sm \left[H^T B \sum_{p=1}^{m} (y^p - Hx) e_k^T B \right]_{jl} \\
&\quad + 0.5s \left[H^T B \sum_{p=1}^{m} (y^p - Hx) e_k^T B \sum_{r=1}^{m} (y^r - Hx)(y^r - Hx)^T B \right]_{jl}. && (3.48)
\end{aligned}
$$

Taking the expected values of both sides given m, we get

$$
\begin{aligned}
E\left[\left[S_x \cdot e_k^T S_X \right]_{jl} \middle| m \right] &= -0.5sm \left[H^T B E \left[\sum_{p=1}^{m} (y^p - Hx) \middle| m \right] e_k^T B \right. \\
&\quad \left. + 0.5s H^T B E \left[\sum_{p=1}^{m} (y^p - Hx) e_k^T \sum_{r=1}^{m} (y^r - Hx)(y^r - Hx)^T \middle| m \right] B \right]_{jl}. && (3.49)
\end{aligned}
$$

Since we have $E[y^p - Hx|m] = E[y^p - Hx] = 0$, the first term of the right hand side of (3.49) vanishes. Hence we have

$$
\begin{aligned}
&E\left[\left[S_x \cdot e_k^T S_X \right]_{jl} \middle| m \right] \\
&= 0.5s \left[H^T B E \left[\sum_{p=1}^{m} (y^p - Hx) e_k^T B \sum_{r=1}^{m} (y^r - Hx)(y^r - Hx)^T \middle| m \right] B \right]_{jl} && (3.50)
\end{aligned}
$$

$$= 0.5s \left[H^T B E \left[\sum_{p=1}^{m} \sum_{r=1}^{m} (y^p - Hx) e_k^T B (y^r - Hx)(y^r - Hx)^T \middle| m \right] B \right]_{jl} \tag{3.51}$$

$$= 0.5s \left[H^T B \sum_{p=1}^{m} \sum_{r=1}^{m} E\left[(y^p - Hx) e_k^T B (y^r - Hx)(y^r - Hx)^T \middle| m \right] B \right]_{jl}. \tag{3.52}$$

When $p \neq r$, due to the independence of the measurements, the expectation inside the summation above should be zero. Hence, we have

$$E\left[\left[S_x \cdot e_k^T S_X \right]_{jl} \middle| m \right] = 0.5s \left[H^T B \sum_{r=1}^{m} E\left[(y^r - Hx) e_k^T B (y^r - Hx)(y^r - Hx)^T \middle| m \right] B \right]_{jl}. \tag{3.53}$$

Inside the expectation above, we have third-order central moments of a Gaussian random variable which are zero. As a result, we have

$$E\left[\left[S_x \cdot e_k^T S_X \right]_{jl} \middle| m \right] = 0 \tag{3.54}$$

for $j = 1, \ldots, 4$, $k, l = 1, 2$ and for all m. As a result, we get

$$E\left[S_x S_{\xi^X}^T \right] = 0. \tag{3.55}$$

- **Calculation of $E\left[S_{\xi^X} S_x^T \right]$:** This term is the transpose of the term $E\left[S_x S_{\xi^X}^T \right]$, hence we have

$$E\left[S_{\xi^X} S_x^T \right] = 0. \tag{3.56}$$

- **Calculation of $E\left[S_{\xi^X} S_{\xi^X}^T \right]$:** Considering the definition of the gradient S_{ξ^X} in (3.38), the matrix $E\left[S_{\xi^X} S_{\xi^X}^T \right]$ can be obtained as follows.

$$E\left[S_{\xi^X} S_{\xi^X}^T \right] = \begin{bmatrix} d_{11,11} & d_{11,12} + d_{11,21} & d_{11,22} \\ d_{12,11} + d_{21,11} & \begin{matrix} d_{12,12} + d_{12,21} \\ + d_{21,12} + d_{21,22} \end{matrix} & d_{12,22} + d_{21,22} \\ d_{22,11} & d_{22,12} + d_{22,21} & d_{22,22} \end{bmatrix}. \tag{3.57}$$

where

$$d_{ij,kl} \triangleq E\left[[S_X]_{ij}[S_X]_{kl}\right]. \tag{3.58}$$

Hence, we have to calculate the expectation of the terms of the form $[S_X]_{ij}[S_X]_{kl}$. We can write these terms as the multiplication $e_i^T S_X e_j e_k^T S_X e_l = [S_X e_j e_k^T S_X]_{il}$ where each of e_i, e_j, e_k and e_l is a column vector composed of all zeros except for its jth entry which is equal to unity. Note that with the extended target state definitions, the possible values for i, j and k, l are $i, j = 1, \ldots, 4$ and $k, l = 1, \ldots, 2$, respectively. As a result, defining $B \triangleq (sX + R)^{-1}$, we can write

$$\begin{aligned}
S_X e_j e_k^T S_X^T =& \left(-0.5smB + 0.5sB\sum_{p=1}^{m}(y^p - Hx)(y^p - Hx)^T B\right) \\
&\times e_j e_k^T \left(-0.5smB + 0.5sB\sum_{r=1}^{m}(y^r - Hx)(y^r - Hx)^T B\right) \\
=& 0.25s^2m^2 B e_j e_k^T B \\
&- 0.25s^2 mB e_j e_k^T B\sum_{r=1}^{m}(y^r - Hx)(y^r - Hx)^T B \\
&- 0.25s^2 mB\sum_{p=1}^{m}(y^p - Hx)(y^p - Hx)^T B e_j e_k^T B \\
&+ 0.25s^2 B\sum_{p=1}^{m}(y^p - Hx)(y^p - Hx)^T B e_j e_k^T B \\
&\times \sum_{r=1}^{m}(y^r - Hx)(y^r - Hx)^T B.
\end{aligned} \tag{3.59}$$

We now define $C \triangleq \sum_{p=1}^{m}(y^p - Hx)(y^p - Hx)^T$ and substitute it into (3.59), which gives

$$\begin{aligned}
S_X e_j e_k^T S_X^T =& 0.25s^2m^2 B e_j e_k^T B - 0.25s^2 mB e_j e_k^T BCB \\
&- 0.25s^2 mBCB e_j e_k^T B + 0.25s^2 BCB e_j e_k^T BCB.
\end{aligned} \tag{3.60}$$

Taking the expected values of both sides given m, we have

$$\begin{aligned}
E[S_X e_j e_k^T S_X^T|m] =& 0.25s^2m^2 B e_j e_k^T B - 0.25s^2 mB e_j e_k^T BE[C|m]B \\
&- 0.25s^2 mBE[C|m]B e_j e_k^T B + 0.25s^2 BE[CB e_j e_k^T BC|m]B.
\end{aligned} \tag{3.61}$$

Noting that C is Wishart distributed with $C \sim \mathcal{W}(m, sX + R)$ given m, we have $E[C|m] = m(sX + R) = mB^{-1}$. Hence, we have

$$E\left[S_X e_j e_k^T S_X^T | m\right] = -0.25 s^2 m^2 B e_j e_k^T B + 0.25 s^2 B E[C B e_j e_k^T B C | m] B. \tag{3.62}$$

In order to compute the expectation in the last term of (3.62), we need the following theorem from [21].

Theorem 3 (Theorem 3.3.15(ii) from [21]). *Let $C \sim \mathcal{W}(m, \Sigma)$ be a Wishart distributed random matrix. Then,*

$$E\left[CAC\right] = m\Sigma A'\Sigma + m \operatorname{tr}\left[\Sigma A\right]\Sigma + m^2 \Sigma A \Sigma. \tag{3.63}$$

■

Using Theorem 3, we can write

$$\begin{aligned}
E[C B e_j e_k^T B C | m] =& m B^{-1} B e_k e_j^T B B^{-1} + m \operatorname{tr}\left(B^{-1} B e_j e_k^T B\right) B^{-1} \\
&+ m^2 B^{-1} B e_j e_k^T B B^{-1} && (3.64)\\
=& m e_k e_j^T + m \operatorname{tr}\left(e_j e_k^T B\right) B^{-1} + m^2 e_j e_k^T && (3.65)\\
=& m e_k e_j^T + m \operatorname{tr}\left(e_k^T B e_j\right) B^{-1} + m^2 e_j e_k^T && (3.66)\\
=& m e_k e_j^T + m B_{kj} B^{-1} + m^2 e_j e_k^T. && (3.67)
\end{aligned}$$

Substituting this result into (3.62) we obtain

$$\begin{aligned}
E\left[S_X e_j e_k^T S_x^T | m\right] =& -0.25 s^2 m^2 B e_j e_k^T B \\
&+ 0.25 s^2 B \left[m e_k e_j^T + m B_{kj} B^{-1} + m^2 e_j e_k^T\right] B && (3.68)\\
=& 0.25 s^2 B \left[m e_k e_j^T + m B_{kj} B^{-1}\right] B && (3.69)\\
=& \frac{s^2}{4} m \left[B e_k e_j^T B + B_{kj} B\right]. && (3.70)
\end{aligned}$$

Taking the expectation of both sides with respect to m, we get

$$E\left[S_X e_j e_k^T S_x^T\right] = \frac{s^2}{4} \bar{m} \left[B e_k e_j^T B + B_{kj} B\right]. \tag{3.71}$$

As a result, $d_{ij,kl}$ used in the result (3.57) is given as

$$d_{ij,kl} \triangleq E\left[[S_X]_{ij}[S_X]_{kl}\right] \tag{3.72}$$

$$= \frac{s^2}{4}\bar{m}\Big[(sX+R)^{-1}e_k e_j^T(sX+R)^{-1} + (sX+R)^{-1}\ \left[(sX+R)^{-1}\right]_{kj}\Big]_{il} \tag{3.73}$$

$$= \frac{s^2}{4}\bar{m}\Big(\left[(sX+R)^{-1}\right]_{ik}\left[(sX+R)^{-1}\right]_{jl} + \left[(sX+R)^{-1}\right]_{il}\ \left[(sX+R)^{-1}\right]_{kj}\Big). \tag{3.74}$$

Combining the results given above, the overall FIM $\mathcal{I}_k$ defined in (3.6) has the following form.

$$\mathcal{I}_k = \begin{bmatrix} I_{11} & \vdots & 0 \\ \cdots & \vdots & \cdots \\ 0 & \vdots & I_{22} \end{bmatrix} \tag{3.75}$$

where I_{11} denoting the FIM for kinematical states is given as

$$I_{11} \triangleq \bar{m}H^T(sX+R)^{-1}H. \tag{3.76}$$

The matrix block I_{22} denoting the FIM for extension is given as

$$I_{22} \triangleq E\left[S_{\xi^X}S_{\xi^X}^T\right] \tag{3.77}$$

where the explicit result of the expectation is given in (3.57). Since the overall FIM $\mathcal{I}_k$ is block diagonal, if the initial covariance $\bar{J}_0$ initial estimation errors in the kinematic state and the extent state is also block diagonal and the dynamics of the kinematic state and the extent state are independent, the parametric CRLBs for the kinematic and extent states can be computed using independent recursions as follows.

- **Parametric CRLB Recursion for the Kinematic State**

$$\mathcal{J}^x_{0|-1} = \bar{J}^x_0, \tag{3.78}$$

$$\mathcal{J}^x_{k|k} = \left(\left(\mathcal{J}^x_{k|k-1}\right)^{-1} + \mathcal{I}^{11}_k\right)^{-1}, \tag{3.79}$$

$$\mathcal{J}^x_{k+1|k} = F^x_k \mathcal{J}^x_{k|k}(F^x_k)^T, \tag{3.80}$$

where

- $\mathcal{J}_{k|k}^{x}$ is the parametric CRLB for the kinematic state,
- $\bar{J}_0^x$ is a fixed covariance matrix representing the estimation error for the initial kinematic state x_0,
- F_k^x is the Jacobian for the state transition function of the kinematic state evaluated at the true kinematic state,
- $\mathcal{I}_k^{11}$ is the FIM for the kinematic state given as I_{11} in (3.76).

- **Parametric CRLB Recursion for the Extent State**

$$\mathcal{J}_{0|-1}^{X} = \bar{J}_0^X, \tag{3.81}$$

$$\mathcal{J}_{k|k}^{X} = \left(\left(\mathcal{J}_{k|k-1}^{X} \right)^{-1} + \mathcal{I}_k^{22} \right)^{-1}, \tag{3.82}$$

$$\mathcal{J}_{k+1|k}^{X} = F_k^X \mathcal{J}_{k|k}^{X} (F_k^X)^T, \tag{3.83}$$

where

- $\mathcal{J}_{k|k}^{X}$ is the parametric CRLB for the extent state,
- $\bar{J}_0^X$ is a fixed covariance matrix representing the estimation error for the initial extent state X_0,
- F_k^X is the Jacobian for the state transition function of the extent state evaluated at the true extent state,
- $\mathcal{I}_k^{22}$ is the FIM for the extent state given as I_{22} in (3.77).

3.3 Initialization of the Parametric CRLB

The initial value of the parametric CRLB for the kinematic state is set to a fixed covariance representing the estimation error for the initial kinematic state x_0. For example, if the initial estimate of an ETT algorithm have the distribution $\hat{x}_{0|-1} \sim p_{\hat{x}_{0|-1}}(\cdot)$ which has a mean equal to the true initial kinematic state x_0, then $\mathcal{J}_{0|-1}^{x}$ is set to be

$$\mathcal{J}_{0|-1}^{x} = P_0 \tag{3.84}$$

where P_0 is the covariance of $p_{\hat{x}_{0|-1}}(\cdot)$. Note that the requirement that the mean of $p_{\hat{x}_{0|-1}}(\cdot)$ is x_0 comes from the requirement of unbiasedness for parametric CRLB, i.e., we need to have $E[\hat{x}_{0|-1}] = x_0$.

The initial value of the parametric CRLB for the kinematic state is set to a fixed covariance representing the estimation error for the initial extension state X_0. Suppose that the distribution of the initial extent estimate for an ETT algorithm is given as $\hat{X}_{0|-1} \sim p_{\hat{X}_{0|-1}}(\cdot)$ which has a mean equal to the true initial extent state, i.e., $E[\hat{X}_{0|-1}] = X_0$, then $\mathcal{J}^X_{0|-1}$ is set to be

$$\mathcal{J}^X_{0|-1} = \Sigma_0 \tag{3.85}$$

where Σ_0 is the covariance of $p_{\hat{X}_{0|-1}}(\cdot)$.

For example, suppose that $\hat{X}_{0|-1}$ is Wishart distributed, i.e., we have $\hat{X}_{0|-1} \sim \mathcal{W}\left(n_0, \frac{X_0}{n_0}\right)$ where n_0 is the initial degrees of freedom. Note that when we have this selection, $E[\hat{X}_{0|-1}] = X_0$ which is a necessary condition for parametric CRLB, since it considers only the unbiased estimators. The covariance of the Wishart distribution is given in the following theorem from [21].

Theorem 4 (3.3.15 (i) from [21])**.** *Let $S \sim \mathcal{W}(n, \Sigma)$, then*

$$cov(S_{ij}, S_{kl}) = n(\Sigma_{ik}\Sigma_{jl} + \Sigma_{il}\Sigma_{jk}). \tag{3.86}$$

■

Using the theorem, we can calculate the initial parametric CRLB for the extent state as follows.

$$\mathcal{J}^X_{0|-1} = \frac{1}{n_0}\begin{bmatrix} 2[\overline{X}_0]^2_{11} & 2[\overline{X}_0]_{11}[\overline{X}_0]_{21} & 2[\overline{X}_0]^2_{21} \\ 2[\overline{X}_0]_{11}[\overline{X}_0]_{21} & 2[\overline{X}_0]_{11}[\overline{X}_0]_{22} + 2[\overline{X}_0]^2_{21} & 2[\overline{X}_0]_{21}[\overline{X}_0]_{22} \\ 2[\overline{X}_0]^2_{21} & 2[\overline{X}_0]_{21}[\overline{X}_0]_{22} & 2[\overline{X}_0]^2_{22} \end{bmatrix}. \tag{3.87}$$

3.4 Parametric CRLB for Semi-Major and Semi-Minor Axes

Semi-major and semi-minor axes of the extension ellipsoid are equal to the square root of the eigenvalues of the extension matrix. The eigenvalues of matrix X can be expressed as follows

$$\lambda_{1,2}(X) = \frac{\operatorname{tr} X \mp \sqrt{(\operatorname{tr} X)^2 - 4 \det X}}{2} \tag{3.88}$$

where + and − signs in $\mp$ correspond to the larger and smaller eigenvalues of X respectively. The semi-major and semi-minor axes of the extension, denoted as a_{major} and a_{minor}, respectively, are given as

$$a_{\text{major,minor}}(X) = \sqrt{\frac{\operatorname{tr} X \mp \sqrt{(\operatorname{tr} X)^2 - 4 \det X}}{2}}, \tag{3.89}$$

$$= \sqrt{\frac{X_{11} + X_{22} \mp \sqrt{(X_{11} + X_{22})^2 - 4\,(X_{11}X_{22} - X_{12}X_{21})}}{2}} \tag{3.90}$$

where + and − signs in $\mp$ correspond to the semi-major and semi-minor axes of the extension, respectively. When we use the fact that X is symmetric, i.e., $X_{12} = X_{21}$, we have

$$a_{\text{major,minor}}(X) = \sqrt{\frac{X_{11} + X_{22} \mp \sqrt{(X_{11} + X_{22})^2 - 4\,(X_{11}X_{22} - X_{12}^2)}}{2}}. \tag{3.91}$$

These expressions describe deterministic nonlinear transformations of the entries of the matrix X and the parametric CRLBs can be obtained using Property 2 from the parametric CRLB of the extent state. In order to obtain the Jacobian of $a_{\text{major,minor}}(\cdot)$ with respect to X, we are going to take the square of both sides above.

$$a^2_{\text{major,minor}}(X) = \frac{X_{11} + X_{22} \mp \sqrt{(X_{11} + X_{22})^2 - 4\,(X_{11}X_{22} - X_{12}^2)}}{2} \tag{3.92}$$

which is correct since the right hand side above is always non-negative. Hence we have

$$\frac{\partial a^2_{\text{major,minor}}(X)}{\partial X_{ij}} = 2a_{\text{major,minor}}(X) \frac{\partial a_{\text{major,minor}}(X)}{\partial X_{ij}} \tag{3.93}$$

which can be written as

$$\frac{\partial a_{\text{major,minor}}(X)}{\partial X_{ij}} = \frac{1}{2a_{\text{major,minor}}(X)} \frac{\partial a^2_{\text{major,minor}}(X)}{\partial X_{ij}}. \tag{3.94}$$

Since we have $\xi^X \triangleq \begin{bmatrix} X_{11} & X_{12} & X_{22} \end{bmatrix}^T$, the Jacobian of $a_{\text{major}}(\cdot)$ and $a_{\text{minor}}(\cdot)$ with respect to ξ^X can be calculated using (3.94) as

$$\nabla_{\xi^X} a_{\text{major}}(X) = \frac{1}{2a_{\text{major}}(X)} \begin{bmatrix} \frac{1}{2} + \frac{X_{11} - X_{22}}{2\sqrt{(\operatorname{tr} X)^2 - 4 \det X}} \\ 2\frac{X_{12}}{\sqrt{(\operatorname{tr} X)^2 - 4 \det X}} \\ \frac{1}{2} + \frac{X_{22} - X_{11}}{2\sqrt{(\operatorname{tr} X)^2 - 4 \det X}} \end{bmatrix}, \tag{3.95}$$

$$\nabla_{\xi^X} a_{\text{minor}}(X) = \frac{1}{2a_{\text{minor}}(X)} \begin{bmatrix} \frac{1}{2} - \frac{X_{11} - X_{22}}{2\sqrt{(\operatorname{tr} X)^2 - 4 \det X}} \\ -2\frac{X_{12}}{\sqrt{(\operatorname{tr} X)^2 - 4 \det X}} \\ \frac{1}{2} - \frac{X_{22} - X_{11}}{2\sqrt{(\operatorname{tr} X)^2 - 4 \det X}} \end{bmatrix}. \tag{3.96}$$

Using the result of Section 2.2.1, we can write the parametric CRLB of the semi-major and semi-minor axes as follows.

$$\mathcal{J}_{k|k}^{a_{\text{major}}} = \nabla_{\xi_k^X}^T a_{\text{major}}(X_k) \mathcal{J}_k^X \nabla_{\xi_k^X} a_{\text{major}}(X_k), \tag{3.97}$$

$$\mathcal{J}_{k|k}^{a_{\text{minor}}} = \nabla_{\xi_k^X}^T a_{\text{minor}}(X_k) \mathcal{J}_k^X \nabla_{\xi_k^X} a_{\text{minor}}(X_k). \tag{3.98}$$

CHAPTER 4

POSTERIOR CRAMÉR-RAO LOWER BOUND FOR EXTENDED TARGET TRACKING

Posterior Cramer-Rao lower bound is the second type of CRLB derived for ETT in this study. The chapter is organized as follows. First the posterior CRLB for dynamic systems is defined in Section 4.1. The posterior CRLB recursion for ETT is derived in Section 4.2. The chapter continues with a discussion of the initialization of the posterior CRLB recursion in Section 4.3. In Section 4.4, the chapter is concluded with posterior CRLB expressions for semi-major and semi-minor axes of the extension.

4.1 Definition of Posterior Cramér-Rao Lower Bound for Dynamic Systems

Posterior CRLB assumes that the parameter, i.e., the state vector in this case, is random and gives a performance measure for both biased and unbiased estimators. We consider the following state space representation.

$$\xi_0 \sim p_{\xi_0}(\xi_0), \tag{4.1}$$

$$\xi_{k+1}|\xi_k \sim p(\xi_{k+1}|\xi_k), \tag{4.2}$$

$$y_k|\xi_k \sim p(y_k|\xi_k) \tag{4.3}$$

where

- $\xi_k \in \mathbb{R}^{n_\xi}$ is the state vector of the dynamic system,

- $p_{\xi_0}(\cdot)$ is a known initial distribution for ξ_0,
- $p(\xi_{k+1}|\xi_k)$ is a known state transition density describing the evolution of the state ξ_k,
- $p(y_k|\xi_k)$ is a known likelihood function for the measurements $y_k \in \mathbb{R}^{n_y}$.

The posterior CRLB recursion derived for this system by Tichavsky et al. in [22] is given as follows.

$$\tilde{\mathcal{I}}_0 = E\left[-\Delta_{\xi_0}^{\xi_0} \log p\left(\xi_0\right)\right] \tag{4.4}$$

$$\tilde{\mathcal{I}}_{k+1} = D_{k+1}^{22} + E\left[-\Delta_{\xi_{k+1}}^{\xi_{k+1}} \log p(y_{k+1}|\xi_{k+1})\right] - D_{k+1}^{21}\left(\tilde{\mathcal{I}}_k + D_{k+1}^{11}\right)^{-1} D_{k+1}^{12} \tag{4.5}$$

$$\tilde{\mathcal{J}}_k = \tilde{\mathcal{I}}_k^{-1} \tag{4.6}$$

where

$$D_{k+1}^{11} \triangleq E\left[-\Delta_{\xi_k}^{\xi_k} \log p(\xi_{k+1}|\xi_k)\right], \tag{4.7}$$

$$D_{k+1}^{12} \triangleq E\left[-\Delta_{\xi_k}^{\xi_{k+1}} \log p(\xi_{k+1}|\xi_k)\right], \tag{4.8}$$

$$D_{k+1}^{21} \triangleq E\left[-\Delta_{\xi_{k+1}}^{\xi_k} \log p(\xi_{k+1}|\xi_k)\right], \tag{4.9}$$

$$D_{k+1}^{22} \triangleq E\left[-\Delta_{\xi_{k+1}}^{\xi_{k+1}} \log p(\xi_{k+1}|\xi_k)\right]. \tag{4.10}$$

The following expressions can be used to calculate the terms D_{k+1}^{ij}, $i,j = 1,2$ and $E\left[-\Delta_{\xi_{k+1}}^{\xi_{k+1}} \log p(y_{k+1}|\xi_{k+1})\right]$ using only first-order derivatives (See [23] for details).

$$E\left[-\Delta_{\xi_0}^{\xi_0} p\left(\xi_0\right)\right] = E\left[\nabla_{\xi_0} p\left(\xi_0\right) \nabla_{\xi_0}^T p\left(\xi_0\right)\right], \tag{4.11}$$

$$E\left[-\Delta_{\xi_k}^{\xi_k} \log p(\xi_{k+1}|\xi_k)\right] = E\left[\nabla_{\xi_k} \log p(\xi_{k+1}|\xi_k) \nabla_{\xi_k}^T \log p(\xi_{k+1}|\xi_k)\right], \tag{4.12}$$

$$E\left[-\Delta_{\xi_k}^{\xi_{k+1}} \log p(\xi_{k+1}|\xi_k)\right] = E\left[\nabla_{\xi_k} \log p(\xi_{k+1}|\xi_k) \nabla_{\xi_{k+1}}^T \log p(\xi_{k+1}|\xi_k)\right], \tag{4.13}$$

$$E\left[-\Delta_{\xi_{k+1}}^{\xi_k} \log p(\xi_{k+1}|\xi_k)\right] = E\left[\nabla_{\xi_{k+1}} \log p(\xi_{k+1}|\xi_k) \nabla_{\xi_k}^T \log p(\xi_{k+1}|\xi_k)\right], \tag{4.14}$$

$$E\left[-\Delta_{\xi_{k+1}}^{\xi_{k+1}} \log p(\xi_{k+1}|\xi_k)\right] = E\left[\nabla_{\xi_{k+1}} \log p(\xi_{k+1}|\xi_k) \nabla_{\xi_{k+1}}^T \log p(\xi_{k+1}|\xi_k)\right], \tag{4.15}$$

$$E\left[-\Delta_{\xi_{k+1}}^{\xi_{k+1}} \log p(y_{k+1}|\xi_{k+1})\right]$$

$$= E\left[\nabla_{\xi_{k+1}} \log p(y_{k+1}|\xi_{k+1}) \nabla_{\xi_{k+1}}^T \log p(y_{k+1}|\xi_{k+1})\right], \tag{4.16}$$

$$= E\left[E\left[\nabla_{\xi_{k+1}} \log p(y_{k+1}|\xi_{k+1}) \nabla_{\xi_{k+1}}^T \log p(y_{k+1}|\xi_{k+1}) \middle| \xi_{k+1}\right]\right], \tag{4.17}$$

$$= E\left[\mathcal{I}_{k+1}(\xi_{k+1})\right], \tag{4.18}$$

where $\mathcal{I}_k(\xi_k)$ is the parametric FIM at the true augmented state ξ_k.

In the next section, the posterior CRLB will be derived for the ETT problem defined in Section 2.1.1.1.

4.2 Derivations of Posterior CRLB for the Case of ETT

In this section, we derive the expressions for the posterior CRLB for ETT. We consider again the augmented state vector ξ_k which is composed of the kinematic state x_k and the extension state X_k as follows.

$$\xi_k \triangleq \begin{bmatrix} \xi_k^x \\ \xi_k^X \end{bmatrix} \tag{4.19}$$

where

$$\xi_k^x \triangleq x_k, \tag{4.20}$$

$$\xi_k^X \triangleq \begin{bmatrix} [X_k]_{11} & [X_k]_{12} & [X_k]_{22} \end{bmatrix}^T. \tag{4.21}$$

The state transition densities for the kinematic and extent states are selected to be independent as follows

$$p(x_{k+1}|x_k) = \mathcal{N}(x_{k+1}; Fx_k, Q), \tag{4.22}$$

$$p(X_{k+1}|X_k) = \mathcal{W}_d\left(X_{k+1}; n_{k+1}, \frac{X_k}{n_{k+1}}\right). \tag{4.23}$$

where $d = 2$. Hence, $p(\xi_{k+1}|\xi_k)$ can be obtained by the multiplication of $p(x_{k+1}|x_k)$ and $p(X_{k+1}|X_k)$ by making the following substitutions.

$$x_k \leftarrow \xi_k^x, \tag{4.24}$$

$$x_{k+1} \leftarrow \xi_{k+1}^x, \tag{4.25}$$

$$X_k \leftarrow \begin{bmatrix} [\xi_k^X]_1 & [\xi_k^X]_2 \\ [\xi_k^X]_2 & [\xi_k^X]_3 \end{bmatrix}, \tag{4.26}$$

$$X_{k+1} \leftarrow \begin{bmatrix} [\xi_{k+1}^X]_1 & [\xi_{k+1}^X]_2 \\ [\xi_{k+1}^X]_2 & [\xi_{k+1}^X]_3 \end{bmatrix}. \tag{4.27}$$

The likelihood $p(Y_k|\xi_k)$ is defined exactly the same as that in the parametric CRLB case. It has been seen in the parametric CRLB case that the likelihood

$p(Y_k|\xi_k)$ results in independent pieces of Fisher information for the kinematic and extent states. Since the transition densities for the kinematic and extent states are also independent, if the initial pieces of Fisher information for the kinematic and extent states are independent, all FIMs and CRLB matrices, $\tilde{\mathcal{I}}_k$ and $\tilde{\mathcal{J}}_k$ as well as the intermediate matrices D_{k+1}^{ij}, $i,j = 1,2$ will be block diagonal. Therefore, posterior CRLBs for the kinematic and extent states can be computed using independent recursions as follows.

- **Posterior CRLB Recursion for the Kinematic State:**

$$\tilde{\mathcal{I}}_0^x = E\left[\nabla_{x_0} \log p_{x_0}(x_0) \nabla_{x_0}^T \log p_{x_0}(x_0)\right], \tag{4.28}$$

$$\tilde{\mathcal{I}}_{k+1}^x = D_{k+1}^{x,22} + E\left[\mathcal{I}_{k+1}^{11}(x_{k+1}, X_{k+1})\right] - D_{k+1}^{x,21}\left(\tilde{\mathcal{I}}_k^x + D_{k+1}^{x,11}\right)^{-1} D_{k+1}^{x,12}, \tag{4.29}$$

$$\tilde{\mathcal{J}}_k^x = \left(\tilde{\mathcal{I}}_k^x\right)^{-1}, \tag{4.30}$$

where $\mathcal{I}_{k+1}^{11}(\cdot,\cdot)$ is the parametric FIM for the kinematic state (evaluated at the true kinematic and extent states x_{k+1} and X_{k+1} respectively) derived in Chapter 3 which is equal to I_{11} in (3.76) and

$$D_{k+1}^{x,11} \triangleq E\left[\nabla_{x_k} \log p(x_{k+1}|x_k) \nabla_{x_k}^T \log p(x_{k+1}|x_k)\right], \tag{4.31}$$

$$D_{k+1}^{x,12} \triangleq E\left[\nabla_{x_k} \log p(x_{k+1}|x_k) \nabla_{x_{k+1}}^T \log p(x_{k+1}|x_k)\right], \tag{4.32}$$

$$D_{k+1}^{x,21} \triangleq E\left[\nabla_{x_{k+1}} \log p(x_{k+1}|x_k) \nabla_{x_k}^T \log p(x_{k+1}|x_k)\right], \tag{4.33}$$

$$D_{k+1}^{x,22} \triangleq E\left[\nabla_{x_{k+1}} \log p(x_{k+1}|x_k) \nabla_{x_{k+1}}^T \log p(x_{k+1}|x_k)\right]. \tag{4.34}$$

- **Posterior CRLB Recursion for the Extent State:**

$$\tilde{\mathcal{I}}_0^X = E\left[\nabla_{\xi_0^X} \log p_{X_0}(X_0) \nabla_{\xi_0^X}^T \log p_{X_0}(X_0)\right], \tag{4.35}$$

$$\tilde{\mathcal{I}}_{k+1}^X = D_{k+1}^{X,22} + E\left[\mathcal{I}_{k+1}^{22}(x_{k+1}, X_{k+1})\right] - D_{k+1}^{X,21}\left(\tilde{\mathcal{I}}_k^X + D_{k+1}^{X,11}\right)^{-1} D_{k+1}^{X,12}, \tag{4.36}$$

$$\tilde{\mathcal{J}}_k^X = \left(\tilde{\mathcal{I}}_k^X\right)^{-1}, \tag{4.37}$$

where $\mathcal{I}_{k+1}^{22}(\cdot,\cdot)$ is the parametric FIM for the extent state (evaluated at the true kinematic and extent states x_{k+1} and X_{k+1} respectively) derived

in Chapter 3 which is equal to I_{22} in (3.77) and

$$D_{k+1}^{X,11} \triangleq E\left[\nabla_{\xi_k^X} \log p(X_{k+1}|X_k) \nabla_{\xi_k^X}^T \log p(X_{k+1}|X_k)\right], \tag{4.38}$$

$$D_{k+1}^{X,12} \triangleq E\left[\nabla_{\xi_k^X} \log p(X_{k+1}|X_k) \nabla_{\xi_{k+1}^X}^T \log p(X_{k+1}|X_k)\right], \tag{4.39}$$

$$D_{k+1}^{X,21} \triangleq E\left[\nabla_{\xi_{k+1}^X} \log p(X_{k+1}|X_k) \nabla_{\xi_k^X}^T \log p(X_{k+1}|X_k)\right], \tag{4.40}$$

$$D_{k+1}^{X,22} \triangleq E\left[\nabla_{\xi_{k+1}^X} \log p(X_{k+1}|X_k) \nabla_{\xi_{k+1}^X}^T \log p(X_{k+1}|X_k)\right]. \tag{4.41}$$

As a result of the discussion above, the posterior CRLB derivations will be made independently in the forthcoming subsections.

4.2.1 Derivations for the Kinematical State

The logarithm of the kinematic state transition density $p(x_{k+1}|x_k)$ is given as

$$\log(p(x_{k+1}|x_k)) = -\frac{1}{2}\log\left(|Q|\right) - \frac{1}{2}(x_{k+1} - Fx_k)^T Q^{-1}(x_{k+1} - Fx_k) \tag{4.42}$$

up to an additive constant independent of x_k and x_{k+1}. Property 5 can easily be applied to obtain the following gradients.

$$\nabla_{x_{k+1}} \log p(x_{k+1}|x_k) = -Q^{-1}(x_{k+1} - Fx_k), \tag{4.43}$$

$$\nabla_{x_k} \log p(x_{k+1}|x_k) = F^T Q^{-1}(x_{k+1} - Fx_k). \tag{4.44}$$

Using the derivatives given above, the expressions for $D_{k+1}^{x,ij}$, $i,j = 1,2$ defined in (4.31) to (4.34) can be calculated as below.

- **Calculation of $D_{k+1}^{x,11}$:**

$$D_{k+1}^{x,11} = E\left[\nabla_{x_k} \log p(x_{k+1}|x_k) \nabla_{x_k}^T \log p(x_{k+1}|x_k)\right], \tag{4.45}$$

$$= E\left[F^T Q^{-1}(x_{k+1} - Fx_k)(x_{k+1} - Fx_k)^T Q^{-1} F\right], \tag{4.46}$$

$$= F^T Q^{-1} E\left[(x_{k+1} - Fx_k)(x_{k+1} - Fx_k)^T\right] Q^{-1} F, \tag{4.47}$$

$$= F^T Q^{-1} F. \tag{4.48}$$

- **Calculation of $D_{k+1}^{x,12}$:**

$$D_{k+1}^{x,12} = E\left[\nabla_{x_k} \log p(x_{k+1}|x_k) \nabla_{x_{k+1}}^T \log p(x_{k+1}|x_k)\right], \tag{4.49}$$

$$= -E\left[F^T Q^{-1}(x_{k+1} - Fx_k)(x_{k+1} - Fx_k)^T Q^{-1}\right], \tag{4.50}$$

$$= -F^T Q^{-1} E\left[(x_{k+1} - Fx_k)(x_{k+1} - Fx_k)^T\right] Q^{-1}, \tag{4.51}$$

$$= -F^T Q^{-1}. \tag{4.52}$$

- **Calculation of $D_{k+1}^{x,21}$:**

$$D_{k+1}^{x,21} = E\left[\nabla_{x_{k+1}} \log p(x_{k+1}|x_k) \nabla_{x_k}^T \log p(x_{k+1}|x_k)\right], \tag{4.53}$$

$$= -E\left[Q^{-1}(x_{k+1} - Fx_k)(x_{k+1} - Fx_k)^T Q^{-1} F\right], \tag{4.54}$$

$$= -Q^{-1} E\left[(x_{k+1} - Fx_k)(x_{k+1} - Fx_k)^T\right] Q^{-1} F, \tag{4.55}$$

$$= -Q^{-1} F. \tag{4.56}$$

- **Calculation of $D_{k+1}^{x,22}$:**

$$D_{k+1}^{x,22} = E\left[\nabla_{x_{k+1}} \log p(x_{k+1}|x_k) \nabla_{x_{k+1}}^T \log p(x_{k+1}|x_k)\right], \tag{4.57}$$

$$= E\left[Q^{-1}(x_{k+1} - Fx_k)(x_{k+1} - Fx_k)^T Q^{-1}\right], \tag{4.58}$$

$$= Q^{-1} E\left[(x_{k+1} - Fx_k)(x_{k+1} - Fx_k)^T\right] Q^{-1}, \tag{4.59}$$

$$= Q^{-1}. \tag{4.60}$$

Substituting the results given above into the recursion (4.29), we get

$$\tilde{\mathcal{I}}_{k+1} = Q^{-1} - Q^{-1} F (\tilde{\mathcal{I}}_k + F^T Q^{-1} F) F^T Q^{-1} + E\left[\mathcal{I}_{k+1}^{11}(x_{k+1}, X_{k+1})\right], \tag{4.61}$$

$$= Q^{-1} - Q^{-1} F (\tilde{\mathcal{I}}_k + F^T Q^{-1} F) F^T Q^{-1} + E\left[\bar{m}_{k+1} H^T (sX_{k+1} + R)^{-1} H\right] \tag{4.62}$$

where $\mathcal{I}_{k+1}^{11}(\cdot,\cdot)$ was substituted from (3.76) to obtain the second equality above. Note that $\bar{m}_k$ denotes the expected number of measurements at time k and it can be dependent on the target kinematic and extent states, i.e., $\bar{m}_k = \bar{m}_k(x_k, X_k)$. This dependence is suppressed in the expressions for the sake of brevity.

A simpler form of (4.62) can be obtained using following well-known lemma.

Lemma 1 (Matrix Inversion Lemma)**.**

$$(A + BCD)^{-1} = A^{-1} - A^{-1} B (C^{-1} + DA^{-1} B)^{-1} DA^{-1}. \tag{4.63}$$

■

Using the matrix inversion lemma on the first two terms on the right hand side of (4.62), we get

$$\tilde{\mathcal{I}}_{k+1} = \left(F\tilde{\mathcal{I}}_k^{-1}F^T + Q\right)^{-1} + E\left[\bar{m}_{k+1}H^T(sX_{k+1}+R)^{-1}H\right]. \tag{4.64}$$

Since there is no analytical form of the expectation on the right hand side of (4.64), it is going to be taken using Monte Carlo integration.

4.2.2 Derivations for the Extent State

The logarithm of the extent state transition density $p(X_{k+1}|X_k)$ is given as

$$\begin{aligned}\log p(X_{k+1}|X_k) =& \frac{n_{k+1}-d-1}{2}\log|X_{k+1}| + \operatorname{tr}\left[-\frac{1}{2}\left(\frac{X_k}{n_{k+1}}\right)^{-1}X_{k+1}\right] \\ &- \frac{n_{k+1}}{2}\log\left|\frac{X_k}{n_{k+1}}\right|\end{aligned} \tag{4.65}$$

up to an additive constant independent of X_k and X_{k+1}. In order to be able to compute the derivatives of $\log p(X_{k+1}|X_k)$, the following properties from matrix calculus are required [20].

Property 8.

$$\frac{\partial \log|X|}{\partial X} = (X^{-1})^T, \tag{4.66}$$

$$\frac{\partial \operatorname{tr}\left[AX^T\right]}{\partial X} = A, \tag{4.67}$$

$$\frac{\partial \operatorname{tr}\left[X^{-1}A\right]}{\partial X} = -X^{-T}A^TX^{-T}. \tag{4.68}$$

■

Using the properties given above, the derivatives of $\log p(X_{k+1}|X_k)$ with respect to X_{k+1} and X_k can be calculated as below.

$$\nabla_{X_{k+1}}\log p(X_{k+1}|X_k) = \frac{n_{k+1}-d-1}{2}\frac{\partial\log|X_{k+1}|}{\partial X_{k+1}} - \frac{n_{k+1}}{2}\frac{\partial\operatorname{tr}\left[X_k^{-1}X_{k+1}\right]}{\partial X_{k+1}}, \tag{4.69}$$

$$= \frac{n_{k+1}-d-1}{2}X_{k+1}^{-1} - \frac{n_{k+1}}{2}{X_k}^{-1}, \tag{4.70}$$

$$\nabla_{X_k}\log p(X_{k+1}|X_k) = -\frac{n_{k+1}}{2}\frac{\partial\operatorname{tr}\left[X_k^{-1}X_{k+1}\right]}{\partial X_k} - \frac{n_{k+1}}{2}\frac{\partial\log|X_k|}{\partial X_k}, \tag{4.71}$$

$$= \frac{n_{k+1}}{2}X_k^{-1}X_{k+1}X_k^{-1} - \frac{n_{k+1}}{2}X_k^{-1}. \tag{4.72}$$

Under the constraints $[X_k]_{12} = [X_k]_{21}$ and $[X_{k+1}]_{12} = [X_{k+1}]_{21}$, the gradient of $\log p(X_{k+1}|X_k)$ with respect to ξ^X_{k+1} and ξ^X_k are given as

$$\nabla_{\xi^X_{k+1}} \log p(X_{k+1}|X_k) = \begin{bmatrix} \left[\nabla_{X_{k+1}} \log p(X_{k+1}|X_k)\right]_{11} \\ \\ \left[\nabla_{X_{k+1}} \log p(X_{k+1}|X_k)\right]_{12} \\ + \left[\nabla_{X_{k+1}} \log p(X_{k+1}|X_k)\right]_{21} \\ \\ \left[\nabla_{X_{k+1}} \log p(X_{k+1}|X_k)\right]_{22} \end{bmatrix}. \tag{4.73}$$

$$\nabla_{\xi^X_k} \log p(X_{k+1}|X_k) = \begin{bmatrix} \left[\nabla_{X_k} \log p(X_{k+1}|X_k)\right]_{11} \\ \\ \left[\nabla_{X_k} \log p(X_{k+1}|X_k)\right]_{12} \\ + \left[\nabla_{X_k} \log p(X_{k+1}|X_k)\right]_{21} \\ \\ \left[\nabla_{X_k} \log p(X_{k+1}|X_k)\right]_{22} \end{bmatrix}. \tag{4.74}$$

The matrices $D^{X,tu}_{k+1}$, $t, u = 1, 2$ defined in (4.38) to (4.41) would then have the following form.

$$D^{X,tu}_{k+1} = \begin{bmatrix} d^{tu}_{11,11} & d^{tu}_{11,12} + d^{tu}_{11,21} & d^{tu}_{11,22} \\ d^{tu}_{12,11} + d^{tu}_{21,11} & d^{tu}_{12,12} + d^{tu}_{12,21} \\ & +d^{tu}_{21,12} + d^{tu}_{21,22} & d^{tu}_{12,22} + d^{tu}_{21,22} \\ d^{tu}_{22,11} & d^{tu}_{22,12} + d^{tu}_{22,21} & d^{tu}_{22,22} \end{bmatrix} \tag{4.75}$$

where

$$d^{11}_{ij,lm} \triangleq E\left[\left[\nabla_{X_k} \log p(X_{k+1}|X_k)\right]_{ij} \left[\nabla_{X_k} \log p(X_{k+1}|X_k)\right]_{lm}\right], \tag{4.76}$$

$$d^{12}_{ij,lm} \triangleq E\left[\left[\nabla_{X_k} \log p(X_{k+1}|X_k)\right]_{ij} \left[\nabla_{X_{k+1}} \log p(X_{k+1}|X_k)\right]_{lm}\right], \tag{4.77}$$

$$d^{21}_{ij,lm} \triangleq E\left[\left[\nabla_{X_{k+1}} \log p(X_{k+1}|X_k)\right]_{ij} \left[\nabla_{X_k} \log p(X_{k+1}|X_k)\right]_{lm}\right], \tag{4.78}$$

$$d^{22}_{ij,lm} \triangleq E\left[\left[\nabla_{X_{k+1}} \log p(X_{k+1}|X_k)\right]_{ij} \left[\nabla_{X_{k+1}} \log p(X_{k+1}|X_k)\right]_{lm}\right]. \tag{4.79}$$

We are now going to calculate the elements of $d^{tu}_{ij,lm}$, $t, u = 1, 2$, one by one below.

- **Calculation of $d_{ij,lm}^{11}$:**

$$\begin{aligned}
d_{ij,lm}^{11} \triangleq & E\left[\left[\nabla_{X_k}\log p(X_{k+1}|X_k)\right]_{ij}\left(\left[\nabla_{X_k}\log p(X_{k+1}|X_k)\right]_{lm}\right)\right] \\
= & E\Bigg[\left[\frac{n_{k+1}}{2}X_k^{-1}X_{k+1}X_k^{-1}-\frac{n_{k+1}}{2}X_k^{-1}\right]_{ij} \\
& \times\left[\frac{n_{k+1}}{2}X_k^{-1}X_{k+1}X_k^{-1}-\frac{n_{k+1}}{2}X_k^{-1}\right]_{lm}\Bigg] \\
= & -\frac{n_{k+1}^2}{4}E\left[\left[X_k^{-1}X_{k+1}X_k^{-1}\right]_{ij}\left[X_k^{-1}\right]_{lm}\right] \\
& -\frac{n_{k+1}^2}{4}E\left[\left[X_k^{-1}\right]_{ij}\left[X_k^{-1}X_{k+1}X_k^{-1}\right]_{lm}\right] \\
& +\frac{n_{k+1}^2}{4}E\left[\left[X_k^{-1}\right]_{ij}\left[X_k^{-1}\right]_{lm}\right] \\
& +\frac{n_{k+1}^2}{4}E\left[\left[X_k^{-1}X_{k+1}X_k^{-1}\right]_{ij}\left[X_k^{-1}X_{k+1}X_k^{-1}\right]_{lm}\right]. \qquad (4.80)
\end{aligned}$$

  - **First term of** (4.80)**:**

$$\begin{aligned}
& E\left[\left[X_k^{-1}X_{k+1}X_k^{-1}\right]_{ij}\left[X_k^{-1}\right]_{lm}\right] \\
& \qquad = E\left[E\left(\left[X_k^{-1}X_{k+1}X_k^{-1}\right]_{ij}\left[X_k^{-1}\right]_{lm}\middle| X_k\right)\right] \qquad (4.81) \\
& \qquad = E\left[\left[X_k^{-1}E\left(X_{k+1}|\,X_k\right)X_k^{-1}\right]_{ij}\left[X_k^{-1}\right]_{lm}\right] \qquad (4.82)
\end{aligned}$$

    It is known that $X_{k+1}|X_k \sim \mathcal{W}_d\left(X_{k+1}; n_{k+1}, \frac{X_k}{n_{k+1}}\right)$ is Wishart distributed. Hence, the inner expectation of (4.82) is given as

$$E\left[X_{k+1}|X_k\right] = n_{k+1}\frac{X_k}{n_{k+1}} = X_k \qquad (4.83)$$

    which gives

$$E\left[\left[X_k^{-1}X_{k+1}X_k^{-1}\right]_{ij}\left[X_k^{-1}\right]_{lm}\right] = E\left[\left[X_k^{-1}\right]_{ij}\left[X_k^{-1}\right]_{lm}\right]. \qquad (4.84)$$

    The expectation on the right hand side above has no analytical form, hence it is going to be taken using Monte Carlo integration.

  - **Second term of** (4.80): This expectation can be computed in the same way as the first term resulting in

$$E\left[\left[X_k^{-1}\right]_{ij}\left[X_k^{-1}X_{k+1}X_k^{-1}\right]_{lm}\right] = E\left[\left[X_k^{-1}\right]_{ij}\left[X_k^{-1}\right]_{lm}\right]. \qquad (4.85)$$

  - **Third term of** (4.80)**:** This term is left as it is.

– **Fourth term of** (4.80)**:**

$$E\left[\left[X_k^{-1}X_{k+1}X_k^{-1}\right]_{ij}\left[X_k^{-1}X_{k+1}X_k^{-1}\right]_{lm}\right] \tag{4.86}$$

$$= E\left[e_i^T X_k^{-1}X_{k+1}X_k^{-1}e_j e_l^T X_k^{-1}X_{k+1}X_k^{-1}e_m\right] \tag{4.87}$$

$$= e_i^T E\left[X_k^{-1}X_{k+1}X_k^{-1}e_j e_l^T X_k^{-1}X_{k+1}\right]e_m \tag{4.88}$$

$$= e_i^T E\left[X_k^{-1}E\left[X_{k+1}X_k^{-1}e_j e_l^T X_k^{-1}X_{k+1}\middle|\, X_k\right]X_k^{-1}\right]e_m \tag{4.89}$$

where $e_\ell \in \mathbb{R}^2$, $\ell = i, j, l, m$ is a vector filled with all zeros except for the ℓth element which is unity. For the inner expectation of (4.89), we are going to use the following theorem.

Theorem 5 (Theorem 3.3.15(ii) from [21])**.** *Let* $X \sim \mathcal{W}_d(n, \Sigma)$

$$E(XAX) = n\Sigma A'\Sigma + n\,\mathrm{tr}(\Sigma A)\Sigma + n^2\Sigma A\Sigma$$

where A *is a constant matrix of size* $d \times d$*.* ■

Using the theorem above, the inner expectation in (4.89) is given as

$$\begin{aligned} E\left[X_{k+1}X_k^{-1}e_j e_l^T X_k^{-1}X_{k+1}|X_k\right] =& n_{k+1}\frac{X_k}{n_{k+1}}X_k^{-1}e_l e_j^T X_k^{-1}\frac{X_k}{n_{k+1}} \\ &+ n_{k+1}\,\mathrm{tr}\left[\frac{X_k}{n_{k+1}}X_k^{-1}e_j e_l^T X_k^{-1}\right]\frac{X_k}{n_{k+1}} \\ &+ n_{k+1}^2\frac{X_k}{n_{k+1}}X_k^{-1}e_j e_l^T X_k^{-1}\frac{X_k}{n_{k+1}}, \qquad (4.90) \\ =& \frac{1}{n_{k+1}}\left(e_l e_j^T + \mathrm{tr}\left[e_j e_l^T X_k^{-1}\right]X_k\right) + e_j e_l^T, \qquad (4.91) \\ =& \frac{1}{n_{k+1}}\left(e_l e_j^T + \left[X_k^{-1}\right]_{lj}X_k\right) + e_j e_l^T. \qquad (4.92) \end{aligned}$$

The fourth term of (4.80) is then obtained as follows.

$$\begin{aligned} &E\left[\left[X_k^{-1}X_{k+1}X_k^{-1}\right]_{ij}\left[X_k^{-1}X_{k+1}X_k^{-1}\right]_{lm}\right] \\ &= \frac{1}{n_{k+1}}E\left[\left[X_k^{-1}\right]_{il}\left[X^{-1}\right]_{jm} + \left[X_k^{-1}\right]_{lj}\left[X_k\right]_{im}\right. \\ &\quad \left. + n_{k+1}\left[X_k^{-1}\right]_{ij}\left[X_k^{-1}\right]_{lm}\right] \qquad (4.93) \end{aligned}$$

Using the individual terms calculated above, the final form of (4.80) that can be reached by analytical manipulations is given as

$$d_{ij,lm}^{11} = \frac{n_{k+1}}{4}\left(E\left[\left[X_k^{-1}\right]_{il}\left[X_k^{-1}\right]_{jm}\right] + E\left[\left[X_k^{-1}\right]_{im}\left[X_k^{-1}\right]_{lj}\right]\right) \tag{4.94}$$

where expectations will be taken using Monte Carlo integration.

- **Calculation of $d_{ij,lm}^{21}$:**

$$\begin{aligned}
d_{ij,lm}^{21} \triangleq & E\left[\left[\nabla_{X_{k+1}} \log p(X_{k+1}|X_k)\right]_{ij}\left[\nabla_{X_k} \log p(X_{k+1}|X_k)\right]_{lm}\right] \\
= & E\Bigg[\left[\frac{n_{k+1}-d-1}{2}X_{k+1}^{-1} - \frac{n_{k+1}}{2}X_k^{-1}\right]_{ij} \\
& \times \left[\frac{n_{k+1}}{2}X_k^{-1}X_{k+1}X_k^{-1} - \frac{n_{k+1}}{2}X_k^{-1}\right]_{lm}\Bigg], \\
= & -\frac{n_{k+1}^2}{4}E\left[\left[X_k^{-1}\right]_{ij}\left[X_k^{-1}X_{k+1}X_k^{-1}\right]_{lm}\right] \\
& -\frac{n_{k+1}(n_{k+1}-d-1)}{4}E\left[\left[X_{k+1}^{-1}\right]_{ij}\left[X_k^{-1}\right]_{lm}\right] \\
& +\frac{n_{k+1}^2}{4}E\left[\left[X_k^{-1}\right]_{ij}\left[X_k^{-1}\right]_{lm}\right] \\
& +\frac{n_{k+1}(n_{k+1}-d-1)}{4}E\left[\left[X_{k+1}^{-1}\right]_{ij}\left[X_k^{-1}X_{k+1}X_k^{-1}\right]_{lm}\right]. \qquad (4.95)
\end{aligned}$$

  - **First term of** (4.95)**:**

$$\begin{aligned}
& E\left[\left[X_k^{-1}\right]_{ij}\left[X_k^{-1}X_{k+1}X_k^{-1}\right]_{lm}\right] \\
& \qquad = E\left[\left[X_k^{-1}\right]_{ij}\left[X_k^{-1}E\left[X_{k+1}|X_k\right]X_k^{-1}\right]_{lm}\right]. \qquad (4.96)
\end{aligned}$$

    The inner expectation is given as X_k as shown in (4.83). Hence, we have

$$E\left[\left[X_k^{-1}\right]_{ij}\left[X_k^{-1}X_{k+1}X_k^{-1}\right]_{lm}\right] = E\left[\left[X_k^{-1}\right]_{ij}\left[X_k^{-1}\right]_{lm}\right]. \qquad (4.97)$$

  - **Second term of** (4.95)**:**

$$E\left[\left[X_{k+1}^{-1}\right]_{ij}\left[X_k^{-1}\right]_{lm}\right] = E\left[\left[E\left[X_{k+1}^{-1}|X_k\right]\right]_{ij}\left[X_k^{-1}\right]_{lm}\right] \qquad (4.98)$$

    For the inner expectation in (4.98) the following theorem is used.

    Theorem 6 (Theorem 3.4.1 from [21])**.** *Let $V \sim \mathcal{IW}_p(m, \Psi)$, then $V^{-1} \sim \mathcal{W}_p(m-p-1, \Psi^{-1})$.* ■

    It is known that $X_{k+1}|X_k \sim \mathcal{W}_d\left(n_{k+1}, \frac{X_k}{n_{k+1}}\right)$ and X_{k+1} is an $d \times d$ matrix. Hence, according to the theorem the distribution of $X_{k+1}^{-1}|X_k$ is given as $X_{k+1}^{-1}|X_k \sim \mathcal{IW}_d\left(n_{k+1}+d+1, \left(\frac{X_k}{n_{k+1}}\right)^{-1}\right)$. Therefore,

the inner expectation in (4.98) can be obtained as

$$E\left[X_{k+1}^{-1}|X_k\right] = \frac{n_{k+1}}{n_{k+1}-d-1}X_k^{-1} \tag{4.99}$$

which yields the following result.

$$E\left[\left[X_{k+1}^{-1}\right]_{ij}\left[X_k^{-1}\right]_{lm}\right] = \frac{n_{k+1}}{n_{k+1}-d-1}E\left[\left[X_k^{-1}\right]_{ij}\left[X_k^{-1}\right]_{lm}\right]. \tag{4.100}$$

– **Third term of** (4.95)**:** This term is left as it is.

– **Fourth term of** (4.95)**:**

$$\begin{aligned} &E\left[\left[X_{k+1}^{-1}\right]_{ij}\left[X_k^{-1}X_{k+1}X_k^{-1}\right]_{lm}\right] \\ &\quad = E\left[e_i^T X_{k+1}^{-1} e_j e_l X_k^{-1} X_{k+1} X_k^{-1} e_m\right] &(4.101)\\ &\quad = E\left[e_i^T E\left[X_{k+1}^{-1} e_j e_l^T X_k^{-1} X_{k+1}\middle| X_k\right] X_k^{-1} e_m\right] &(4.102)\end{aligned}$$

where $e_\ell \in \mathbb{R}^2$, $\ell = i, j, l, m$ is a vector filled with all zeros except for the ℓth element which is unity. For calculating the inner expectation of (4.102), the following corollary from [24] is required.

Corollary 1 ([24])**.** *Let $X \sim \mathcal{W}_d(k, V)$ with V nonsingular and $k \geq d+1$, and suppose that the $d \times d$ constant matrix A is not necessarily symmetric. Then*

$$E\left[XAX^{-1}\right] = (k-d-1)^{-1}\left(kVAV^{-1} - A^T - \operatorname{tr}[A]\, I_d\right) \tag{4.103}$$

where I_d denotes a $d \times d$ identity matrix. ■

Notice that if the transpose of the argument of the inner expectation of (4.102), i.e., $X_{k+1}^{-1} e_j e_l^T X_k^{-1} X_{k+1}$, is taken, it will have the same form given in the corollary. Hence we have

$$\left(X_{k+1}^{-1} e_j e_l^T X_k^{-1} X_{k+1}\right)^T = X_{k+1} X_k^{-1} e_l e_j^T X_{k+1}^{-1}. \tag{4.104}$$

Now, the expectation of both sides of (4.104) can be taken and, using

the corollary, the expectation can be calculated as

$$E\left[X_{k+1}^{-1}e_l e_j^T X_k^{-1} X_{k+1}\right] = \frac{1}{n_{k+1}-d-1}\Big(n_{k+1}e_l e_j^T X_k^{-1} - e_j e_l^T X_k^{-1} - \mathrm{tr}\left[X_k^{-1}e_l e_j^T\right] I_d\Big) \tag{4.105}$$

$$= \frac{1}{n_{k+1}-d-1}\Big(n_{k+1}e_l e_j^T X_k^{-1} - e_j e_l^T X_k^{-1} - \left[X_k^{-1}\right]_{jl} I_d\Big). \tag{4.106}$$

Taking the transpose of both sides of (4.106), we get

$$E\left[X_{k+1}^{-1}e_j e_l^T X_k^{-1} X_{k+1}^{-1}\right] = \frac{1}{n_{k+1}-d-1}\Big(n_{k+1}X_k^{-1}e_j e_l^T - X_k^{-1}e_l e_j^T - \left[X_k^{-1}\right]_{jl} I_d\Big). \tag{4.107}$$

After substituting (4.107) into (4.102), with some analytical manipulations, we obtain

$$E\left[\left[X_{k+1}^{-1}\right]_{ij}\left[X_k^{-1}X_{k+1}X_k^{-1}\right]_{lm}\right] = \frac{1}{n_{k+1}-d-1}\Big(n_{k+1}\left[X_k^{-1}\right]_{ij}\left[X_k^{-1}\right]_{lm} - \left[X_k^{-1}\right]_{il}\left[X_k^{-1}\right]_{jm} - \left[X_k^{-1}\right]_{jl}\left[X_k^{-1}\right]_{im}\Big). \tag{4.108}$$

Combining the individual equations obtained above, with some algebra, $d_{ij,lm}^{21}$ can be found as below.

$$d_{ij,lm}^{21} = -\frac{n_{k+1}}{4}\left(E\left[\left[X_k^{-1}\right]_{ij}\left[X_k^{-1}\right]_{lm}\right] + E\left[\left[X_k^{-1}\right]_{jl}\left[X_k^{-1}\right]_{im}\right]\right) \tag{4.109}$$

where the expectations should be computed using Monte Carlo integration.

- **Calculation of $d_{ij,lm}^{12}$:** There is no need for a detailed calculation of this term because we have

$$d_{ij,lm}^{12} = d_{lm,ij}^{21}. \tag{4.110}$$

- **Calculation of $d^{22}_{ij,lm}$:**

$$d^{22}_{ij,lm} \triangleq E\left[\left[\nabla_{X_{k+1}} \log p(X_{k+1}|X_k)\right]_{ij}\left[\nabla_{X_{k+1}} \log p(X_{k+1}|X_k)\right]_{lm}\right] \quad (4.111)$$

$$= E\Bigg[\left[\frac{n_{k+1}-d-1}{2}X^{-1}_{k+1} - \frac{n_{k+1}}{2}X^{-1}_{k}\right]_{ij} \times \left[\frac{n_{k+1}-d-1}{2}X^{-1}_{k+1} - \frac{n_{k+1}}{2}X^{-1}_{k}\right]_{lm}\Bigg], \quad (4.112)$$

$$= \left(\frac{n_{k+1}-d-1}{2}\right)^2 E\left[\left[X^{-1}_{k+1}\right]_{ij}\left[X^{-1}_{k+1}\right]_{lm}\right] + \left(\frac{n_{k+1}}{2}\right)^2 E\left[\left[X^{-1}_{k}\right]_{ij}\left[X^{-1}_{k}\right]_{lm}\right] - \frac{(n_{k+1}-d-1)n_{k+1}}{4}E\left[\left[X^{-1}_{k+1}\right]_{ij}\left[X^{-1}_{k}\right]_{lm}\right] - \frac{(n_{k+1}-d-1)n_{k+1}}{4}E\left[\left[X^{-1}_{k}\right]_{ij}\left[X^{-1}_{k+1}\right]_{lm}\right]. \quad (4.113)$$

– **First term of** (4.113)**:** The expectation $E\left[\left[X^{-1}_{k+1}\right]_{ij}\left[X^{-1}_{k+1}\right]_{lm}\right]$ can be written as follows.

$$E\left[\left[X^{-1}_{k+1}\right]_{ij}\left[X^{-1}_{k+1}\right]_{lm}\right] = E\left[e_i^T X^{-1}_{k+1} e_j e_l^T X^{-1}_{k+1} e_m\right] \quad (4.114)$$

$$= E\left[e_i^T E\left[X^{-1}_{k+1} e_j e_l^T X^{-1}_{k+1}\middle|\, X_k\right] e_m\right] \quad (4.115)$$

where $e_\ell \in \mathbb{R}^2$, $\ell = i, j, l, m$ is a vector filled with all zeros except for the ℓth element which is unity. In order to take the inner expectation in (4.115), the following theorem is required.

Theorem 7 (Theorem 3.4.5(i) from [21])**.** *Let $X \sim \mathcal{IW}_d(n, \Psi)$. Then*

$$E\left[XAX\right] = c_1 \Psi A \Psi + c_2\left[\Psi A^T \Psi + \mathrm{tr}\left(A\Psi\right)\Psi\right] \quad (4.116)$$

where A is a constant matrix of size $d \times d$ and the scalars c_1 and c_2 are defined as follows.

$$c_1 = (n-2d-3)c_2, \quad (4.117)$$

$$c_2 = \left[(n-2d-1)(n-2d-2)(n-2d-4)\right]^{-1}. \quad (4.118)$$

■

Noting that $X^{-1}_{k+1}|X_k \sim \mathcal{IW}\left(n_{k+1}+d+1, n_{k+1}X^{-1}_k\right)$, Theorem 7 can

be applied to take the inner expectation in (4.115) as follows.

$$\begin{aligned} E\left[X_{k+1}^{-1}e_j e_l^T X_{k+1}^{-1}\middle|\, X_k\right] =& c_1 n_{k+1}^2 X_k^{-1}e_j e_l^T X_k^{-1} \\ &+ c_2 n_{k+1}^2\Big(X_k^{-1}e_l e_j^T X_k^{-1} \\ &+ \mathrm{tr}[e_j e_l^T X_k^{-1}]X_k^{-1}\Big), \qquad (4.119) \\ =& c_1 n_{k+1}^2 X_k^{-1}e_j e_l^T X_k^{-1} \\ &+ c_2 n_{k+1}^2\Big(X_k^{-1}e_l e_j^T X_k^{-1} \\ &+ [X_k^{-1}]_{lj}X_k^{-1}\Big). \qquad (4.120) \end{aligned}$$

Substituting (4.120) into (4.115), we get

$$\begin{aligned} E\left[\left[X_{k+1}^{-1}\right]_{ij}\left[X_{k+1}^{-1}\right]_{lm}\right] =& E\Big[c_1 n_{k+1}^2\left[X_k^{-1}\right]_{ij}\left[X_k^{-1}\right]_{lm} \\ &+ c_2 n_{k+1}^2\Big(\left[X_k^{-1}\right]_{il}\left[X_k^{-1}\right]_{jm} \\ &+ \left[X_k^{-1}\right]_{lj}\left[X_k^{-1}\right]_{im}\Big)\Big] \qquad (4.121) \end{aligned}$$

where

$$c_1 = (n_{k+1}-d-2)c_2, \qquad (4.122)$$

$$c_2 = \left[(n_{k+1}-d)(n_{k+1}-d-1)(n_{k+1}-d-3)\right]^{-1}. \qquad (4.123)$$

– **Second term of** (4.113)**:** This term is left as it is.

– **Third term of** (4.113)**:**

$$E\left[\left[X_{k+1}^{-1}\right]_{ij}\left[X_k^{-1}\right]_{lm}\right] = E\left[\left[E\left[X_{k+1}^{-1}|X_k\right]\right]_{ij}\left[X_k^{-1}\right]_{lm}\right]. \qquad (4.124)$$

The inner expectation above is the same as that in (4.98). Hence we have

$$E\left[\left[X_{k+1}^{-1}\right]_{ij}\left[X_k^{-1}\right]_{lm}\right] = \frac{n_{k+1}}{n_{k+1}-d-1}E\left[\left[X_k^{-1}\right]_{ij}\left[X_k^{-1}\right]_{lm}\right]. \qquad (4.125)$$

– **Fourth term of** (4.113)**:** This term is calculated in the same way as the third term as follows.

$$\begin{aligned} E\left[\left[X_k^{-1}\right]_{ij}\left[X_{k+1}^{-1}\right]_{lm}\right] &= E\left[\left[X_k^{-1}\right]_{ij}\left[E\left[X_{k+1}^{-1}|X_k\right]\right]_{lm}\right] \\ &= \frac{n_{k+1}}{n_{k+1}-d-1}E\left[\left[X_k^{-1}\right]_{ij}\left[X_k^{-1}\right]_{lm}\right]. \qquad (4.126) \end{aligned}$$

Using the individual terms calculated above, the final form of (4.113) that can be reached by analytical manipulations is given as

$$\begin{aligned} d^{22}_{ij,lm} =& \frac{n^2_{k+1}}{4}\left(c_1\left(n_{k+1}-d-1\right)^2-1\right) E\left[\left[X_k^{-1}\right]_{ij}\left[X_k^{-1}\right]_{lm}\right] \\ &+ c_2\frac{n^2_{k+1}}{4}\left(n_{k+1}-d-1\right)^2 E\left[\left[X_k^{-1}\right]_{il}\left[X_k^{-1}\right]_{jm}\right] \\ &+ c_2\frac{n^2_{k+1}}{4}\left(n_{k+1}-d-1\right)^2 E\left[\left[X_k^{-1}\right]_{lj}\left[X_k^{-1}\right]_{im}\right]. \end{aligned} \tag{4.127}$$

The expectations above are also taken using Monte Carlo integration.

The last term that needs to be calculated for the posterior CRLB of the extent state is the term $E\left[\mathcal{I}^{22}_{k+1}(x_{k+1}, X_{k+1})\right]$ in (4.36). Here $\mathcal{I}^{22}_{k+1}(\cdot,\cdot)$ is the parametric FIM for the extent state (evaluated at the true kinematic and extent states x_{k+1} and X_{k+1} respectively) derived in Chapter 3 which is equal to I_{22} in (3.77). For the sake of completeness, we show $\mathcal{I}^{22}_{k+1}(\cdot,\cdot)$ below as well.

$$\mathcal{I}^{22}_{k+1}(\cdot,\cdot) = \begin{bmatrix} d_{11,11} & d_{11,12}+d_{11,21} & d_{11,22} \\ d_{12,11}+d_{21,11} & \begin{array}{c} d_{12,12}+d_{12,21} \\ +d_{21,12}+d_{21,22} \end{array} & d_{12,22}+d_{21,22} \\ d_{22,11} & d_{22,12}+d_{22,21} & d_{22,22} \end{bmatrix} \tag{4.128}$$

where

$$\begin{aligned} d_{ij,lm} \triangleq& \frac{s^2}{4}\bar{m}_{k+1}\Big(\left[(sX_{k+1}+R)^{-1}\right]_{il}\left[(sX_{k+1}+R)^{-1}\right]_{jm} \\ &+ \left[(sX_{k+1}+R)^{-1}\right]_{im}\ \left[(sX_{k+1}+R)^{-1}\right]_{lj}\Big). \end{aligned} \tag{4.129}$$

Note here again that $\bar{m}_k$ denotes the expected number of measurements at time k and it can be dependent on the target kinematic and extent states, i.e., $\bar{m}_k = \bar{m}_k(x_k, X_k)$. This dependence is suppressed in the expressions for the sake of brevity. Hence, $E\left[\mathcal{I}^{22}_{k+1}(x_{k+1}, X_{k+1})\right]$ is given as

$$\mathcal{I}^{22}_{k+1}(\cdot,\cdot) = \begin{bmatrix} \bar{d}_{11,11} & \bar{d}_{11,12}+\bar{d}_{11,21} & \bar{d}_{11,22} \\ \bar{d}_{12,11}+\bar{d}_{21,11} & \begin{array}{c} \bar{d}_{12,12}+\bar{d}_{12,21} \\ +\bar{d}_{21,12}+\bar{d}_{21,22} \end{array} & \bar{d}_{12,22}+\bar{d}_{21,22} \\ \bar{d}_{22,11} & \bar{d}_{22,12}+\bar{d}_{22,21} & \bar{d}_{22,22} \end{bmatrix} \tag{4.130}$$

where

$$\bar{d}_{ij,lm} = 0.25s^2 \Big(E\left[\bar{m}_{k+1}\left[(sX_{k+1}+R)^{-1}\right]_{il}\left[(sX_{k+1}+R)^{-1}\right]_{jm}\right] + E\left[\bar{m}_{k+1}\left[(sX_{k+1}+R)^{-1}\right]_{im}\left[(sX_{k+1}+R)^{-1}\right]_{lj}\right]\Big). \quad (4.131)$$

Here, Monte Carlo integration should again be used for taking the expectations.

4.3 Initialization of Posterior Cramér-Rao Lower Bound

The initial posterior CRLB's for the kinematic and extent states are examined separately below.

4.3.1 Initialization for the Posterior CRLB of the Kinematic State

The initial posterior FIM for the kinematic state is set as follows.

$$\tilde{\mathcal{I}}_0^x = E\left[\nabla_{x_0} \log p_{x_0}(x_0) \nabla_{x_0}^T \log p_{x_0}(x_0)\right]. \quad (4.132)$$

Assuming that $p_{x_0}(x_0) = \mathcal{N}(x_0; \bar{x}, P_0)$ would easily give us the following gradient.

$$\frac{\partial \log p_{x_0}(x_0)}{\partial x_0} = -Q^{-1}(x_0 - \bar{x}). \quad (4.133)$$

Hence, $\tilde{\mathcal{I}}_0^x$ is given as

$$\tilde{\mathcal{I}}_0^x = P_0^{-1} E\left[(x_0 - \bar{x})^T (x_0 - \bar{x})\right] P_0^{-1} \quad (4.134)$$

$$= P_0^{-1} \quad (4.135)$$

which means that

$$\tilde{\mathcal{I}}_0^x = P_0^{-1}. \quad (4.136)$$

This would yield the initial posterior CRLB given below.

$$\tilde{\mathcal{J}}_0^x = P_0. \quad (4.137)$$

4.3.2 Initialization for the Posterior CRLB of the Extent State

The initial posterior FIM for the extent state is set as follows.

$$\tilde{\mathcal{I}}_0^X = E\left[\nabla_{\xi_0^X} \log p_{X_0}(X_0)\, \nabla_{\xi_0^X}^T \log p_{X_0}(X_0)\right]. \tag{4.138}$$

We here assume that

$$p(X_0) = \mathcal{W}\left(X_0; \bar{n}, \frac{\bar{X}}{\bar{n}}\right) \tag{4.139}$$

which gives us the following gradient with respect to X_0.

$$\nabla_{X_0} \log p_{X_0}(X_0) = \frac{\bar{n} - d - 1}{2} X_0^{-1} - \frac{\bar{n}}{2} \bar{X}^{-1}. \tag{4.140}$$

Under the constraint $[X_0]_{12} = [X_0]_{21}$, the gradient of $\log p_{X_0}(X_0)$ with respect to ξ_0^X is given as

$$\nabla_{\xi_0^X} \log p_{X_0}(X_0) = \begin{bmatrix} [\nabla_{X_0} \log p_{X_0}(X_0)]_{11} \\ \\ [\nabla_{X_0} \log p_{X_0}(X_0)]_{12} \\ +[\nabla_{X_0} \log p_{X_0}(X_0)]_{21} \\ \\ [\nabla_{X_0} \log p_{X_0}(X_0)]_{22} \end{bmatrix}. \tag{4.141}$$

As a result, the matrix $\tilde{\mathcal{I}}_0^X$ will have the following form.

$$\tilde{\mathcal{I}}_0^X = \begin{bmatrix} d_{0,11,11} & d_{0,11,12} + d_{0,11,21} & d_{0,11,22} \\ d_{0,12,11} + d_{0,21,11} & \begin{matrix} d_{0,12,12} + d_{0,12,21} \\ +d_{0,21,12} + d_{0,21,22} \end{matrix} & d_{0,12,22} + d_{0,21,22} \\ d_{0,22,11} & d_{0,22,12} + d_{0,22,21} & d_{0,22,22} \end{bmatrix} \tag{4.142}$$

where

$$d_{0,ij,kl} \triangleq E\left[[\nabla_{X_0} \log p_{X_0}(X_0)]_{ij} [\nabla_{X_0} \log p_{X_0}(X_0)]_{kl}\right]. \tag{4.143}$$

The term $d_{0,ij,kl}$ can be calculated as follows.

$$\begin{aligned} d_{0,ij,kl} =& E\left[\left[\frac{\bar{n}-d-1}{2}X_0^{-1}-\frac{\bar{n}}{2}\bar{X}^{-1}\right]_{ij}\left[\frac{\bar{n}-d-1}{2}X_0^{-1}-\frac{\bar{n}}{2}\bar{X}^{-1}\right]_{kl}\right] \\ =& \frac{(\bar{n}-d-1)^2}{4}E\left[\left[X_0^{-1}\right]_{ij}\left[X_0^{-1}\right]_{kl}\right]+\frac{\bar{n}^2}{4}E\left[\left[\bar{X}^{-1}\right]_{ij}\left[\bar{X}^{-1}\right]_{kl}\right] \\ & -\frac{\bar{n}(\bar{n}-d-1)}{4}\left(E\left[\left[X_0^{-1}\right]_{ij}\left[\bar{X}^{-1}\right]_{kl}\right]+E\left[\left[\bar{X}^{-1}\right]_{ij}\left[X_0^{-1}\right]_{kl}\right]\right) \end{aligned} \tag{4.144}$$

The expectations involved in (4.144) are calculated one by one below.

- **First expectation of** (4.144)**:** This expectation involves the multiplication of two inverse Wishart distributed random matrices. By using Theorem 7 we can write

$$\begin{aligned} E\left[\left[X_0^{-1}\right]_{ij}\left[X_0^{-1}\right]_{kl}\right] =& c_1\bar{n}^2\left[\bar{X}^{-1}\right]_{ij}\left[\bar{X}^{-1}\right]_{kl}+c_2\bar{n}^2\left[\bar{X}^{-1}\right]_{ik}\left[\bar{X}^{-1}\right]_{jl} \\ & +c_2\bar{n}^2\left[\bar{X}^{-1}\right]_{kj}\left[\bar{X}^{-1}\right]_{il} \end{aligned} \tag{4.145}$$

  where

$$c_1 = c_2(\bar{n}-d-2), \tag{4.146}$$

$$c_2 = \left[(\bar{n}-d)(\bar{n}-d-1)(\bar{n}-d-3)\right]^{-1}. \tag{4.147}$$

- **Second expectation of** (4.144)**:** This expectation is left as it is.

- **Third expectation of** (4.144)**:** This expectation can be taken using Theorem 6 as follows.

$$E\left[\left[X_0^{-1}\right]_{ij}\left[\bar{X}^{-1}\right]_{kl}\right] = E\left[\left[X_0^{-1}\right]_{ij}\right]\left[\bar{X}^{-1}\right]_{kl} \tag{4.148}$$

$$= \frac{\bar{n}}{\bar{n}-d-1}\left[\bar{X}^{-1}\right]_{ij}\left[\bar{X}^{-1}\right]_{kl}. \tag{4.149}$$

- **Fourth expectation of** (4.144)**:** This expectation gives the same result as the previous case.

$$E\left[\left[\bar{X}^{-1}\right]_{ij}\left[X_0^{-1}\right]_{kl}\right] = \frac{\bar{n}}{\bar{n}-d-1}\left[\bar{X}^{-1}\right]_{ij}\left[\bar{X}^{-1}\right]_{kl}. \tag{4.150}$$

Combining the individual terms given above, we obtain $d_{0,ij,kl}$ as follows.

$$\begin{aligned} d_{0,ij,kl} =& \frac{\bar{n}^2}{4}\left(c_1\left(\bar{n}-d-1\right)^2-1\right)\left[\bar{X}^{-1}\right]_{ij}\left[\bar{X}^{-1}\right]_{kl} \\ & +c_2\frac{\bar{n}^2(\bar{n}-d-1)^2}{4}\left(\left[\bar{X}^{-1}\right]_{ik}\left[\bar{X}^{-1}\right]_{jl}+\left[\bar{X}^{-1}\right]_{kj}\left[\bar{X}^{-1}\right]_{il}\right) \end{aligned} \tag{4.151}$$

where the coefficients c_1 and c_2 are defined in (4.146) and (4.147) respectively.

4.4 Computation of Posterior Cramér-Rao Lower Bound for Semi-Major and Semi-Minor Axes

Derivation of posterior CRLB for semi-major and semi-minor axes of the extent ellipsoid follows the same procedure as the one in Section 3.3 except that an expectation has to be taken over the Jacobian of the nonlinear transformation as described in Section 2.2.2. Note that we have the semi-major and semi-minor axes given as

$$a^2_{\text{major,minor}}(X) = \frac{X_{11} + X_{22} \mp \sqrt{(X_{11} + X_{22})^2 - 4\left(X_{11}X_{22} - X_{12}^2\right)}}{2} \tag{4.152}$$

where $+$ and $-$ signs in $\mp$ correspond to the semi-major and semi-minor axes of the extension respectively. The gradients for $a_{\text{major}}(\cdot)$ and $a_{\text{minor}}(\cdot)$ are given as

$$\nabla_{\xi^X} a_{\text{major}}(X) = \frac{1}{2a_{\text{major}}(X)} \begin{bmatrix} \frac{1}{2} + \frac{X_{11} - X_{22}}{2\sqrt{(\operatorname{tr} X)^2 - 4\det X}} \\ 2\frac{X_{12}}{\sqrt{(\operatorname{tr} X)^2 - 4\det X}} \\ \frac{1}{2} + \frac{X_{22} - X_{11}}{2\sqrt{(\operatorname{tr} X)^2 - 4\det X}} \end{bmatrix}, \tag{4.153}$$

$$\nabla_{\xi^X} a_{\text{minor}}(X) = \frac{1}{2a_{\text{minor}}(X)} \begin{bmatrix} \frac{1}{2} - \frac{X_{11} - X_{22}}{2\sqrt{(\operatorname{tr} X)^2 - 4\det X}} \\ -2\frac{X_{12}}{\sqrt{(\operatorname{tr} X)^2 - 4\det X}} \\ \frac{1}{2} - \frac{X_{22} - X_{11}}{2\sqrt{(\operatorname{tr} X)^2 - 4\det X}} \end{bmatrix}. \tag{4.154}$$

Using the result of Section 2.2.2, we can write the posterior CRLB of the semi-major and semi-minor axes as follows.

$$\tilde{\mathcal{J}}_k^{a_{\text{major}}} = E\left[\nabla^T_{\xi_k^X} a_{\text{major}}(X_k)\right] \tilde{\mathcal{J}}_k^X E\left[\nabla_{\xi_k^X} a_{\text{major}}(X_k)\right], \tag{4.155}$$

$$\tilde{\mathcal{J}}_k^{a_{\text{minor}}} = E\left[\nabla^T_{\xi_k^X} a_{\text{minor}}(X_k)\right] \tilde{\mathcal{J}}_k^X E\left[\nabla_{\xi_k^X} a_{\text{minor}}(X_k)\right] \tag{4.156}$$

where the expectations are taken using Monte Carlo integration.

CHAPTER 5

SIMULATIONS

In this chapter, the performance of the ETT algorithm proposed in [11] and described in Chapter 2 is compared to the parametric and posterior CRLBs in MATLAB environment. The organization of the chapter is given as follows. In Sections 5.1 and 5.2, parametric and posterior bound simulations are made respectively. In each respective section, first, the implementation of the corresponding bound is described and then the simulation results are presented. Finally, in Section 5.3, the dependence of the performance of the ETT algorithm is tested with respect to some parameters of interest.

5.1 Parametric Cramér-Rao Lower Bound

5.1.1 Implementation

The definition and the details of parametric CRLB were presented in Chapter 3. The most important remark concerning this bound is that the states are considered to be deterministic parameters with measurements which are contaminated with noise.

5.1.1.1 True Target & Measurement Parameters

During the realization of the algorithm, a scenario that includes a target moving with constant velocity, having a fixed extension size and orientation is considered. Hence, the true trajectory of the extension center is generated using a

nearly constant velocity (CV) model. The system dynamics of the CV model is determined by the state equation given below.

$$x_{k+1} = Fx_k + Bw_k \tag{5.1}$$

where F is the state transition matrix for a target moving on 2 dimensional space, defined as

$$F \triangleq \begin{bmatrix} 1 & 0 & T & 0 \\ 0 & 1 & 0 & T \\ 0 & 0 & 1 & 0 \\ 0 & 0 & 0 & 1 \end{bmatrix} \tag{5.2}$$

and B is the noise gain matrix,

$$B \triangleq \begin{bmatrix} \frac{T^2}{2} & 0 & T & 0 \\ 0 & \frac{T^2}{2} & 0 & T \end{bmatrix}^T. \tag{5.3}$$

w_k is the process noise with $w_k \sim \mathcal{N}(0, Q)$ and T is the sampling time. In all simulations, the sampling time T is set to be $T = 1\,\mathrm{s}$. The total duration of the scenario is $100\,\mathrm{s}$.

The matrix Q represents the process noise covariance matrix. For the parametric CRLB, the true target trajectories are generated by taking the matrix Q to be a zero matrix. The fixed true initial state is selected to be $x_0 = \begin{bmatrix} 0\,\mathrm{m} & 0\,\mathrm{m} & 500\,\mathrm{m/s} & 500\,\mathrm{m/s} \end{bmatrix}^T$. Note that in this case, the true motion of the target does not contain any acceleration, and therefore fixed and deterministic which is a requirement of the parametric CRLB.

The extension of the target which is ellipsoidal is represented by a positive definite symmetric matrix with dimension of 2×2. The orientation and the size of the ellipsoid are determined by two sets of parameters; two eigenvectors which control the extent direction and two eigenvalues that represent the semi-major and semi-minor axes of the ellipsoid. The true extension state X_k is assumed to be constant along time, i.e., we have

$$X_{k+1} = X_k. \tag{5.4}$$

The fixed extent state X_k is formed as follows.

$$X_k = E\Lambda E^T \tag{5.5}$$

for all k where the eigenvector matrix, E, is determined by the object orientation angle, α, as given below.

$$E = \begin{bmatrix} \cos\alpha & -\sin\alpha \\ \sin\alpha & \cos\alpha \end{bmatrix}. \tag{5.6}$$

The diagonal matrix Λ containing the eigenvalues in its diagonal is given as follows.

$$\Lambda = \begin{bmatrix} a^2_{\text{major}} & 0 \\ 0 & a^2_{\text{minor}} \end{bmatrix}. \tag{5.7}$$

In the experiments, the true values of the extent parameters are taken to be $\alpha = 45^\circ$, $a_{\text{major}} = 300\,\text{m}$, $a_{\text{minor}} = 100\,\text{m}$.

The position measurements are generated by drawing random numbers from the following Gaussian distribution at each scan.

$$y^i_k \sim \mathcal{N}(Hx_k, sX_k + R) \tag{5.8}$$

where

$$H = \begin{bmatrix} 1 & 0 & 0 & 0 \\ 0 & 1 & 0 & 0 \end{bmatrix}, \tag{5.9}$$

$$R = \sigma^2_v \begin{bmatrix} 1 & 0 \\ 0 & 1 \end{bmatrix}, \tag{5.10}$$

where $\sigma^2_v = 1000\,\text{m}^2$ and the scalar s is taken to be $s = 1$ in all simulations. The number of measurements generated per scan is taken to be non-random and constant for all time instants, i.e., $m_k = m$ for all k. Monte Carlo simulations are conducted for different numbers of measurements. The selected values for this purpose are $m = 5$, $m = 20$ and $m = 80$.

A segment of the fixed true target trajectory and a single realization of the random measurements are displayed in Figure 5.1.

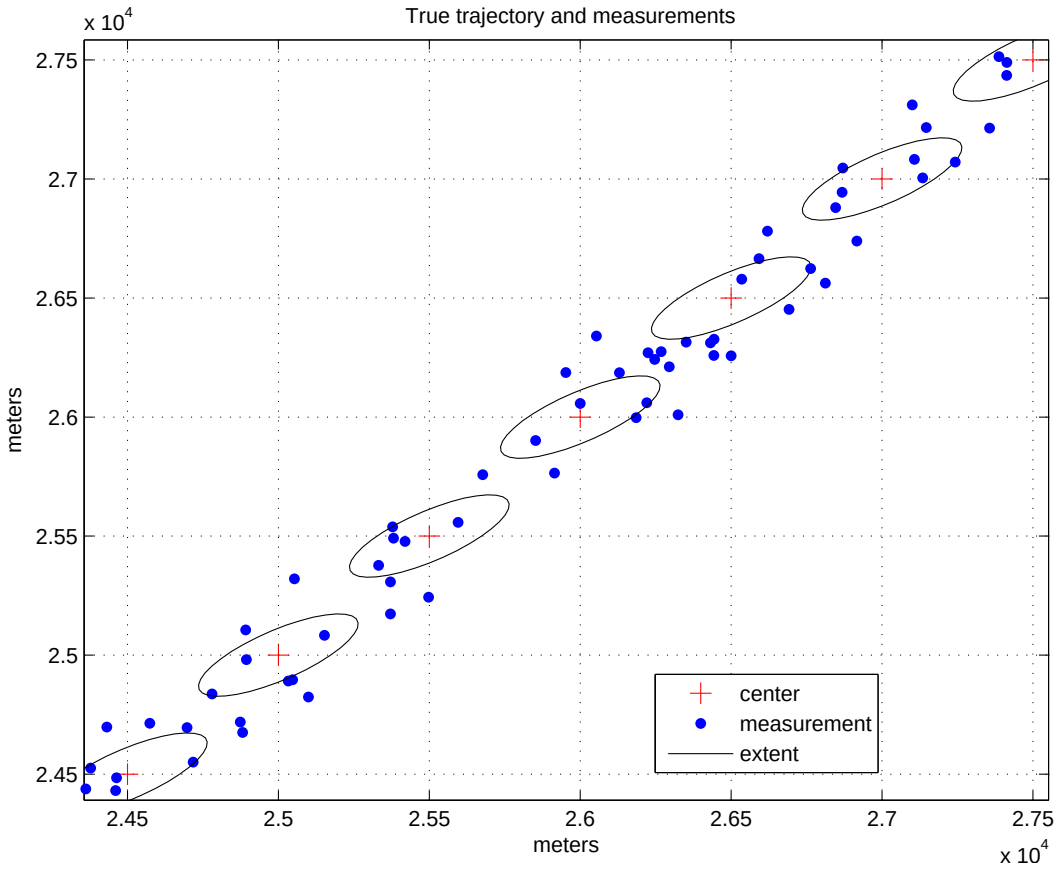

Figure 5.1: True trajectory and a single realization of measurements.

5.1.1.2 ETT Algorithm Parameters

After the measurements are generated, they are supplied to the ETT algorithm described in Section 2.1.1. The parameters of the ETT algorithm are selected as follows.

The initial kinematic and extent state estimates of the algorithm, i.e., $x_{0|-1}$ and $X_{0|-1}$ are selected randomly for each Monte Carlo run as follows.

$$x_{0|-1} \sim \mathcal{N}(x_0, P_0) \tag{5.11}$$

$$X_{0|-1} \sim \mathcal{W}_2\left(n_0, \frac{X_0}{n_0}\right) \tag{5.12}$$

where x_0 and X_0 are the true initial kinematic and extent states respectively and

$$P_0 = \text{diag}\left[75\,\text{m}^2, 75\,\text{m}^2, 15\,\text{m}^2/\text{s}^2, 15\,\text{m}^2/\text{s}^2\right], \tag{5.13}$$

$$n_0 = 10. \tag{5.14}$$

As a result, the parametric CRLB for the kinematic state has been initialized with P_0. The parametric CRLB for the extent state is initialized with the covariance of the Wishart distribution in (5.12) whose explicit expression is given in (3.87) in Chapter 3.

Other initial parameters for the ETT algorithm are given as

$$P_{0|-1} = P_0, \tag{5.15}$$

$$\alpha_{0|-1} = 2.1. \tag{5.16}$$

The ETT algorithm uses the state model in (5.1) where the process noise covariance Q is selected to be

$$Q = \sigma_v^2 \begin{bmatrix} 1 & 0 \\ 0 & 1 \end{bmatrix}. \tag{5.17}$$

where $\sigma_v^2 = 1\,\text{m}^2/\text{s}^4$. The prediction for the extent is made using the forgetting parameter $\tau = 5$.

5.1.2 Results

In this subsection, the performance of the ETT algorithm is evaluated by analyzing the RMS errors for its estimates and comparing these errors to (the square root of) the CRLB results. Moreover, the changes in the RMS errors of the ETT estimator and CRLBs are observed for different deterministic number of measurements, m_k, received in a scan. As mentioned earlier, the number of measurements is set to 5, 20 and 80 for different Monte Carlo simulations each involving 10000 Monte Carlo runs.

The RMS position and velocity errors in x and y axes are illustrated in Figure 5.2 along with the corresponding parametric CRLB values. It is worth to remind that FIM of the kinematical states is directly proportional to the (expected) number of measurements as shown in (3.76). A close examination of the results reveals that the square-roots of the parametric CRLBs are halved as the number of measurements is quadrupled.

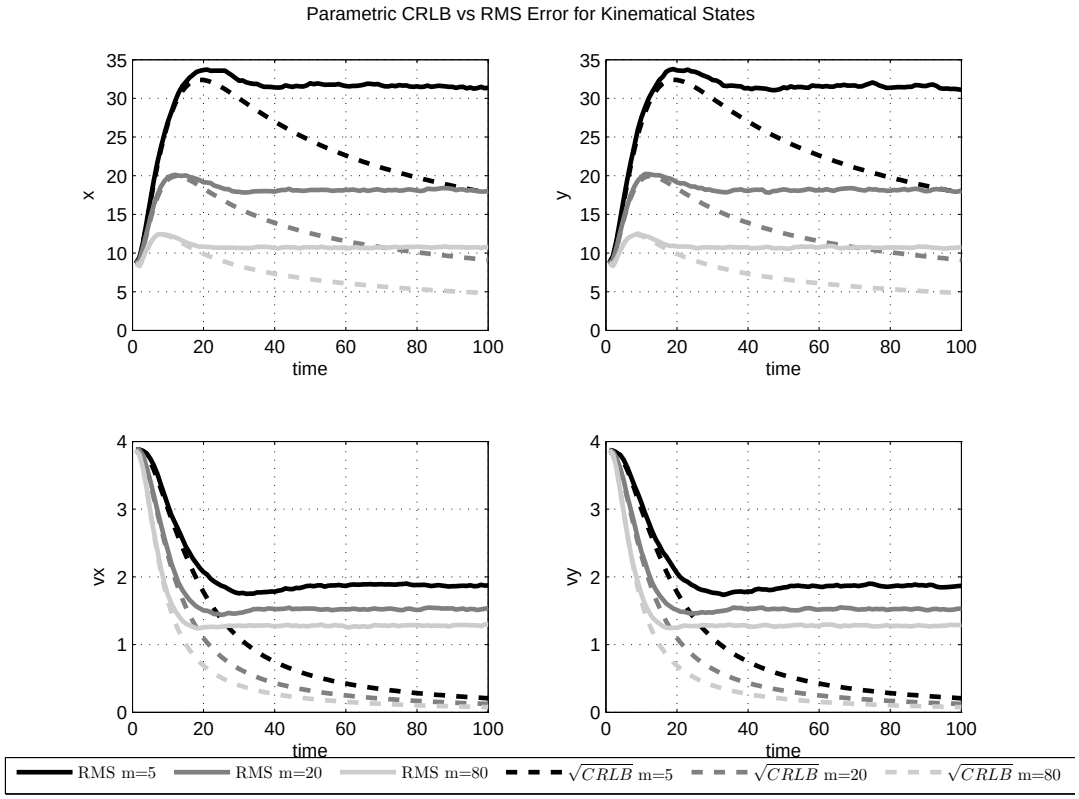

Figure 5.2: RMS errors and parametric CRLB values for kinematical states with $m = 5$, $m = 20$ and $m = 80$.

Figure 5.3 shows the parametric CRLBs and the RMS errors for the extents. The extent matrix elements mentioned in the figure are defined as below.

$$X \triangleq \begin{bmatrix} a_{11} & a_{12} \\ a_{21} & a_{22} \end{bmatrix} \tag{5.18}$$

where $a_{12} = a_{21}$. Similar to the previous results, a four-fold increase in the number of measurements yields a reduction by one-half on the parametric bounds due to the direct relationship between the (expected) number of measurements and the FIM of the extension, which is described in (3.74).

RMS errors obtained for the semi-major and semi-minor axes of the extension are compared to the corresponding parametric CRLB's in Figure 5.4. The results in the figure look quite similar to those for the extension matrix elements.

One major observation that is obtained by examining the figures for the parametric CRLB is that although the RMS errors follow the corresponding bounds at the onset of the scenario, the bound decreases so fast that the RMS error cannot follow it any longer. This is a characteristics of the parametric CRLB where the state is assumed to be deterministic with no process noise. The estimation algorithms like Kalman filters or the ETT algorithm we work with, on the other hand, have to use a non-zero process noise covariance matrix Q for avoiding divergence. Hence for the parametric CRLB there is always a mismatch between the truth and the model parameters used in the estimation algorithms.

We now examine the average CRLBs and average RMS values along time. We define these values as the square root of the mean of CRLB values along time and root-mean-square of the RMS values along time, respectively. Tables 5.1, 5.2 and 5.3 summarize the estimator performances and CRLBs for the kinematic states, extent states and the semi-major semi-minor axes, respectively. It is clear from the tables that the derived expressions ensure a lower bound to the estimation errors. Increasing number of measurements yields to better estimates in terms of error variances. Additionally, it can be claimed that the considered estimator is almost efficient for kinematical state estimation, in contrast to the extension estimation performance which fails to get closer to the bound for small number of measurements. Similar to the extension results, semi-major and semi-

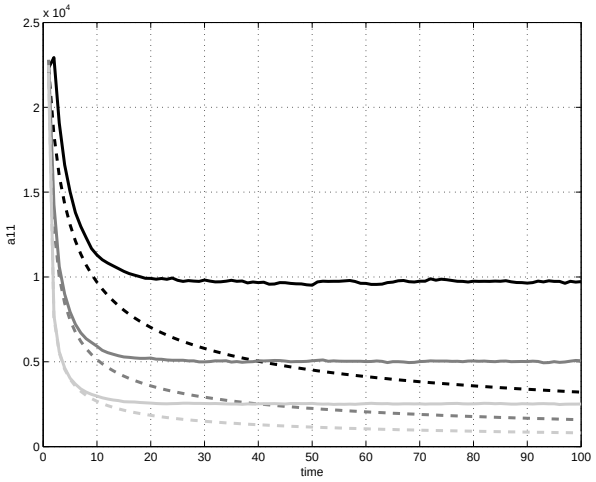

(a) a_{11} (m^2)

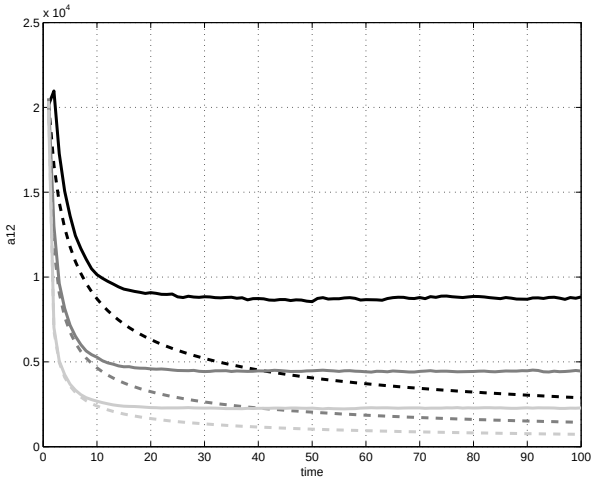

(b) a_{12} (m^2)

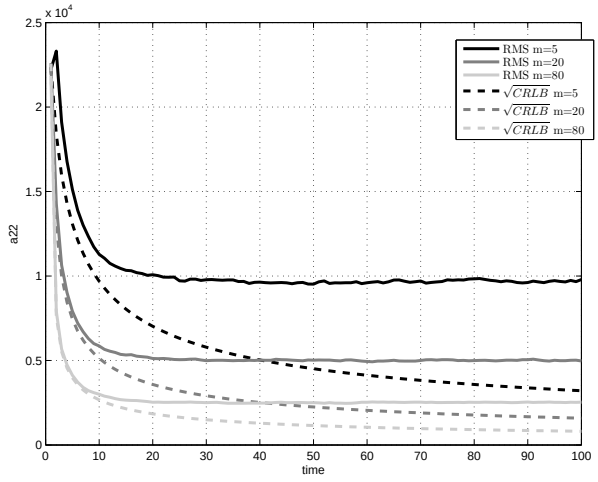

(c) a_{22} (m^2)

Figure 5.3: RMS errors and parametric CRLB values for extension with $m = 5$, $m = 20$ and $m = 80$.

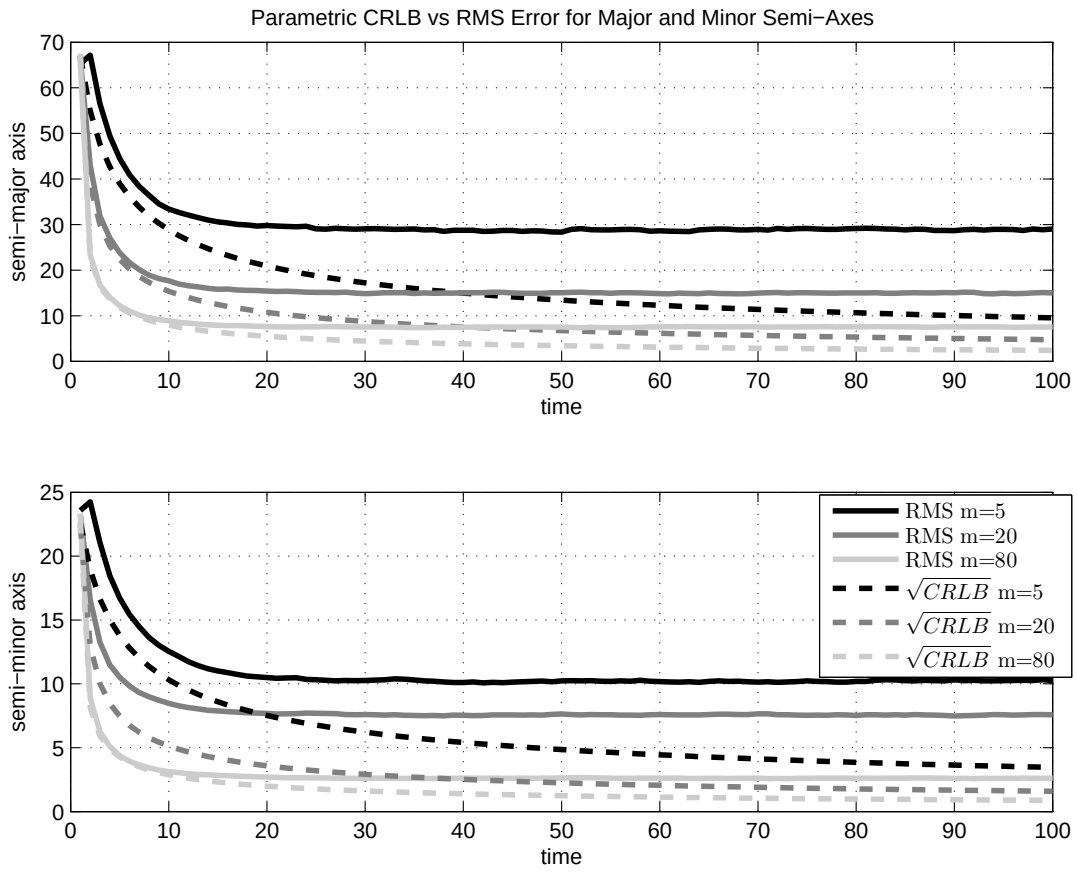

Figure 5.4: RMS errors and parametric CRLB values for major and minor semi-axes with $m = 5$, $m = 20$ and $m = 80$.

minor axes estimation performance degrades a lot with decreasing number of measurements. Nevertheless, the errors for all states can decrease substantially with sufficient measurement numbers.

It is also worth to mention that when the number of measurements is quadrupled, the RMS errors in the position estimates drop with $\sqrt{2}$, while the velocity errors are divided by $\sqrt[4]{2}$. A similar inference can be made for the extension performances as follows. When the number of measurements is quadrupled, errors in the extension entries and semi-major, semi-minor axes are approximately divided by $\sqrt{2}$.

Tables 5.4 and 5.5 present the average standard deviations of RMS errors (along both Monte Carlo runs and time) for the kinematic states and extension states respectively. It is seen that the average standard deviations are quite large meaning that the variation in the performance of the algorithm is quite large

among the Monte Carlo runs.

Table 5.1: Average RMS errors and average parametric CRLBs for kinematical states.

m	Kinematical state RMS errors				Kinematical state parametric CRLB			
	x[m]	y[m]	v_x[m/s]	v_y[m/s]	x[m]	y[m]	v_x[m/s]	v_y[m/s]
5	30.5	30.5	2.1	2.1	24.0	24.0	1.5	1.5
20	18.1	18.1	1.8	1.8	13.5	13.5	1.2	1.2
80	10.8	10.8	1.5	1.5	7.7	7.7	1.0	1.0

Table 5.2: Average RMS errors and average parametric CRLBs for extension.

m	Extension RMS error			Extension parametric CRLB		
	a_{11}[m^2]	a_{12}[m^2]	a_{22}[m^2]	a_{11}[m^2]	a_{12}[m^2]	a_{22}[m^2]
5	10542	9520	10519	6492	5885	6502
20	5916	5277	5896	4051	3667	4050
80	3535	3189	3525	2881	2602	2886

Table 5.3: Average RMS errors and average parametric CRLBs for semi-major and semi-minor axes.

m	RMS error		Parametric CRLB	
	Semi-major axis[m]	Semi-minor axis[m]	Semi-major axis[m]	Semi-minor axis[m]
5	12.92	31.54	6.47	19.50
20	8.29	17.60	4.05	12.14
80	3.74	10.53	2.99	8.61

Table 5.4: Average standard deviations of RMS errors for kinematical states.

m	x[m]	y[m]	v_x[m/s]	v_y[m/s]
5	36.5	36.5	2.6	2.6
20	21.7	21.7	2.2	3.05
80	12.9	12.9	1.8	1.8

Table 5.5: Average standard deviations of RMS errors for extension states.

m	$a_{11}[\mathrm{m}^2]$	$a_{21}[\mathrm{m}^2]$	$a_{22}[\mathrm{m}^2]$
5	13378	12155	13372
20	7224	6556	6556
80	4486	3971	4419

5.2 Posterior Cramér-Rao Lower Bound

5.2.1 Implementation

The definition and the details of the posterior CRLB were presented in Chapter 4. As explained in Chapter 4, the most distinctive feature of the posterior CRLB is that it considers states as random variables in contrast to parametric CRLB. As a result of this property, complicated expected values appear in its formulation, which makes the application of Monte Carlo integration techniques necessary.

5.2.1.1 Trajectory and Measurement Generation

The implementation of the posterior CRLB requires using Monte Carlo techniques to take the expectations. In order to do so, multiple random target and measurement scenarios are generated. The initial states for the kinematic and extent states of the target are selected from the following pdfs.

$$x_0 \sim \mathcal{N}(\bar{x}_0, P_0) \tag{5.19}$$

$$X_0 \sim \mathcal{W}_2\left(n_0, \frac{\overline{X}_0}{n_0}\right) \tag{5.20}$$

where $\overline{X}_0$ a fixed extent state with $a_{\mathrm{major}} = 300\,\mathrm{m}$, $a_{\mathrm{minor}} = 100\,\mathrm{m}$, and the orientation $\alpha = 45°$. The parameters $\bar{x}_0$, P_0 and n_0 are given as

$$\bar{x}_0 = x_0, \tag{5.21}$$

$$P_0 = \mathrm{diag}\left[75\,\mathrm{m}^2, 75\,\mathrm{m}^2, 15\,\mathrm{m}^2/\mathrm{s}^2, 15\,\mathrm{m}^2/\mathrm{s}^2\right], \tag{5.22}$$

$$n_0 = 20000. \tag{5.23}$$

The kinematic and extent states evolve in time according to the following transition pdfs.

$$p(x_{k+1}|x_k) = \mathcal{N}(x_{k+1}; Fx_k, Q) \tag{5.24}$$

$$p(X_{k+1}|X_k) = \mathcal{W}\left(X_{k+1}; n_{k+1}, \frac{X_k}{n_{k+1}}\right) \tag{5.25}$$

where F is the CV state transition matrix defined in (5.2) with the sampling period $T = 1\,\text{s}$; the process noise covariance Q is given in (5.17) and $n_{k+1} = 20000$ for all k. The total duration of the scenarios is $100\,\text{s}$.

Once the random trajectories are obtained, measurements are produced for each trajectory from the corresponding randomly generated kinematical states and extensions. The measurement pdf from which the measurements are drawn is the same as the one used in the parametric CRLB which is given below.

$$y_k^i \sim \mathcal{N}(Hx_k, sX_k + R)$$

where H and R are given in (5.9) and (5.10), respectively and $s = 1$. The number of measurements generated per scan is again taken to be non-random and constant for all time instants, i.e., $m_k = m$ for all k. Monte Carlo simulations are conducted for different numbers of measurements. The selected values for this purpose are $m = 5$, $m = 20$ and $m = 80$ as before.

Some examples of the random kinematical state trajectories and the measurements generated from one of the random trajectories are shown in Figure 5.5.

5.2.1.2 Computation of Posterior Cramér-Rao Lower Bound

Posterior CRLB is implemented using the expressions derived in Chapter 4. Many of these expressions involve the expected values whose computations are analytically impossible. Therefore, Monte Carlo integration method is used to take the expectations numerically. In this subsection, we explain what this technique is by providing the theory behind it.

Monte Carlo is defined loosely by Anderson in [25] as "the art of approximating an expectation by the sample mean of a function of simulated random variables".

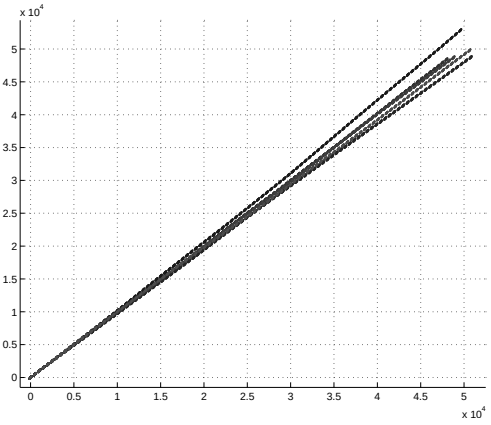

(a) Samples from random trajectories.

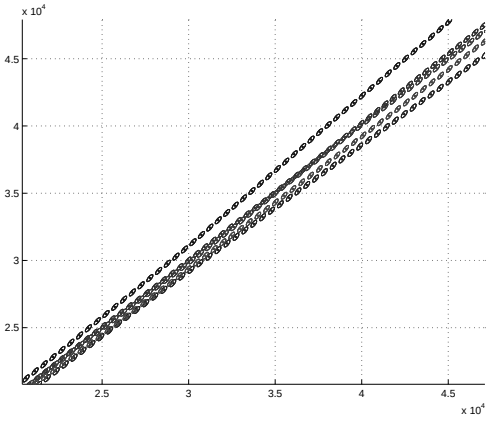

(b) A segment from random trajectories.

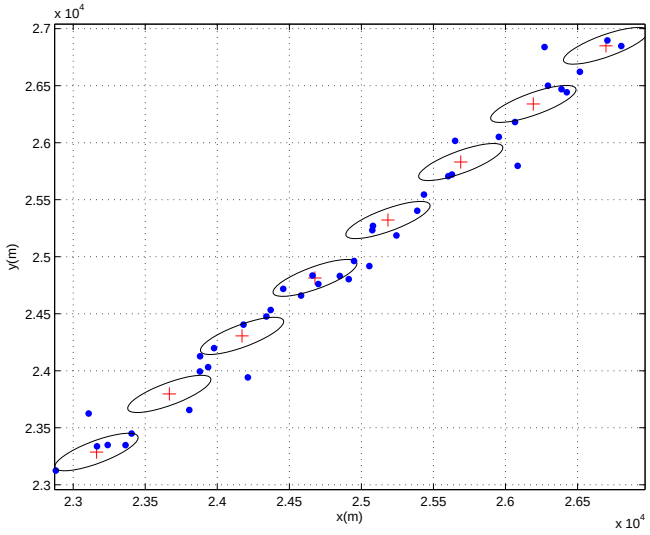

(c) Random measurements.

Figure 5.5: Random trajectories and a single realization of measurements.

Though there are many other definitions in the literature, this one is quite meaningful for the problem considered in this study. A Monte Carlo integration method is applied when the integration of a function is not possible by means of analytical manipulations due to nonlinearities or dimensions. Contrary to other integration techniques, the Monte Carlo technique makes use of statistical inference.

Let us assume that x is a random variable having the pdf $f_X(x)$ defined in $\mathcal{X}$, i.e., $x \in \mathcal{X}$. Then, the expected value of a function $g(\cdot)$ of x can be written as follows.

$$E\left\{g(x)\right\} = \int_{x \in \mathcal{X}} g(x) f_X(x) dx. \tag{5.26}$$

This expectation can be approximated via Monte Carlo integration by considering N independent samples of x as follows.

$$\hat{g}(x) = \frac{1}{N} \sum_{i=1}^{N} g(x_i). \tag{5.27}$$

According to the strong law of large numbers, the greater the number of samples, the closer the estimate gets to the true value which is mathematically expressed as follows.

$$\lim_{N \to \infty} \frac{1}{N} \sum_{i=1}^{N} g(x_i) = E\left[g(x)\right]. \tag{5.28}$$

If the variance of this estimator is investigated, it can be seen that the estimation errors decrease with $1/\sqrt{N}$.

The expectations derived in Section 4.2 require the application of Monte Carlo integration for two main reasons. First of all, the expected values are to be taken with respect to the random variable X_k whose pdf is unidentified. Secondly, even if the pdf were known, it might be still unachievable to compute these expectations analytically, since they are highly nonlinear in matrix variables.

In the experiments, randomly generated kinematical states and extensions are employed as samples in Monte Carlo integration, and the number of samples, N_{mc}, is set to 10000.

5.2.1.3 ETT Algorithm Parameters

ETT algorithm is run on N_{mc} sets of measurements that are generated from the random trajectories. The differences between the estimates of the ETT algorithm and randomly generated states are calculated for each run, and the RMS errors of estimates are computed by averaging the individual errors over the Monte Carlo runs.

While executing the algorithm, the kinematic and extent estimates, $x_{0|-1}$ and $X_{0|-1}$,respectively, are initialized as described below for each Monte Carlo run.

$$x_{0|-1} \sim \mathcal{N}(\bar{x}_0, P_0) \tag{5.29}$$

$$X_{0|-1} \sim \mathcal{W}_2\left(n_0, \frac{\overline{X}_0}{n_0}\right) \tag{5.30}$$

where $\overline{X}_0$ is the same fixed extent as in (5.20) in Section 5.1.1.1 and

$$\bar{x}_0 = x_0, \tag{5.31}$$

$$P_0 = \text{diag}\left[75\,\text{m}^2, 75\,\text{m}^2, 15\,\text{m}^2/\text{s}^2, 15\,\text{m}^2/\text{s}^2\right], \tag{5.32}$$

$$n_0 = 10. \tag{5.33}$$

The initial covariance matrix of kinematical estimate and the initial value of the parameter $\alpha_{0|-1}$ are given below.

$$P_{0|-1} = P_0, \tag{5.34}$$

$$\alpha_{0|-1} = 2.1. \tag{5.35}$$

The process noise covariance Q used in the ETT filter is given in (5.17) and the forgetting parameter is set to be $\tau = 5$.

5.2.2 Results

This section provides the performance comparison of the ETT algorithm by means of the posterior CRLB. The comparison is made in the same way as the previous section by using the RMS errors and the square roots of the posterior CRLB. Similar to the parametric bound case, the results are produced for three different measurement numbers: $m = 5$, $m = 20$ and $m = 80$.

The first set of results to be analyzed is the RMS errors for the kinematical states which consist of positions and velocities in x and y coordinates. Figure 5.6 presents these results for all numbers of measurements simultaneously. It is apparent from the figure that as the number of measurements increases, the bounds and the errors decrease. If one examines the expressions derived for the information submatrices and the recursion for posterior FIM in (4.4) carefully, it can be seen that FIM is an affine function of the number of measurements which is the main reason for the drops in the bounds.

Another observation that is quite significant is that RMS errors for all kinematical states follow the posterior CRLB almost perfectly after an initial convergence

period, which is a strong indication that the estimator under investigation is almost optimal in the MMSE sense.

The observations above can be repeated for the extension estimation as well considering Figure 5.7. Larger numbers of measurements result in smaller RMS errors and bounds. The reasoning that the relationship between the bound and the number of measurements being affine is valid also for the extension. Contrary to the previous results, the RMS errors cannot reach the bounds which indicates that a superior estimator might be developed in order to estimate extension.

The results corresponding to semi-major and semi-minor axes are shown in Figure 5.8. Since the bounds for the axes are linked to those of the extension with a transformation independent from the number of measurements, the errors and bounds change in a similar fashion. Furthermore, the bounds always stay below the errors meaning that the estimation of major and minor semi-axes are not efficient (in an estimation theoretical sense).

The comparison of average RMS errors and posterior CRLB is provided in Tables 5.6, 5.7 and 5.8. It is easy to see the decrease in the error and the bound with respect to increasing number of measurements. The average RMS errors for the kinematical states are pretty close to the posterior bound indicating that estimator is almost optimal and hence efficient (in an estimation theoretical sense) for kinematic states. Furthermore, the position errors and velocity errors decrease by $\sqrt{2}$ and $\sqrt[4]{2}$, respectively with quadrupled number of measurements, as in the parametric case. There is still room for an improvement in the estimation of extension and its features, since the average RMS errors are rather above the bounds. A reduction by $\sqrt{2}$ is seen in the errors of extension and semi-major, semi-minor axes estimates when the number of measurements is quadrupled.

Tables 5.9 and 5.10 illustrate the average standard deviations of the RMS errors in kinematic and extent states, respectively. The variations in the RMS errors again seem to be too large over the Monte Carlo runs although they become lower as the number of measurements grows.

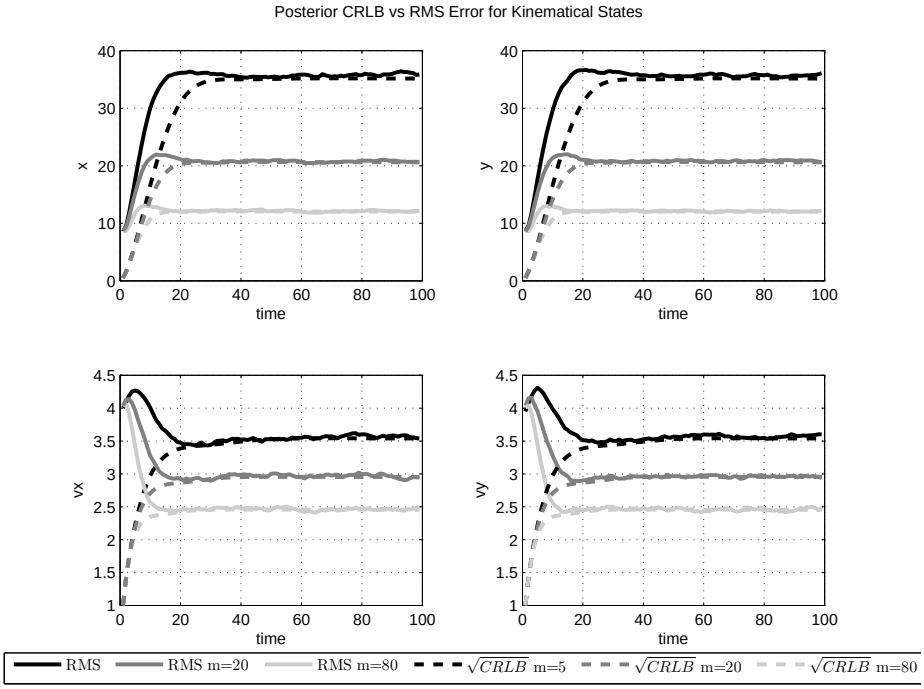

Figure 5.6: RMS errors and posterior CRLB values for kinematical states with $m = 5$, $m = 20$ and $m = 80$.

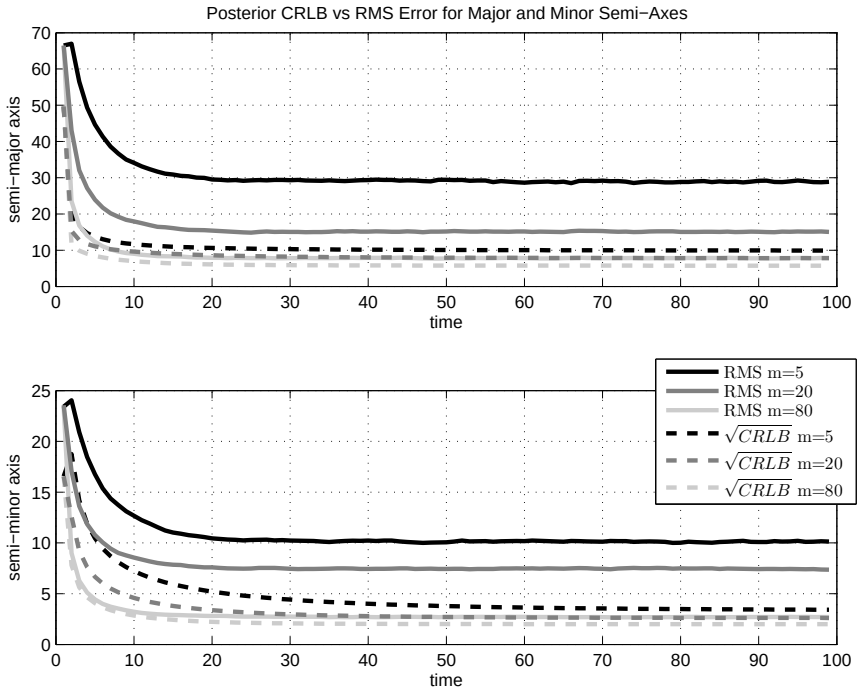

Figure 5.8: RMS errors and posterior CRLB values for major and minor semi-axes with $m = 5$, $m = 20$ and $m = 80$.

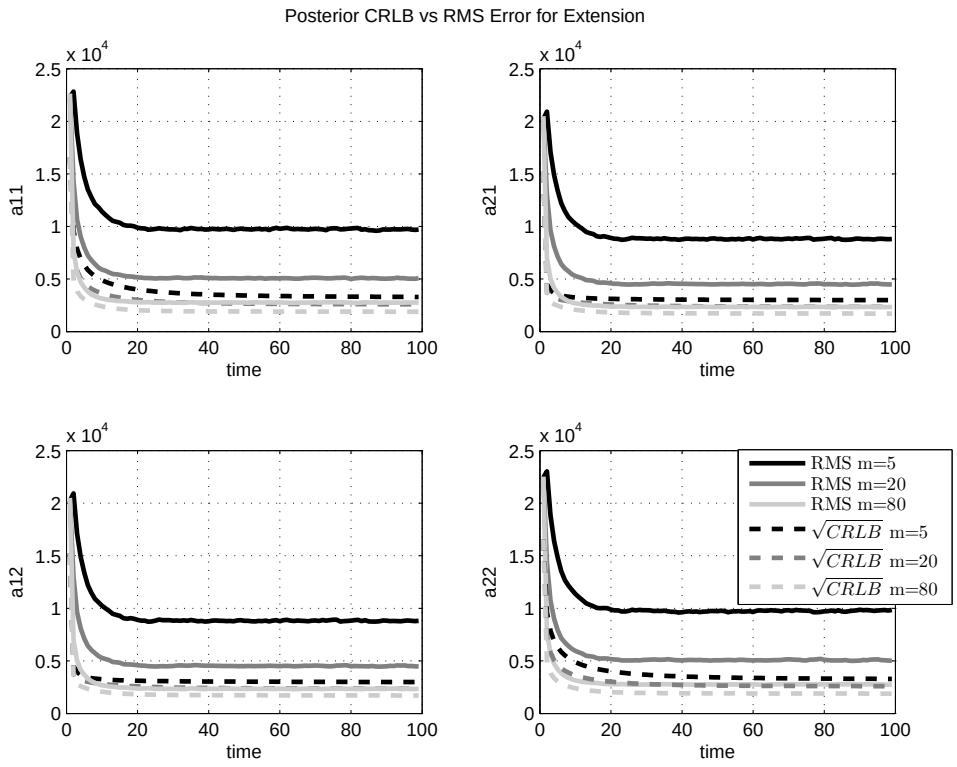

Figure 5.7: RMS errors and posterior CRLB values for extension states with $m = 5$, $m = 20$ and $m = 80$.

Table 5.6: Average RMS errors and average posterior CRLB values for kinematical states.

m	Kinematical state RMS errors				Kinematical state posterior CRLB			
	x[m]	y[m]	v_x[m/s]	v_y[m/s]	x[m]	y[m]	v_x[m/s]	v_y[m/s]
5	33.2	33.2	3.4	3.4	31.9	31.9	3.3	3.3
20	19.8	19.8	2.9	2.9	19.2	19.2	2.8	2.8
80	11.9	11.9	2.4	2.4	9.3	13.3	2.4	2.4

Table 5.7: Average RMS errors and average posterior CRLB values for extension.

m	Extension RMS errors			Extension posterior CRLB		
	a_{11}[m^2]	a_{21}[m^2]	a_{22}[m^2]	a_{11}[m^2]	a_{21}[m^2]	a_{22}[m^2]
5	10588	9577	10584	4226	3422	4225
20	5941	5318	5948	3401	2908	3399
80	3604	3296	3652	2676	2375	2677

Table 5.8: Average RMS errors and average posterior CRLB values for semi-major and semi-minor axes.

m	RMS error		Posterior CRLB	
	Semi-major axis[m]	Semi-minor axis[m]	Semi-major axis[m]	Semi-minor axis[m]
5	12.763	31.69	5.25	11.57
20	8.224	17.72	3.87	9.72
80	3.8	10.79	2.89	7.86

Table 5.9: Average standard deviations of RMS errors for kinematical states.

m	x[m]	y[m]	v_x[m/s]	v_y[m/s]
5	41.1	41.1	4.3	4.3
20	24.3	24.4	3.6	2.2
80	14.4	14.4	3.1	3.1

Table 5.10: Average standard deviations of RMS errors for extension states.

m	a_{11}[m^2]	a_{12}[m^2]	a_{22}[m^2]
5	13714	12155	13657
20	7364	6634	6634
80	4509	4032	4703

5.3 Dependence of the Estimator Performance on Some Parameters

In the experiments of the previous subsections, the same set of parameters (except the number of measurements) is used in the ETT filter. These parameters are given as

$$Q = \begin{bmatrix} 1 & 0 \\ 0 & 1 \end{bmatrix}, \quad R = \begin{bmatrix} 1000 & 0 \\ 0 & 1000 \end{bmatrix}, \quad \tau = 5. \tag{5.36}$$

The algorithm performance with different numbers of measurements was investigated and it was realized that the performance becomes acceptable when the number of measurements exceeds 20, which is so high that it may not be attainable even with the state of the art radars today for even the largest targets.

Therefore, in this section we investigate whether the performance of the algorithm, the extent estimation performance in particular, can be improved for low number of measurements by adjusting some parameters properly.

Several trials are made by adjusting the process noise covariance matrix, Q, measurement noise covariance matrix, R, and the time constant τ used in the ETT algorithm. Due to the fact that the experiments with the numbers of measurements $m_k = 20$ and $m_k = 80$ result in acceptable performances, we only consider the low number of measurements, $m_k = 5$.

5.3.1 Dependence on Process Noise Covariance Matrix Q

In this subsection, the sensitivity of RMS estimation errors to the process noise covariance matrix used in the ETT algorithm is examined. Three different process noise covariance matrices are used, namely, Q_{normal}, Q_{high} and Q_{low}. The covariance matrix Q_{normal} is the one used in the previous simulations and is given as

$$Q_{\text{normal}} = \begin{bmatrix} 1 & 0 \\ 0 & 1 \end{bmatrix} \text{m}^2/\text{s}^4. \tag{5.37}$$

The standard deviations are tripled for the high process noise covariance matrix Q_{high} and reduced by three times to obtain the low process noise covariance matrix Q_{low}. Hence, we have

$$Q_{\text{high}} = 3^2 \begin{bmatrix} 1 & 0 \\ 0 & 1 \end{bmatrix} \text{m}^2/\text{s}^4, \tag{5.38}$$

$$Q_{\text{low}} = \left(\frac{1}{3}\right)^2 \begin{bmatrix} 1 & 0 \\ 0 & 1 \end{bmatrix} \text{m}^2/\text{s}^4. \tag{5.39}$$

Note that the process noise covariance matrices given above are used only in the ETT algorithm. The process noise covariance matrices used for generating the true kinematical states remain the same as those in the previous subsections. For this reason, the parametric and posterior CRLB values will remain the same as those shown in the previous subsections.

RMS estimation errors for the kinematical states for the cases of parametric CRLB and posterior CRLB are shown in Figures 5.9 and 5.10 respectively. For the case of parametric CRLB, in Figure 5.9, we see that the errors in kinematic state estimation decrease considerably as the process noise covariances get smaller. Since in the case of parametric CRLB, there is no process noise in the states, the smaller the process noise covariance used in the ETT algorithm, the more there is model match in the filter. Hence the results get better as the process noise covariance gets smaller.

For the case of posterior CRLB in Figure 5.10, the best estimates are obtained when the ETT algorithm uses the process noise covariance matrix Q_{normal} which is employed in the generation of the true state trajectories. The other process noise covariance matrices result in larger estimation errors due to the model mismatch in the filter.

The results for the extent states, semi-major and semi-minor axes are not shown here since it has been observed that these results are insensitive to the process noise covariance used in the ETT algorithm.

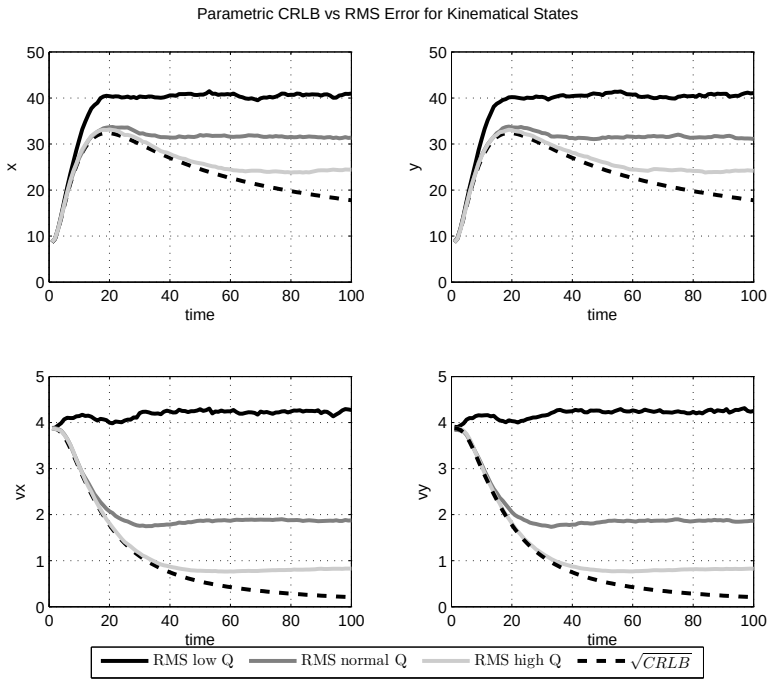

Figure 5.9: RMS errors and parametric CRLB values for kinematical states with different process noise covariance matrices.

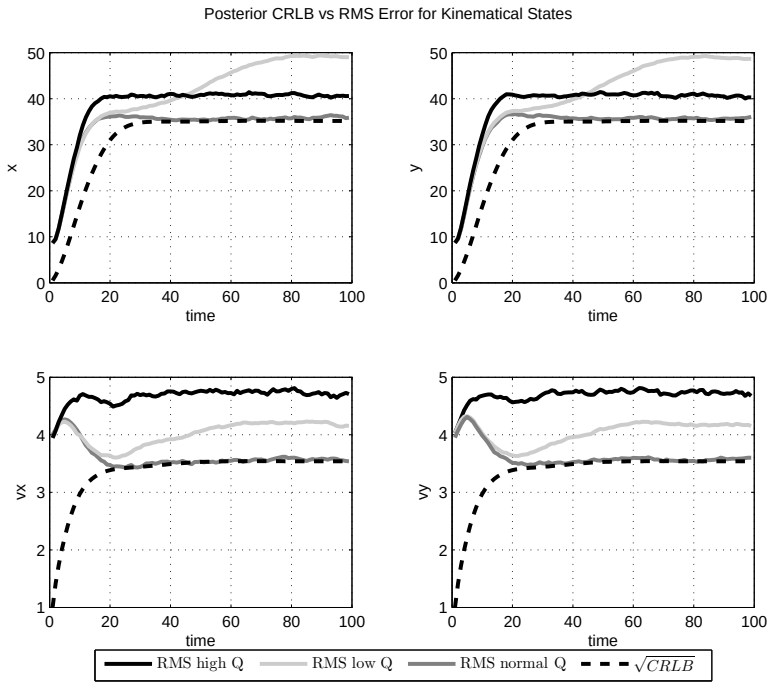

Figure 5.10: RMS errors and posterior CRLB values for kinematical states with different process noise covariance matrices.

5.3.2 Dependence on Measurement Noise Covariance Matrix R

In this subsection, the sensitivity of RMS estimation errors to the measurement noise covariance matrix used in the ETT algorithm is examined. Three different measurement noise covariance matrices are used, namely, R_{normal}, R_{high} and R_{low}. The covariance matrix R_{normal} is the one used in the simulations of the previous subsections and is given as

$$R_{\text{normal}} = \begin{bmatrix} 1000 & 0 \\ 0 & 1000 \end{bmatrix} \text{m}^2 \tag{5.40}$$

The standard deviations are tripled for the high measurement noise covariance matrix R_{high} and reduced by three times to obtain the low measurement noise covariance matrix R_{low}. Hence, we have

$$R_{\text{high}} = 3^2 \begin{bmatrix} 1000 & 0 \\ 0 & 1000 \end{bmatrix} \text{m}^2, \tag{5.41}$$

$$R_{\text{low}} = \left(\frac{1}{3}\right)^2 \begin{bmatrix} 1000 & 0 \\ 0 & 1000 \end{bmatrix} \text{m}^2. \tag{5.42}$$

Note that the measurement noise covariance matrices given above are used only in the ETT algorithm. The measurement noise covariance matrices used for generating the measurements remain the same as those in the previous subsections. For this reason, the parametric and posterior CRLB values will remain the same as those shown in the previous subsections.

It has been observed in the simulations that the measurement noise covariance has almost no effect on kinematical state estimation performance. Therefore, the kinematical state estimation results are not shown. Figures 5.11 and 5.12 show the extent estimation performance for the parametric and posterior CRLB cases respectively. Figures 5.13 and 5.14 illustrate the RMS errors for major and minor semi-axes estimates for the parametric and posterior CRLB cases respectively. It is seen in the figures that the extent estimation performance depends on the measurement noise covariance used in the filter. The dependence of the extent estimates on the measurement noise covariance appears significantly only in the diagonal entries of the extent. The dependence is stronger in semi-minor axis than in semi-major axis. It is seen that the measurement noise covariances R_{normal} and R_{low} yield almost the same results which indicates that using smaller measurement noise covariances than the actual measurement noise covariances does not affect the extent estimation results much. This phenomenon arise from the fact that measurement noise covariance matrix become negligible compared to extent matrix X_k as it gets smaller. On the other hand, the use of R_{high} noticeably degrades the estimation performance. This happens because when the filter thinks that the measurement noise covariance is higher than its true value, it tries to make the extent estimate considerably smaller than the true extent to take care of the increased measurement noise covariance.

5.3.3 Dependence on Forgetting Factor τ

The final trials are made by changing the time constant τ used in the ETT algorithm. Since the trajectories obey a CV model with a static or almost static extension size and orientation, the parameter τ which is described as "a time constant related to the agility with which the object may change its extension

over time" in [11] can be set to a greater value.

It has been observed that the kinematical estimation errors are rather insensitive to the value of τ used in the ETT algorithm. Therefore the results for the kinematical states are not shown here.

In Figures 5.15 and 5.16, extent estimation performances are shown for the cases of parametric and posterior CRLB respectively. Figures 5.17 and 5.18 illustrate the performance for the estimates of the semi-major and semi-minor axes for the cases of parametric and posterior CRLB respectively. Note that the parametric and posterior CRLBs shown in these figures are the same as the ones obtained for $m = 5$ in the figures presented in the previous subsections. It is observed that increasing the time constant leads to considerable reductions in the estimation errors which is due to the increased model match between the filter and the true extent. By increasing τ from 5 to 20, the errors of the extent estimates are decreased so much that the performance with 20 measurements is achieved only with 5 measurements. In order to find the limits of the performance dependence on this parameter, different trials with time constants $\tau = 60$, $\tau = 80$ and $\tau = 100$ are made. By doing so, it is revealed that the estimation performance converges to a limit which is depicted by the results obtained for $\tau = 100$ in the figures. In the case of parametric CRLB a very high value for τ means an almost perfect model match between the filter and the true extent. Therefore, the RMS errors almost reach the parametric CRLB values making the ETT algorithm (almost) efficient. In the case of posterior CRLB, there is still a significant gap between the CRLB and the corresponding RMS errors for $\tau = 100$. Therefore, for random parameter cases, there is still a chance for an improvement. Note that it is important to emphasize here that if a more random and dynamic extent scenario was used in the posterior CRLB case, there might have been a significant degradation in the extent estimation performances for very high values of τ. Overall, the time constant τ should be seen as a critical parameter which determines the extension estimation performance for the extent estimation scenarios considered in this work.

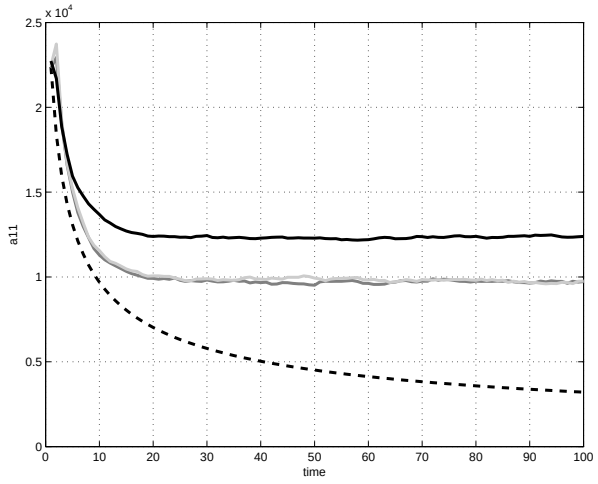

(a) a_{11} (m^2)

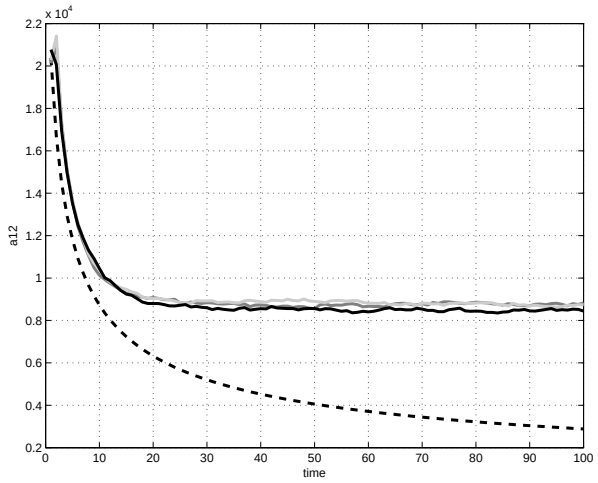

(b) a_{12} (m^2)

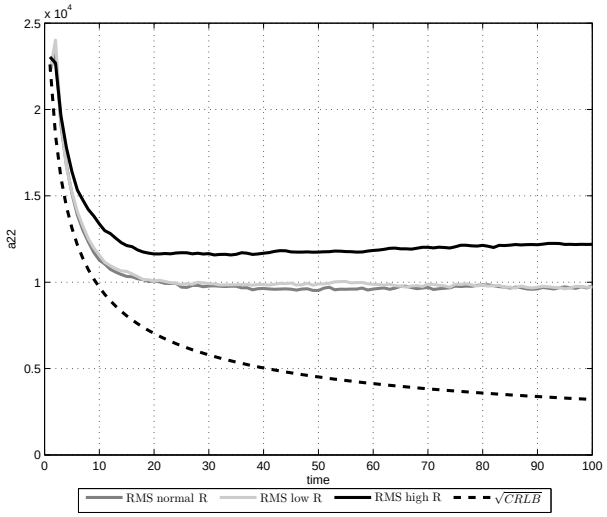

(c) a_{22} (m^2)

Figure 5.11: RMS errors and parametric CRLB values for extension with different measurement noise covariance matrices.

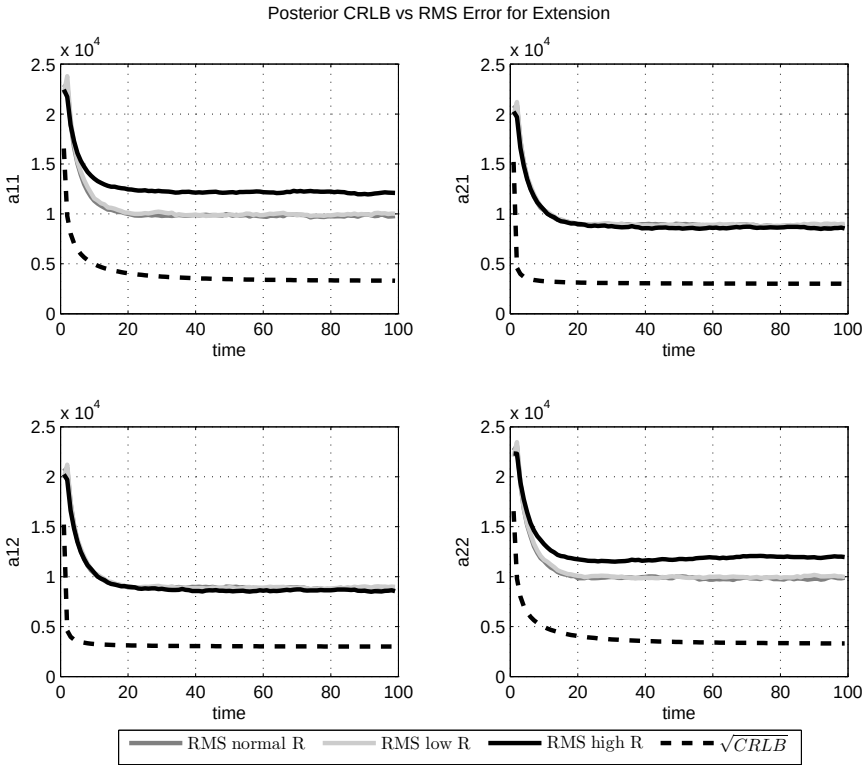

Figure 5.12: RMS errors and posterior CRLB values for extension estimates with different measurement noise covariance matrices.

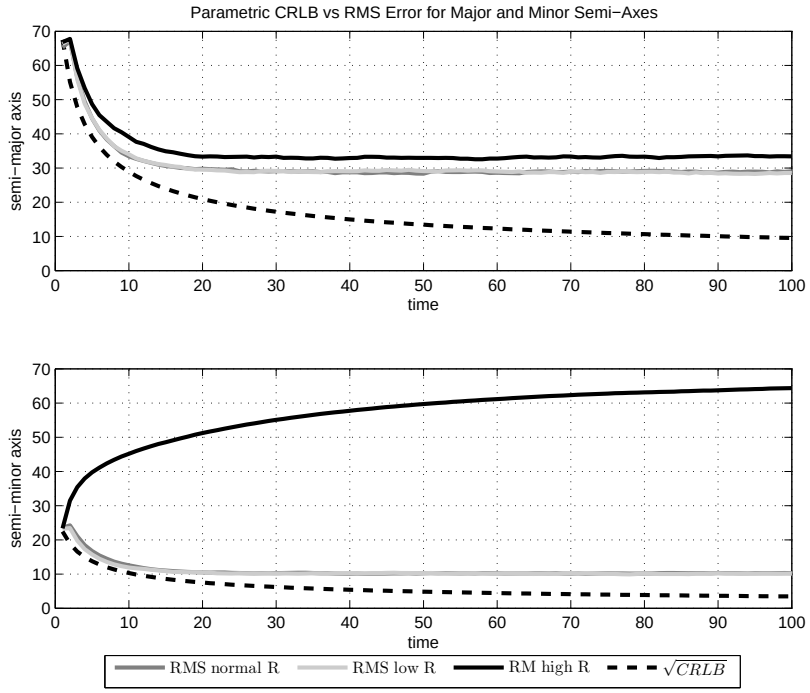

Figure 5.13: RMS errors and parametric CRLB values for semi-major and semi-minor axes estimates with different measurement noise covariance matrices.

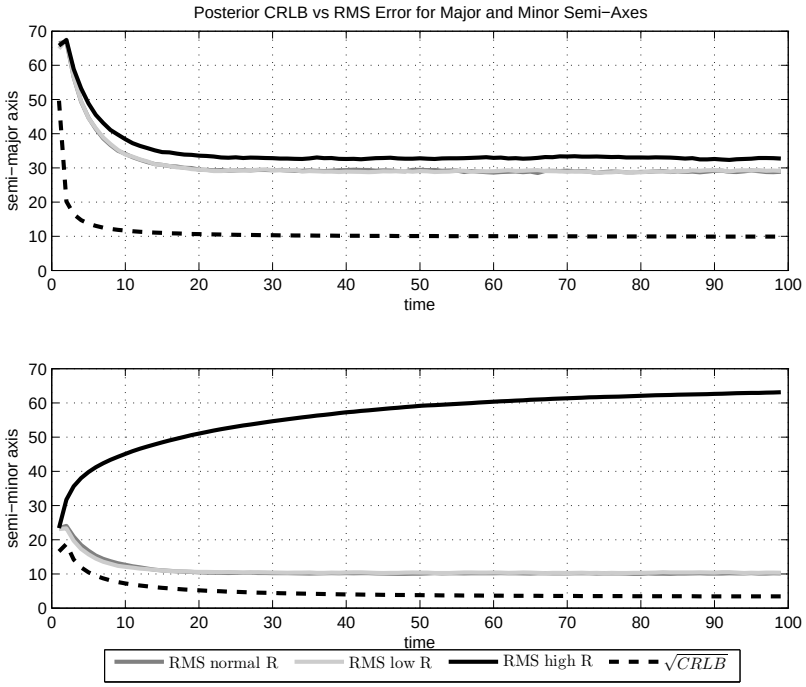

Figure 5.14: RMS errors and posterior CRLB values for semi-major and semi-minor axes estimates with different measurement noise covariance matrices.

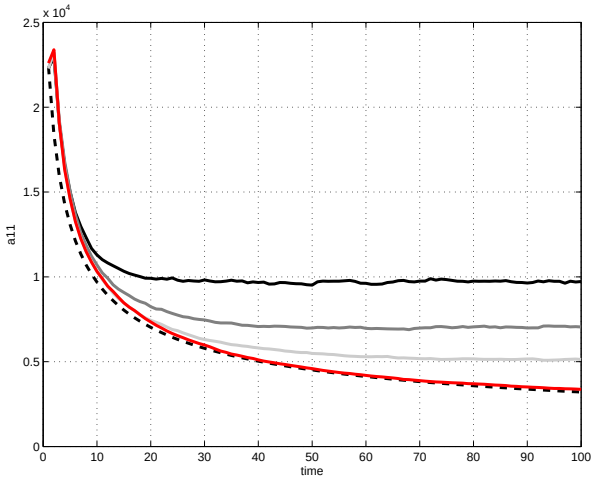

(a) a_{11} (m^2)

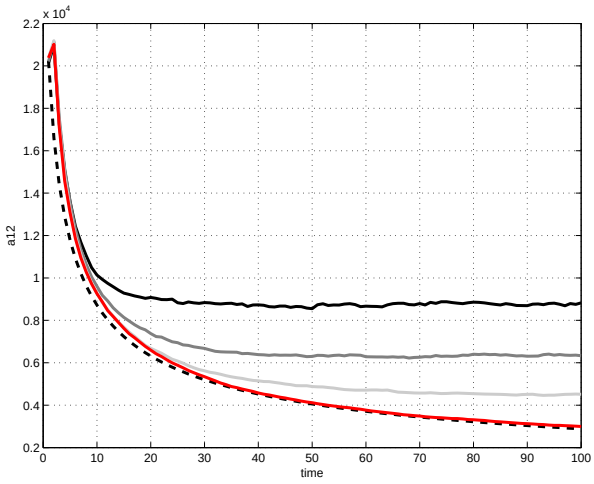

(b) a_{12} (m^2)

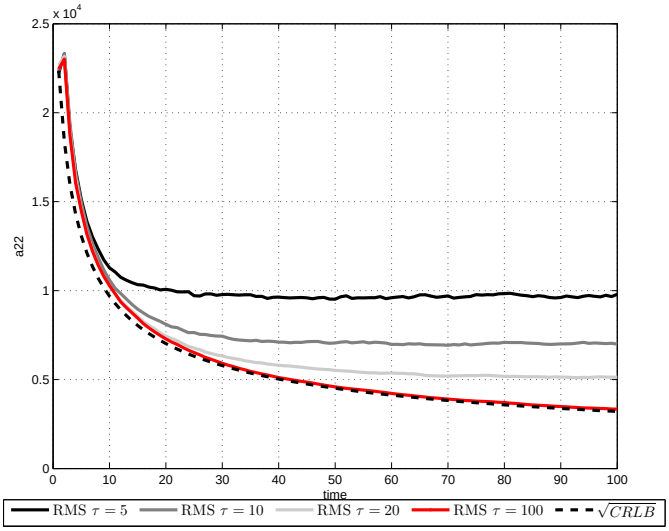

(c) a_{22} (m^2)

Figure 5.15: RMS errors and parametric CRLB values for extension with $\tau = 5$, $\tau = 10$, $\tau = 20$ and $\tau = 100$.

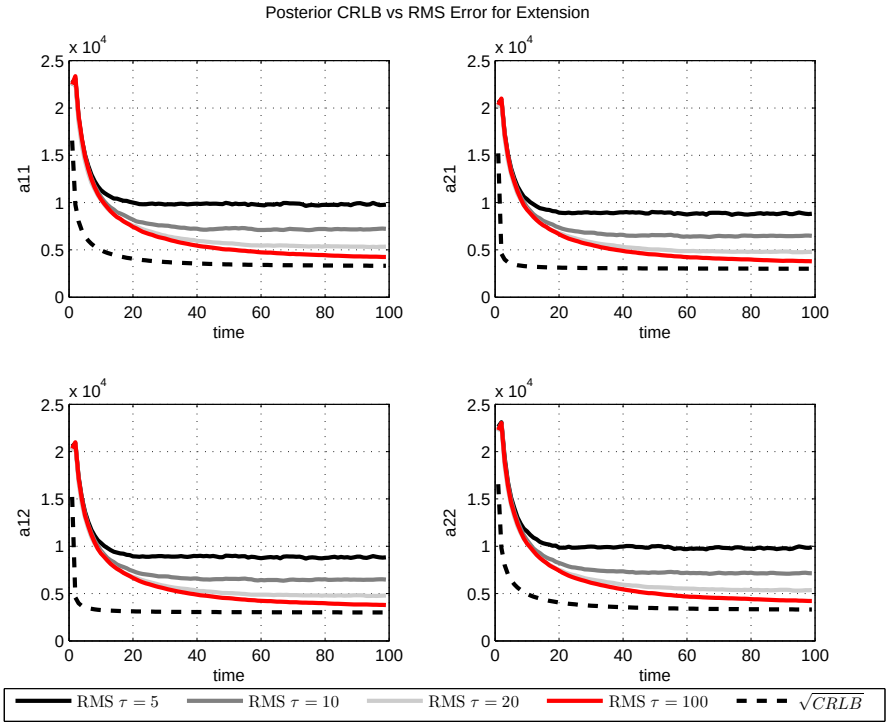

Figure 5.16: RMS errors and posterior CRLB values for extension with $\tau = 5$, $\tau = 10$, $\tau = 20$ and $\tau = 100$.

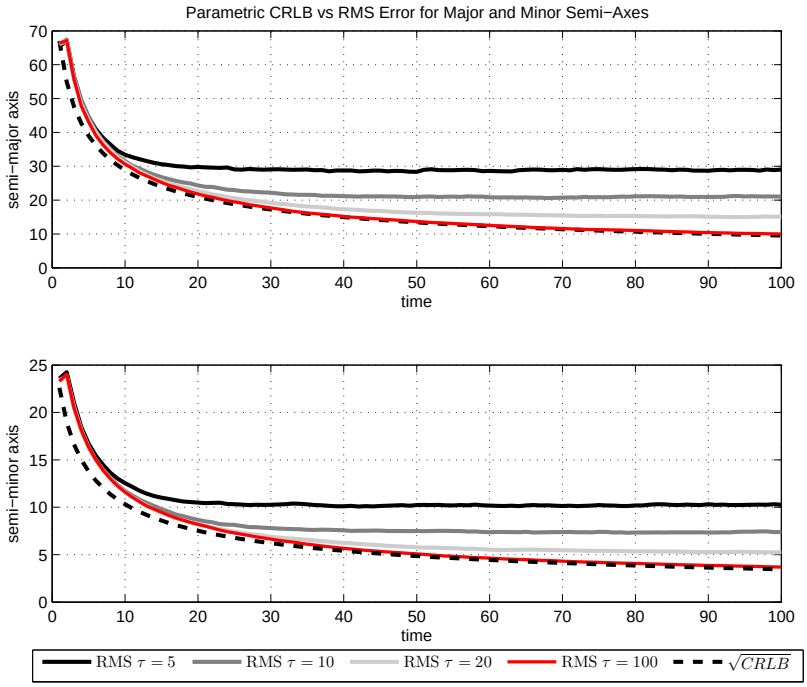

Figure 5.17: RMS errors and parametric CRLB for major and minor semi-axes with $\tau = 5$, $\tau = 10$, $\tau = 20$ and $\tau = 100$.

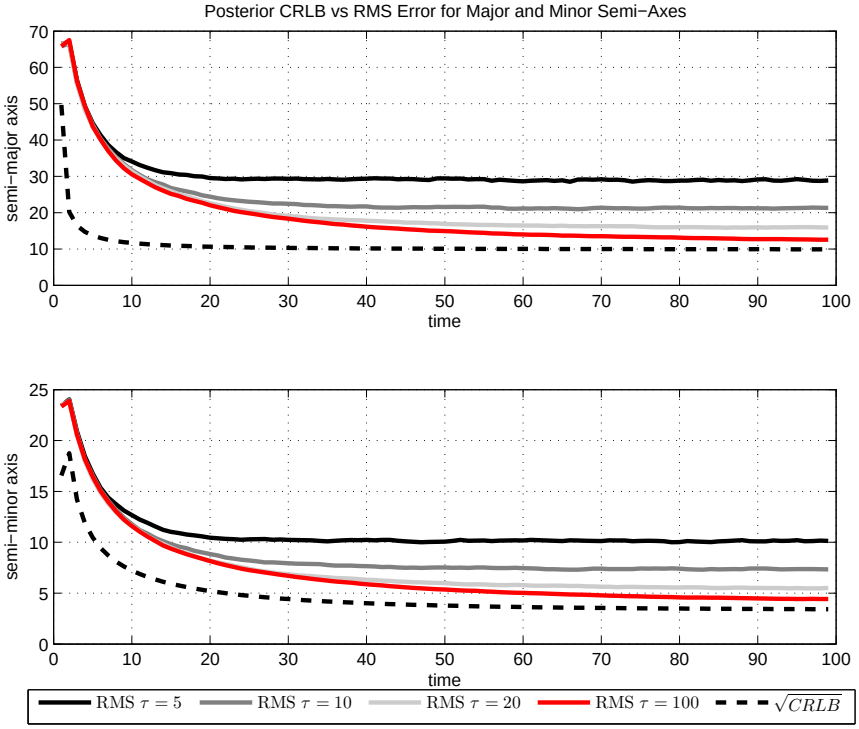

Figure 5.18: RMS errors and posterior CRLB values for major and minor semi-axes with $\tau = 5$, $\tau = 10$, $\tau = 20$ and $\tau = 100$.

CHAPTER 6

CONCLUSIONS

The aim of this thesis has been to evaluate the performance of a state-of-the-art ETT algorithm proposed by Feldmann et al. in [11] by means of CRLBs. The parameters whose estimates are included in the performance analysis are: kinematical states, extension and its semi-major and semi-minor axes. The problem is defined as a discrete time, nonlinear filtering problem which brings along the necessity to establish a recursion for the assessment of the performance.

Two different CRLBs have been derived in this work; namely, the parametric CRLB and posterior CRLB. In parametric CRLB, the system is modeled in such a way that states to be estimated are deterministic, yet unknown and the measurements are random. The expressions of FIM related to this bound are derived by employing the likelihood function of the noisy measurements. This bound is only useful for dynamic systems which has no process noise and for evaluating the performance of unbiased estimates. For posterior CRLB, which can be used for performance evaluation of both biased and unbiased estimators for dynamic systems with random states, the state space representation of the model involves the transition pdfs of the states and the likelihood function of the observations. Using these distributions, the FIM expressions are obtained with the help of analytical and numerical techniques. The recursion from [22] is employed for the posterior bound; and while implementing the bound Monte Carlo techniques are exploited.

The simulations show that the ETT algorithm can be described as an (almost) efficient estimator for kinematical state estimation. Moreover, it has been proved

that the estimator is capable of estimating extension and its semi-major and semi-minor axes satisfactorily with a CV motion model. Investigation of the effects of the number of measurements reveals that increasing the number of measurements results in higher-quality estimates, as expected. For reaching close extent RMS error values to the CRLB, many measurements above 10 are required under model-mismatch conditions.

Dependence of the performance of the algorithm on several parameters has been tested. It was seen that

- The process noise covariance matrix used in the ETT algorithm does not affect the extent estimation performance much.
- The measurement noise covariance matrix used in the ETT algorithm does not affect the kinematic estimation performance much.
- The time constant used in the ETT algorithm does not affect the kinematic estimation performance much.

In addition to these, it was observed that

- The measurement noise covariance matrix used in the ETT algorithm affects the extent error performance, especially for the diagonal elements of the extent matrix and the semi-minor axis of the extent ellipse.
- The extent estimation performance is more sensitive to large values of measurement noise covariance than small values compared to the true measurement noise covariance.
- The extent estimation performance is closely dependent on the forgetting time constant used in the ETT algorithm.

To the author's best knowledge, this is the first study which derives and uses CRLBs for examining the performance of an ETT algorithm in a random matrix framework.

The subject of this thesis is a fruitful research area for further work. Firstly, more studies need to be carried out in order to examine the performance of

the algorithm under different motion models, such as a coordinated-turn model. As a further work, the CRLB expressions for the orientation of the target extent should be derived as well. Additionally, the performance for problems that involve agile target extents should be explored by further research. In some extended target scenarios, the target extent might be dependent on the kinematic target states, see e.g., [1]. For these types of scenarios, it would be interesting to derive coupled/joint CRLBs for the target kinematic and extent states.

REFERENCES

[1] K. Granstrom and U. Orguner, "New prediction for extended targets with random matrices," *IEEE Transactions on Aerospace and Electronic Systems*, vol. 50, no. 2, pp. 1577–1589, April 2014.

[2] S. S. Blackman and R. Popoli, *Design and analysis of modern target tracking systems*. Artech House, 1999.

[3] Y. Bar-Shalom, X. Li, and T. Kirubarajan, *Estimation with applications to tracking and navigation*. Wiley, 2001.

[4] D. J. Salmond and M. C. Parr, "Track maintenance using measurements of target extent," *IEE Proceedings-Radar, Sonar and Navigation*, vol. 150, no. 6, pp. 389–395, 2003.

[5] D. Salmond and K. Gilholm, "Spatial distribution model for tracking extended objects," *IEE Proceedings-Radar, Sonar and Navigation*, vol. 152, no. 5, pp. 364–371, 2005.

[6] Y. Boers and J. N. Driessen, "A track before detect approach for extended objects," in *Proceedings of the 9th International Conference on Information Fusion*, July 2006, pp. 1–7.

[7] Z. Zhong, H. Meng, and X. Wang, "Extended target tracking using an IMM based Rao-Blackwellised unscented Kalman filter," in *Proceedings of the 9th International Conference on Signal Processing (ICSP 2008)*, Oct 2008, pp. 2409–2412.

[8] D. Angelova and L. Mihaylova, "Extended object tracking using Monte Carlo methods," *IEEE Transactions on Signal Processing*, vol. 56, no. 2, pp. 825–832, Feb 2008.

[9] K. Granstrom, C. Lundquist, and O. Orguner, "Extended target tracking using a Gaussian-mixture PHD filter," *IEEE Transactions on Aerospace and Electronic Systems*, vol. 48, no. 4, pp. 3268–3286, October 2012.

[10] J. W. Koch, "Bayesian approach to extended object and cluster tracking using random matrices," *IEEE Transactions on Aerospace and Electronic Systems*, vol. 44, no. 3, pp. 1042–1059, July 2008.

[11] M. Feldmann, D. Franken, and W. Koch, "Tracking of extended objects and group targets using random matrices," *IEEE Transactions on Signal Processing*, vol. 59, no. 4, pp. 1409–1420, April 2011.

[12] S. M. Kay, *Fundamentals of Statistical Signal Processing: Estimation theory.* Prentice Hall, 1993.

[13] H. L. Van Trees, *Detection, Estimation, and Modulation Theory*, ser. Detection, Estimation, and Modulation Theory. Wiley, 2004, no. 1.

[14] H. L. V. Trees and K. L. Bell, *Bayesian Bounds for Parameter Estimation and Nonlinear Filtering/Tracking.* Wiley-IEEE Press, 2007.

[15] B. Ristic and D. J. Salmond, "A study of a nonlinear filtering problem for tracking an extended target," in *Proceedings of the 12th International Conference on Information Fusion (FUSION'04)*, 2004.

[16] L. Xu and X. R. Li, "Hybrid Cramer-Rao lower bound on tracking ground moving extended target," in *Proceedings of the 12th International Conference on Information Fusion (FUSION'09)*, July 2009, pp. 1037–1044.

[17] Z. Zhong, H. Meng, and X. Wang, "A comparison of posterior Cramer-Rao bounds for point and extended target tracking," *IEEE Signal Processing Letters*, vol. 17, no. 10, pp. 819–822, Oct 2010.

[18] ——, "Performance bound for extended target tracking using high resolution sensors," *Sensors*, vol. 10, no. 12, pp. 11 618–11 632, 2010.

[19] H. Meng, Z. Zhong, and X. Wang, "Performance bounds of extended target tracking in cluttered environments," *Science China Information Sciences*, vol. 56, no. 7, pp. 1–12, 2013.

[20] K. B. Petersen and M. S. Pedersen, "The matrix cookbook," http://www.math.uwaterloo.ca/~hwolkowi/matrixcookbook.pdf, 11 2012, accessed: 2015-09-04.

[21] A. K. Gupta and D. K. Nagar, *Matrix Variate Distributions.* Chapman and Hall/CRC, 1999.

[22] P. Tichavsky, C. H. Muravchik, and A. Nehorai, "Posterior Cramer-Rao bounds for discrete-time nonlinear filtering," *IEEE Transactions on Signal Processing*, vol. 46, no. 5, pp. 1386–1396, May 1998.

[23] U. Orguner. (2015, Sep.) Using first-order derivatives for calculating posterior CRLB instead of second-order derivatives. [Online]. Available: http://www.eee.metu.edu.tr/~umut/files/PosteriorCRLBtricks.pdf

[24] Y. Dodge, Ed., *Statistical Data Analysis and Inference.* Elsevier Science Publisher, 1989.

[25] E. C. Andersson, "Monte Carlo methods and importance sampling," http://ib.berkeley.edu/labs/slatkin/eriq/index.htm, 10 1999, accessed : 2015-9-4.